

AD-A112 421

AIR FORCE ACADEMY CO

F/6 20/4

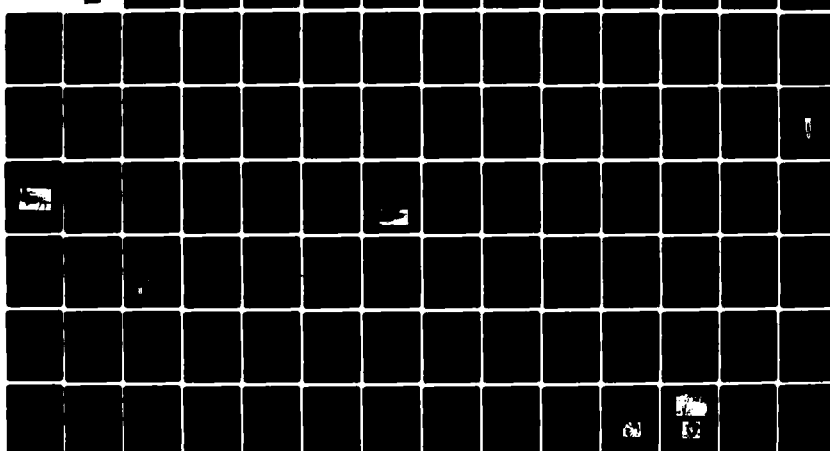
AIR FORCE ACADEMY AERONAUTICS DIGEST - SPRING/SUMMER 1981.(U)

DEC 81 A M HIGGINS, F M JONAS, E J JUMPER

UNCLASSIFIED USAFA-TR-81-11

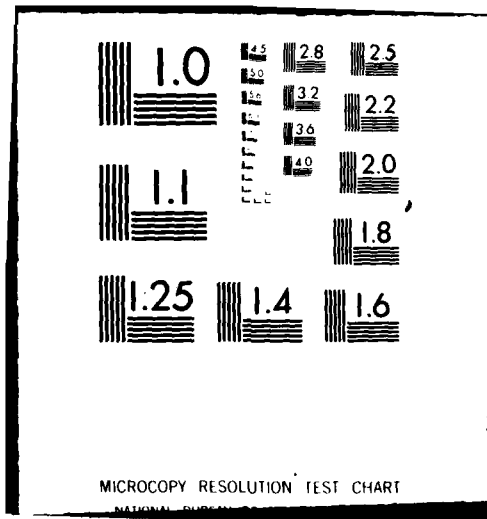
NL

1 x 2  
2 x 4  
[ ]



6a

6b



ADA112421



# AIR FORCE ACADEMY

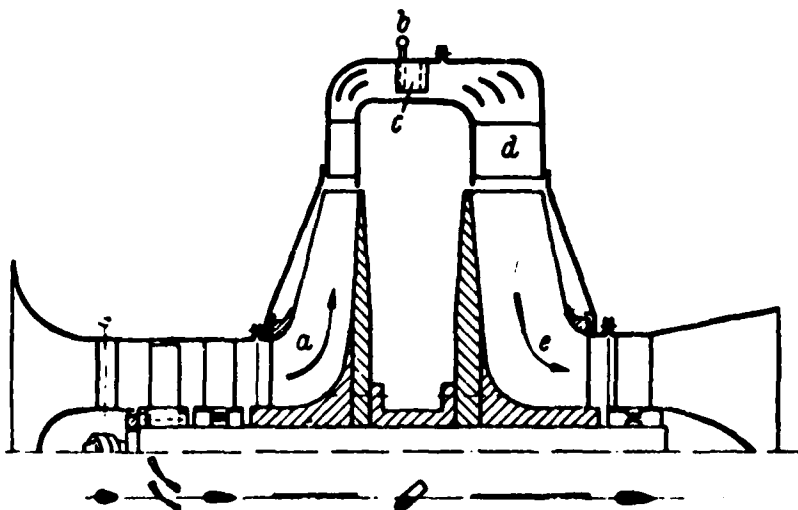
## Aeronautics Digest – Spring/Summer 1981

12  
USAFA-TR-81-11

### RADIAL TURBOJET – He.S.1

DECEMBER 1981

Final Report



Built 1936; Tested 1937

APPROVED FOR PUBLIC RELEASE: DISTRIBUTION UNLIMITED

AMC FILE COPY

Department of Aeronautics  
Dean of the Faculty  
United Air Force Academy  
Colorado 80840

DTIC  
FCTE  
MAR 23 1982  
D  
H

012

COVER:

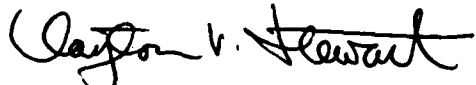
The cover shows a schematic diagram of Germany's first turbojet engine, the He.S.1, which was built by the Heinkel company under the direction of Dr. Hans von Ohain. If you are interested in the beginnings and development of jet propulsion, see Dr. von Ohain's article in this Digest entitled "The Evolution of Aero-Propulsion Systems."

Editorial Review by Capt James M. Kempf, Department of English,  
USAF Academy, Colorado 80840

This document is presented as a compilation of monographs worthy of publication. The United States Air Force Academy vouches for the quality of research, without necessarily endorsing the opinions and conclusions of the authors.

This Digest has been cleared for open publication and/or public release by the appropriate Office of Information in accordance with AFR 190-17 and DODD 5230.9. There is no objection to unlimited distribution of the Digest to the public at large, or by DDC to the National Technical Information Service.

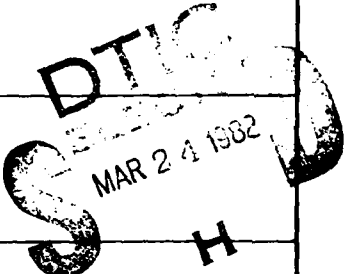
This Digest has been reviewed and is approved for publication.



Clayton V. Stewart, Lt. Colonel, USAF  
Director of Research and Continuing Education

## UNCLASSIFIED

SECURITY CLASSIFICATION OF THIS PAGE (When Data Entered)

REPORT DOCUMENTATION PAGE		READ INSTRUCTIONS BEFORE COMPLETING FORM
1. REPORT NUMBER USAFA-TR-81-11	2. GOVT ACCESSION NO. <i>AD-A412424</i>	3. RECIPIENT'S CATALOG NUMBER
4. TITLE (and Subtitle)  Air Force Academy Aeronautics Digest Spring/Summer 1981	5. TYPE OF REPORT & PERIOD COVERED  Final Report	
7. AUTHOR(s)  EDITORS: A.M. Higgins E.J. Jumper B.Gregory F.M. Jonas J.M. Kempf	6. PERFORMING ORG. REPORT NUMBER	
9. PERFORMING ORGANIZATION NAME AND ADDRESS  Department of Aeronautics United States Air Force Academy, CO 80840	10. PROGRAM ELEMENT, PROJECT, TASK AREA & WORK UNIT NUMBERS	
11. CONTROLLING OFFICE NAME AND ADDRESS	12. REPORT DATE December 1981	
14. MONITORING AGENCY NAME & ADDRESS(if different from Controlling Office)	13. NUMBER OF PAGES 106	
	15. SECURITY CLASS. (of this report)	
	15a. DECLASSIFICATION DOWNGRADING SCHEDULE	
16. DISTRIBUTION STATEMENT (of this Report)	<div style="border: 1px solid black; padding: 5px; display: inline-block;"> <b>DISTRIBUTION STATEMENT A</b>            Approved for public release;            Distribution is unlimited         </div> <div style="margin-top: 10px;">  </div>	
17. DISTRIBUTION STATEMENT (of the abstract entered in Block 20, if different from Report)		
18. SUPPLEMENTARY NOTES		
19. KEY WORDS (Continue on reverse side if necessary and identify by block number)	Aerodynamics, Propulsion, Thermodynamics, Wind Tunnel, Aeronautical Instrumentation, Aeronautical History, Engineering Education	
20. ABSTRACT (Continue on reverse side if necessary and identify by block number)	<p>This <u>Digest</u> covers unclassified research in aeronautics performed at the United States Air Force Academy during the six months ending 15 July 1981. This report includes technical papers in the specific areas of aerodynamics, propulsion, experimental instrumentation, engineering education, and aeronautical history.</p>	

PREFACE

This report is the seventh issue of the Air Force Academy Aeronautics Digest.\* Our policy is to print articles which represent recent scholarly work by students and faculty of the Department of Aeronautics members of other departments of the Academy and the Frank J. Seiter Research Laboratory, researchers directly or indirectly involved with USAFA-sponsored projects, and authors in fields of interest to the USAFA.

In addition to complete papers, the Digest also includes, when appropriate, abstracts of lengthier reports and articles published in other formats. The editors will consider for publication contributions in the general field of Aeronautics, including:

- Aeronautical Engineering
- Aerodynamics
- Flight Mechanics
- Propulsion
- Structures
- Instrumentation
- Fluid Dynamics
- Thermodynamics and Heat Transfer
- Biomechanics
- Engineering Education
- Aeronautical History

Papers on other topics will be considered on an individual basis. Contributions should be sent to:

Editor, Aeronautics Digest  
DFAN  
US Air Force Academy, CO 80840

The Aeronautics Digest is presently edited by Maj A.M. Higgins, PhD; Capt F.M. Jonas, PhD; Maj E.J. Jumper, PhD; and Capt J.M. Kempf, PhD, Department of English, who provided the final editorial review. Our thanks also to our Associate Editor, Barbara J. Gregory, of Contract Technical Services, Inc.

Accession For	
NTIS CRA&I	<input checked="" type="checkbox"/>
DTIC TAB	<input type="checkbox"/>
Unpublished	<input type="checkbox"/>
Justification	
By	
Distribution	
Available to DDC	
DDC	
COPY	
REF ID	

A

\* The first five issues of the Digest can be ordered from the Defense Documentation Center (DDC), Cameron Station, Alexandria, VA 22324. Use the following AD numbers: Aeronautics Digest - Spring 1978, ADA060207; Aeronautics Digest - Fall 1978, ADA069044; Aeronautics Digest - Spring 1979, ADA075419; Aeronautics Digest - Fall 1979, ADA085770; and Aeronautics Digest - Spring/Summer 1980, ADA096678.

## CONTENTS

<u>Section</u>		<u>Page</u>
I. AERODYNAMICS		1
THE MASS FLUX SURFACE BOUNDARY CONDITION FOR LINEARIZED POTENTIAL FLOW ----F.M. Jonas		2
A NUMERICAL INVESTIGATION OF THE EFFECTS OF FIN PLANFORM PARAMETERS ON THE SUBSONIC CRUISE PERFORMANCE OF A SUPERSONIC ARROW WING CONFIGURATION ----G.T. Matsuyama and C.E. Lan		17
II. PROPULSION		33
AN IMPROVED METHOD FOR CALCULATION OF STATIC THRUST FOR THE USAFA J-85/13 TURBOJET ENGINE ----M.K. Reagan, P.D. Thornley, and A.M. Higgins		34
III. INSTRUMENTATION AND HARDWARE		51
PRESSURE MEASUREMENT USING A HIGH-SPEED DATA ACQUISITION AND ON-LINE CALIBRATION SYSTEM ----J.A. Wright and W.A. Buzzell		52
IV. ENGINEERING EDUCATION		64
CADET PERFORMANCE DURING SUMMER ACADEMICS: REPEAT VERSUS NON-REPEAT STUDENTS ----J.H. Russell		65
REFLECTIONS OF AN ENGLISH LITERATURE MAJOR ON OUR TECHNOLOGICAL SOCIETY ----J.M. Kempf		70
V. AERONAUTICAL HISTORY		79
THE EVOLUTION AND FUTURE OF AEROPROPULSION SYSTEMS ----Hans von Ohain		80

USAF-A-TR-81-11

**SECTION I**

**Aerodynamics**

THE MASS FLUX SURFACE BOUNDARY CONDITION  
FOR LINEARIZED POTENTIAL FLOW

F.M. Jonas\*

Abstract

This paper discusses and demonstrates mathematically the use of consistent boundary conditions when solving equations which approximate real fluid flow relationships. In particular, potential flow equations are examined and appropriate boundary conditions are presented. Furthermore, these exact potential flow equations are simplified by assuming small perturbations to the flow field about a body, and boundary conditions consistent with this approximation are developed. The paper closes by presenting an analytic solution to the linearized small perturbation potential equation, or Prandtl-Glauert equation, for the idealized flow about an elliptic cylinder. This solution is obtained only after the successful application of consistent boundary conditions.

I. Introduction

Potential flow theory has been a useful tool for aerodynamic engineers. Potential flow theory, of course, is based on the assumption that a given fluid flow is inviscid (frictionless) and irrotational (i.e., the fluid elements may deform but may not rotate as they move with the fluid). Although potential flow theory represents a highly idealized condition which actual fluid flow never achieves, the mathematical equations which are derived from the idealized theoretical condition can be used by engineers to provide accurate estimates of some of the aerodynamic forces generated by a body as it moves through a real fluid. These aerodynamic forces include: lift, pitching moment, and inviscid drag-due-to-lift.

Due to the increased sophistication of computer technology in recent years, aeronautical engineers have demonstrated a renewed interest in developing numerical techniques that can be used along with the equations derived from potential flow theory for practical analysis of aerodynamic fluid flow phenomena. This renewed interest is largely due to the fact that the use of these numerical techniques and modern computers can, in combination, solve difficult potential flow problems that arise from fluid flows around very complex aerodynamic shapes such as a complete aircraft or a specific missile configuration. For compressible (subsonic or supersonic) fluid flows the most useful method that has been used to date for predicting the inviscid aerodynamic characteristics of aeronautical designs or arbitrary configurations has been the distributed surface singularity or panel method (Ref. 1-3).

Classically, analytical methods for evaluating potential fluid flows such as the panel method have been based on a further assumption that the disturbances created by an aerodynamic body as it moves through the fluid are small (i.e., the changes in velocity of the fluid as it moves around the body are small compared to the free stream velocity). This assumption serves as the basis for thin airfoil/slender body theory and is a reasonable assumption for most streamlined aerodynamic shapes. Making this assumption allows one, through physical reasoning, to reduce the exact mathematical expression describing potential flow, which is a highly nonlinear equation, to a linear equation. The Prandtl-Glauert (P-G) equation (or the linearized potential equation) results from the simplifying assumptions of thin airfoil theory and is an

---

\*Captain, USAF, Assistant Professor of Aeronautics, DFAN

approximation for analyzing the aerodynamic performance of slender or thin bodies in subsonic or supersonic fluid flows. The P-G equation, and the exact mathematical expression describing potential flow from which the P-G equation is derived, are both expressed as second-order partial differential equations. As such, two boundary conditions must be specified before one can obtain a specific solution describing the potential flow field about a given body. These two boundary conditions are specified where the theoretician or engineer knows something (or can make a reasonable assumption) about the fluid flow as it interacts with the body of interest. Normally the two boundary conditions are specified at (1) the surface of the body of interest, and (2) far away from the body of interest. For the first boundary condition, since the potential flow is frictionless, it is reasonable to assume that the velocity or surface flow must parallel the surface (for real fluids with friction or viscosity we know that this boundary condition is specified by requiring the velocity to be zero at the surface). This is called the no-slip condition for frictionless flows and can be restated by requiring the velocity vector of the fluid flow normal to the surface of interest to be zero. This is the velocity surface boundary condition (VBC). For the second boundary condition far away from the body it is reasonable to assume for both frictionless and real fluids that the disturbances created by the body disappear (or at least remain finite, small, and do not grow).

In the process of arriving at the approximate formulation of the potential flow field about an aerodynamic body, as represented by the P-G equation (i.e., the reduction of the exact mathematical expression for potential flow from a nonlinear to a linear equation when one assumes small perturbations), to be consistent one needs to apply the same reasoning to the exact mathematical formulations of the boundary conditions. This is indeed done in thin airfoil/slender body theory and one arrives at an approximate formulation of the velocity surface boundary condition to be used in conjunction with the P-G equation. The boundary condition far away from the body, however, remains the same as exactly formulated. In an attempt to obtain more accurate solutions to the P-G equation (solutions which represent the velocity field about the body of interest and thus the resulting distribution of surface pressure), especially when using numerical techniques, some have resorted to using the exact and not the approximate surface boundary condition.

It is the purpose of this paper to demonstrate that a more consistent boundary condition to apply at the surface of interest when using the P-G equation (i.e., consistent with the approximation implied by the P-G equation) is not the exact velocity boundary condition, but an approximation to the mass flux surface boundary condition (MFBC). The mass flux boundary condition requires that there be no mass flowing through the aerodynamic surface.

The reasons for using the mass flux boundary condition and not the exact velocity boundary condition at the surface of interest in conjunction with the P-G equation will be developed in the following manner. First, the exact mathematical formulation describing the potential flow of a fluid will be presented showing the problem formulation to be highly nonlinear. The exact mathematical expressions for the surface

boundary condition (velocity and mass flux) and infinity boundary condition (far away from the body of interest) will also be presented. Next, the assumption of small perturbations will be introduced, and the resulting approximate equations (i.e., the P-G equation) derived. This process is necessary to arrive at the formulation of the problem as most commonly presented and applied. The velocity surface boundary condition will only be presented in its exact formulation as the approximate formulation has already been thoroughly developed and verified (Ref. 4) in thin airfoil/slender body theory applications. At this point an attempt to obtain an analytic solution to the P-G equation for an elliptic cylinder (two-dimensional) in subsonic compressible flow will be made, applying the exact velocity surface boundary condition and then the appropriate mass flux surface boundary condition. It will be shown that an analytic solution can be successfully obtained only by applying the latter surface boundary condition (the infinity boundary condition remains unchanged). Finally, the analytic solution, in terms of the surface velocity distribution at a zero-lift condition, will be presented for selected Mach numbers.

## II. Statement of Exact Problem

The steady, inviscid, irrotational (potential) flow past an arbitrary configuration (Figure 1) is formulated in terms of the velocity potential,  $\Phi$ , where the velocity  $\vec{V} = \nabla \Phi$  as follows:

A. Governing equation (governing the flow field or velocity about the body)

$$\nabla^2 \Phi = \frac{1}{a^2} [\vec{V} \cdot \nabla \left( \frac{V^2}{2} \right)] \quad (1)$$

where the local speed of sound at any point in the flow is given by

$$a^2 = a_\infty^2 - \frac{(\gamma - 1)}{2} (V^2 - U_\infty^2) \quad (2)$$

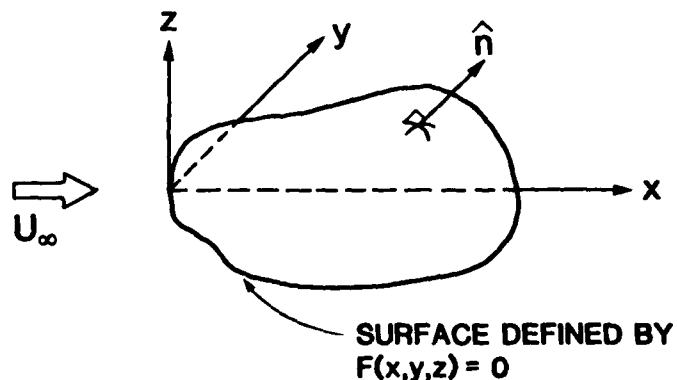


Figure 1. Axis System Rotation

Eqn. (1) is a second-order partial differential equation which requires that two boundary conditions be specified before one can attempt to obtain a solution. Two convenient locations to specify boundary conditions are at the surface of interest and far away from the body.

B. Surface boundary Condition

Velocity (VBC):

$$\hat{\mathbf{v}} \cdot \hat{\mathbf{n}} = 0 \text{ on } F(x,y,z) = 0 \quad (3)$$

Eqn. (3) requires the velocity to be parallel to the surface or that the velocity vector normal to the surface is zero (inviscid or frictionless flow).

Mass Flux (MFBC):

$$\rho \hat{\mathbf{v}} \cdot \hat{\mathbf{n}} = 0 \text{ on } F(x,y,z) = 0 \quad (4)$$

Eqn. (4) requires that the mass flux perpendicular to the surface be zero or that there is no mass flow into the body.

C. Fluid boundary condition at infinity (far away from the body)

$$\nabla \phi \rightarrow \hat{\mathbf{U}}_{\infty} \hat{\mathbf{i}} \text{ at infinity} \quad (5)$$

This requires that any disturbances in the fluid due to the presence of the body disappear when one gets very far away from the body.

Note that the velocity boundary condition (Eqn. (3)) and the mass flux boundary condition (Eqn. (4)) at the surface differ only by the inclusion of the local density,  $\rho$ , which changes the physical interpretation of what is being imposed at the surface. At first glance this difference appears superfluous. Since the fluid is assumed to be a continuum (no holes), and subsequently the density of the fluid is nowhere zero, then one can eliminate density from Eqn. (3) making the two surface boundary conditions identical. In fact, if Eqn. (1) could be solved exactly at every point in the flow field, and since the density of the fluid is not zero anywhere, then the standard velocity boundary condition should be enforced. Eqn. (1) cannot be solved for arbitrary configurations, thus one must resort to an approximate method. One approach is to use numerical techniques, such as finite difference, to solve Eqn. (1) with the appropriate boundary conditions for a given configuration. For this case the velocity boundary condition (Eqn. (3)) is used at the surface (Ref. 5). Another approach is to solve an equation which approximates Eqn. (1). The Prandtl-Glauert or linearized potential equation is an example of this latter technique. It is the purpose of this paper to show, with respect to the P-G equation, that the mass flux boundary

condition (Eqn. (4)), with its subsequent approximations, is the correct boundary condition to apply at the surface in order to obtain valid solutions.

The exact problem can be restated in terms of a non-dimensional perturbation velocity potential,  $\phi$ , where

$$\phi = U_\infty l (x + \phi) \quad (6)$$

The problem is nondimensionalized to permit application of perturbation theory as presented in the next section. The length,  $l$ , represents some characteristic body length (such as the chord length) which also is used to non-dimensionalize the coordinate directions  $(x, y, z)$ . The reason for introducing the perturbation parameter  $\phi$  is to measure directly the effects of the body on the fluid. The gradient of the perturbation velocity potential,  $\nabla\phi$ , thus represents the perturbation velocity components  $(u/U_\infty, v/U_\infty, w/U_\infty)$  because of the presence of the body. Replacing the local speed of sound in Eqn. (1) with Eqn. (2) and rewriting Eqns. (1, 3-5) in terms of the non-dimensionalized quantities results in:

#### A. Governing equation

$$\begin{aligned} (1 - M_\infty^2) \phi_{xx} + \phi_{yy} + \phi_{zz} &= M_\infty^2 [(\gamma + 1)\phi_x + (\frac{\gamma + 1}{2})\phi_x^2 + (\frac{\gamma - 1}{2})(\phi_y^2 + \phi_z^2)]\phi_{xx} \\ &+ M_\infty^2 [(\gamma - 1)\phi_x + (\frac{\gamma + 1}{2})\phi_y^2 + (\frac{\gamma - 1}{2})(\phi_x^2 + \phi_z^2)]\phi_{yy} \\ &+ M_\infty^2 [(\gamma - 1)\phi_x + (\frac{\gamma + 1}{2})\phi_z^2 + (\frac{\gamma - 1}{2})(\phi_x^2 + \phi_y^2)]\phi_{zz} \\ &+ 2M_\infty^2 [(\phi_y + \phi_x\phi_y)\phi_{xy} + (\phi_z + \phi_x\phi_z)\phi_{xz} + \phi_y\phi_z\phi_{yz}] \end{aligned} \quad (7)$$

#### B. Surface boundary condition

Velocity (VBC):

$$(1 + \phi_x)n_x + \phi_y n_y + \phi_z n_z = 0 \text{ on } F(x, y, z) = 0 \quad (8)$$

Mass Flux (MFBC):

$$\frac{\rho}{\rho_\infty} [(1 + \phi_x)n_x + \phi_y n_y + \phi_z n_z] = 0 \text{ on } F(x, y, z) = 0 \quad (9)$$

where

$$n_x = \frac{\partial F}{\partial x} / |\nabla F|, n_y = \frac{\partial F}{\partial y} / |\nabla F|, n_z = \frac{\partial F}{\partial z} / |\nabla F|$$

#### C. Fluid infinity boundary condition

$$\nabla\phi \rightarrow 0 \text{ at infinity} \quad (10)$$

Eqn. (7) dramatically shows the highly nonlinear nature of the problem. Analytic solutions for arbitrary configurations cannot be obtained and one is forced to seek numerical or approximate solutions.

### III. Small Perturbation Theory

Probably the most used approximation of Eqn. (7) for compressible flow is the equation that results when one assumes that the body to be analyzed is thin or slender and the resulting perturbations are small. Since  $\phi$  represents the perturbations due to the body (e.g., change in velocity due to presence of the body), one can examine the relative magnitude of terms in Eqn. (7) and neglect those that are small based on physical reasoning. The governing equation resulting from this assumption (Ref. 4 and 6) is:

$$\beta^2 \phi_{xx} + \phi_{yy} + \phi_{zz} = 0 \quad (11)$$

(Note that this approximation is linear.)

where

$$\beta^2 = 1 - M_\infty^2$$

Eqn. (11) forms the basis for thin airfoil/slender body theory and predictive inviscid aerodynamics, and it is valid for subsonic or supersonic potential flows. It must be remembered that this equation applies to small perturbations and will yield valid solutions only in those regions where this assumption is valid (Ref. 6). Note that for incompressible flow ( $M_\infty \rightarrow 0$ ) Eqn. (11) is exact regardless of the body; for example, Eqn. (11) is identical to Eqn. (7) for incompressible flow.

### IV. Boundary Conditions

In order to obtain a solution to Eqn. (11) one must apply the appropriate boundary conditions at the body and fluid infinity. It would be ideal to apply boundary conditions such that the problem could be transformed to an equivalent incompressible flow problem (Laplace's equation), which has known analytic solutions. The application of thin airfoil/slender body theory accomplished this and provided aerodynamicists the first opportunity to make accurate estimates of the potential flow field about arbitrary configurations, especially those immersed in a compressible flow. With the advent of computer capabilities and associated numerical techniques such as the panel method (Ref. 1-3), the emphasis has been on the application of more exact boundary conditions (as opposed to thin airfoil theory), especially at the surface of the body. The most obvious candidate is the exact velocity boundary condition or:

$$(1 + \phi_x)n_x + \phi_y n_y + \phi_z n_z = 0 \text{ on } F(x, y, z) = 0 \quad (12)$$

Eqn. (7), the exact governing equation, is a mathematical statement that represents the conservation of mass (the continuity equation). An approximation of this equation, such as the P-G equation (Eqn. (11)), does not assure mass conservation. If we use Eqn. (11) and apply the VBC (Eqn. (12)) at the surface, we still have not assured continuity. Chin (Ref. 7) has claimed that to obtain analytic solutions to the P-G equation, it is necessary to reinforce this lost continuity condition by imposing the zero-mass flux condition at the surface (MFBC). In fact, it appears impossible to transform the P-G equation to Laplace's equations and simultaneously maintain a zero-net flux condition through the closed-body streamline (Ref. 7) when trying to obtain analytic solutions, unless one uses a consistent approximation (to the approximation implied by the P-G equation) to the mass flux surface boundary condition, Eqn. (9). (This is demonstrated in the next section as applied to the elliptic cylinder.) It can be shown that this consistent approximation derived from Eqn. (9) (Ref. 6-8) is

$$(1 + \beta^2 \phi_x) n_x + \phi_y n_y + \phi_z n_z = 0 \text{ on } F(x, y, z) = 0 \quad (13)$$

This then is the boundary condition to be applied at the surface when using the P-G equation. This mass flux boundary condition approximation differs from the velocity boundary condition by the inclusion of  $\beta^2$ , and is identical for incompressible flow ( $\beta^2 = 1$ ). The boundary condition to be applied at fluid infinity requires that the disturbances due to the presence of the body disappear, or as previously presented

$$\nabla \phi \rightarrow 0 \text{ at infinity} \quad (14)$$

The problem now is well posed, and thus one is guaranteed that analytic solutions exist.

It should be noted that the necessity for applying the mass flux boundary condition in thin airfoil/slender body theory does not arise (although for higher order approximations it may be necessary). This is because the  $x$ -component of the perturbation velocity ( $\phi_x$ ) in Eqn. (12) (VBC) is neglected (Ref. 4) in the surface boundary condition, and thus when one also neglects this term in Eqn. (13) (MFBC) the two boundary conditions become identical. Whether or not this is fortuitous, it illustrates the use of a boundary condition consistent with the assumptions made in the derivation and application of thin airfoil/slender body theory.

#### V. Elliptic Cylinder in Subsonic Potential Flow

To illustrate the necessity for applying the MFBC approximation, Eqn. (13), as opposed to the exact VBC, Eqn. (12), when solving the P-G equation we will attempt to obtain an analytic solution. The problem to be solved is the nonlifting elliptical cylinder (two-dimensional) in subsonic potential flow as shown in

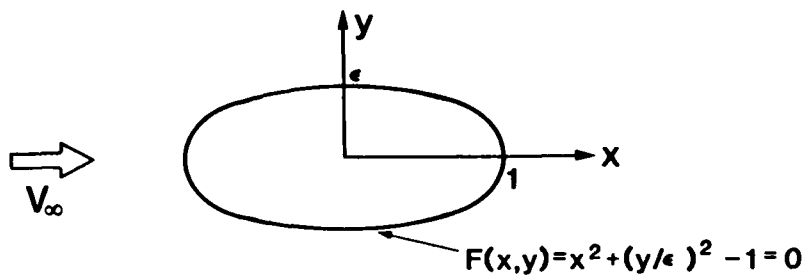


Figure 2. Elliptic Cylinder

Figure 2. First we will apply the exact VBC, then the MFBC approximation, demonstrating that a valid analytic solution can only be obtained in the latter approach.

The approach involves transforming the problem (Eqn. (11) with either the VBC, Eqn. (12), or the MFBC, Eqn. (13), applied at the surface, and the infinity boundary condition, Eqn. (14)) to the flow about an equivalent circular cylinder in incompressible flow or

$$\begin{aligned} \nabla^2 \phi &= 0 \\ \mathbf{V} \cdot \hat{\mathbf{n}} &= 0 \text{ on surface, circular cylinder} \\ \mathbf{V} &\rightarrow \mathbf{U}_\infty \text{ at infinity} \end{aligned}$$

At this point the known solution about the circular cylinder can then be transformed back to the ellipse in compressible flow. This in essence involves eliminating the  $\beta^2$  terms in Eqns. (11) and (13) through a coordinate transform and a transform of the perturbation potential function  $\phi$ . If successful, the final step will be to apply the Joukowski transform, mapping the equivalent ellipse to the known solution about a circular cylinder in incompressible flow. First let us consider the statement of the problem applying the VBC at the surface:

A. Governing P-G equation for two-dimensional flow

$$\beta^2 \phi_{xx} + \phi_{yy} = 0 \quad (15)$$

B. Exact VBC ( $n_x \sim x$ ,  $n_y \sim y/\epsilon^2$ )

$$(1 + \phi_x)(x) + \phi_y (y/\epsilon^2) = 0 \text{ on } F(x,y) = x^2 + (y/\epsilon)^2 - 1 = 0 \quad (16)$$

C. Infinity boundary condition

$$\phi_x \rightarrow 0, \phi_y \rightarrow 0 \text{ at infinity} \quad (17)$$

Applying the P-G coordinate transform,  $\bar{x} = x/\beta$  ( $\beta \neq 0$ ) results in:

$$\phi_{\bar{x}\bar{x}} + \phi_{yy} = 0 \quad (18)$$

$$(1 + \frac{1}{\beta} \phi_{\bar{x}})(\beta \bar{x}) + \phi_y (y/\epsilon^2) = 0 \text{ on } F(\bar{x}, y) = (\beta \bar{x})^2 + (y/\epsilon)^2 - 1 = 0 \quad (19)$$

$$\phi_{\bar{x}} \rightarrow 0, \phi_y \rightarrow 0 \text{ at infinity} \quad (20)$$

Now let  $\tilde{\phi} = \phi/\beta$ , resulting in

$$\tilde{\phi}_{\bar{x}\bar{x}} + \tilde{\phi}_{yy} = 0 \quad (21)$$

$$(1 + \tilde{\phi}_{\bar{x}})(\bar{x}) + \tilde{\phi}_y (y/\epsilon^2) = 0 \quad (22)$$

$$\tilde{\phi}_{\bar{x}} \rightarrow 0, \tilde{\phi}_y \rightarrow 0 \text{ at infinity} \quad (23)$$

Finally, let  $\tilde{\phi} = \bar{x} + \phi$ , resulting in

$$\tilde{\phi}_{\bar{x}\bar{x}} + \tilde{\phi}_{yy} = 0 \quad (24)$$

$$\tilde{\phi}_{\bar{x}} (\bar{x}) + \tilde{\phi}_y (y/\epsilon^2) = 0 \quad (25)$$

$$\tilde{\phi}_{\bar{x}} \rightarrow 1, \tilde{\phi}_y \rightarrow 0 \text{ at infinity} \quad (26)$$

The problem has been successfully transformed to an incompressible flow problem. However, upon examining the surface normals in Eqn. (25) we see that the surface boundary condition is satisfied on the surface specified by

$$\left. \begin{aligned} \bar{F}(\bar{x}, y) &= \bar{x}^2 + (y/\epsilon)^2 - 1 = 0 \\ \bar{F}(x, y) &= (x/\beta)^2 + (y/\epsilon)^2 - 1 = 0 \end{aligned} \right\} \quad (27)$$

and not the original surface specified by the following equation:

$$\left. \begin{aligned} F(\bar{x}, y) &= (\beta \bar{x})^2 + (y/\epsilon)^2 - 1 = 0 \\ F(x, y) &= x^2 + (y/\epsilon)^2 - 1 = 0 \end{aligned} \right\} \quad (28)$$

Thus, while one may obtain a solution that appears correct, since both surfaces have the same maximum thickness (only the chord lengths are different) and yield approximately the same maximum velocity, it is clearly for the wrong surface.

Now let us attempt the same problem applying the MFBC at the surface. The statement of the problem is as follows:

A. P-G equation

$$\beta^2 \phi_{xx} + \phi_{yy} = 0 \quad (29)$$

B. Approximate MFBC

$$(1 + \beta^2 \phi_x) (x) + \phi_y (y/\epsilon^2) = 0 \text{ on } F(x, y) = x^2 + (y/\epsilon)^2 - 1 = 0 \quad (30)$$

C. Infinity boundary condition

$$\phi_x \rightarrow 0, \phi_y \rightarrow 0 \quad (31)$$

Applying the P-G transformation,  $\tilde{x} = x/\beta$  ( $\beta \neq 0$ ), results in

$$\phi_{\tilde{x}\tilde{x}} + \phi_{yy} = 0 \quad (32)$$

$$(1 + \beta \phi_{\tilde{x}})(\beta \tilde{x}) + \phi_y (y/\epsilon^2) = 0 \text{ on } F(\tilde{x}, y) = 0 \quad (33)$$

$$\phi_{\tilde{x}} \rightarrow 0, \phi_y \rightarrow 0 \text{ at infinity} \quad (34)$$

Now let  $\tilde{\phi} = \beta \phi$ , resulting in

$$\tilde{\phi}_{\tilde{x}\tilde{x}} + \tilde{\phi}_{yy} = 0 \quad (35)$$

$$(1 + \tilde{\phi}_{\tilde{x}})(\beta^2 \tilde{x}) + \tilde{\phi}_y (y/\epsilon^2) = 0 \text{ on } F(\tilde{x}, y) = 0 \quad (36)$$

$$\tilde{\phi}_{\tilde{x}} \rightarrow 0, \tilde{\phi}_y \rightarrow 0 \text{ at infinity} \quad (37)$$

Finally, let  $\tilde{\phi} = \tilde{x} + \tilde{\phi}$ , resulting in

$$\tilde{\phi}_{xx} + \tilde{\phi}_{yy} = 0 \quad (38)$$

$$\tilde{\phi}_x (\beta^2 \tilde{x}) + \tilde{\phi}_y (y/\epsilon^2) = 0 \text{ on } F(\tilde{x}, y) = 0 \quad (39)$$

$$\tilde{\phi}_x \rightarrow 1, \tilde{\phi}_y \rightarrow 0 \text{ at infinity} \quad (40)$$

Again, the problem has been successfully transformed to an incompressible flow problem, but this time for the correct surface:

$$F(\tilde{x}, y) = (\beta \tilde{x})^2 + (y/\epsilon)^2 - 1 = 0 \quad (41)$$

or

$$F(x, y) = x^2 + (y/\epsilon)^2 - 1 = 0 \quad (42)$$

One can now proceed to transform this problem to the known solution about a circular cylinder in incompressible flow using the Joukowski transform. The resulting analytic solution (Ref. 6) is

$$\phi(x, y) = \frac{kQ}{2B} \left\{ P + \sqrt{P^2 - 1} \right\} \left\{ 1 + R^2 \right\} - \frac{x}{\beta^2} + \text{constant} \quad (43)$$

where

$$k = \frac{1}{\beta} \sqrt{1 - (\beta \epsilon)^2} \quad (44)$$

$$P = \sqrt{y^2 + \left( \frac{x}{\beta} + k \right)^2} \quad (45)$$

$$q = \sqrt{y^2 + \left( \frac{x}{\beta} - k \right)^2} \quad (46)$$

$$P = P + q/2k \quad (47)$$

$$Q = P - q/2k \quad (48)$$

$$R = \sqrt{\frac{1 + \beta \epsilon}{1 - \beta \epsilon}} \quad (P + \sqrt{P^2 - 1}) \quad (49)$$

As demonstrated, this problem cannot be successfully transformed to an equivalent incompressible flow problem for the same or given surface using the exact VBC. An analytic solution is successfully obtained only after one uses a consistent approximation (to the approximation implied by the P-G equation) to the MFBC at the surface. It may be concluded from this that the attempt to use the more exact VBC at the

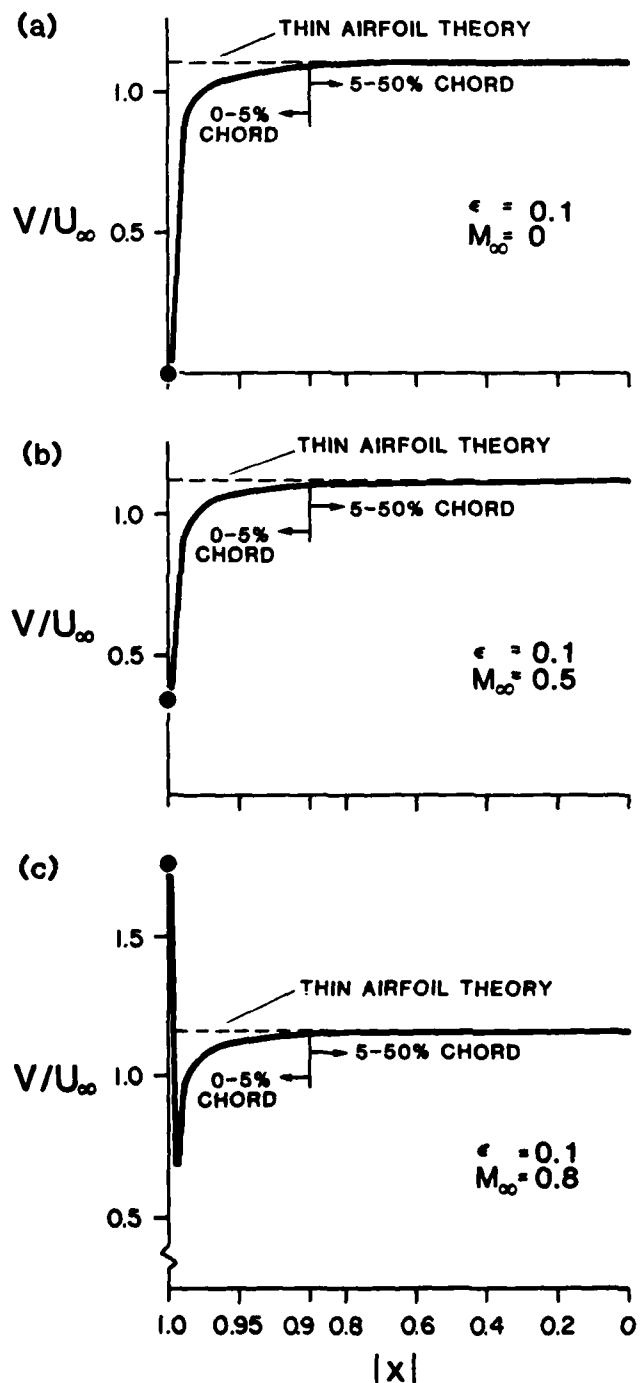


Figure 3. P-G Solution, Two-Dimensional Ellipse, MFBC,  $\epsilon = 0.1$ .  
 (a)  $M_\infty = 0$ ; (b)  $M_\infty = 0.5$ ; (c)  $M_\infty = 0.8$

surface in numerical techniques solving the P-G equation may lead to incorrect results. Therefore, to be consistent one should apply the MFBC at the surface for compressible flows. This applies to any surface and is not peculiar to the ellipse.

In Figure 3 the solution (Eqn. (43)) is presented in terms of the total velocity,  $V/U_\infty$ , where

$$\frac{V}{U_\infty} = \sqrt{(1+\phi_x)^2 + \phi_y^2} \quad (50)$$

for an elliptic cylinder,  $\epsilon = 0.1$ , at freestream Mach numbers of 0, 0.5, and 0.8.

For comparison, the thin airfoil theory solution (Ref. 6)

$$\frac{V}{U_\infty} = 1 + \epsilon/\beta \quad (51)$$

is shown in these figures and represents an asymptotic limit for the more exact solution using the MFBC. For incompressible flow the MFBC solution is exact, as shown in Figure 3a, while for compressible flows (Figures 3b and 3c) the MFBC solutions are approximations to the exact problem. In Figures 3b and 3c the velocity at the stagnation points ( $|x| = 1$ ) is not zero but some finite value. This is not an error, but it is consistent with the approximation implied by the P-G equation, since the perturbations are no longer small in the stagnation region ( $V \rightarrow 0$ ). In fact, the perturbation velocity component,  $\phi_x$  or  $u/U_\infty$ , is on the order of the freestream velocity in this region. The fact that small perturbation theory breaks down in this region has been noted by many investigators (Ref. 6, 9-13) and is dramatically illustrated by the results of thin airfoil theory for all Mach numbers. This result does not hinder the calculation of inviscid lift or pitching moments but is of concern for inviscid drag calculations (Ref. 6, 9-12). If one attempted to numerically apply the VBC, the velocity at the stagnation point would be forced to zero for all freestream Mach numbers. Although this is physically true, one must ask if this is a reasonable result of a method based on small perturbations.

#### VI. Conclusions

It has been successfully demonstrated that in the effort to obtain more exact solutions to the Prandtl-Glauert equation, one should apply the mass flux boundary condition approximation at the surface and not the exact VBC. This boundary condition approximation (MFBC) is consistent with the approximation implied by the Prandtl-Glauert equation. The fact that one cannot obtain analytic solutions to the Prandtl-Glauert equation using the exact velocity boundary condition has implications concerning the validity of solutions obtained using numerical techniques which solve the P-G equation applying the exact velocity surface boundary condition.

Symbols

a	speed of sound
$F(x,y,z)$	surface equation, $F(x,y,z) = 0$
$l$	characteristic length
M	Mach number
$\hat{n}$	outward surface normal
u	velocity
v	velocity
$(u,v,w)$	perturbation velocity components in Cartesian coordinates system
$(x,y,z)$	Cartesian coordinates, unit vectors $(\hat{i}, \hat{j}, \hat{k})$
$\beta^2$	$1 - M_\infty^2$
$\gamma$	ratio of specific heats
$\epsilon$	thickness parameter
$\rho$	density
$\phi(x,y,z)$	perturbation potential function
$\psi(x,y,z)$	Potential function
$\infty$	freestream conditions

References

1. Woodward, F. A. An Improved Method for Aerodynamic Analysis of Wing-Body-Tail Configurations in Subsonic and Supersonic Flow. NASA CR-2228, Part 1, 1973.
2. Hess, J. L. "The Problem of Three-Dimensional Lifting Potential Flow and Its Solution by Means of Surface Singularity Distribution." Computer Methods in Applied Mechanics and Engineering, Vol. 4, 1974.
3. Ehlers, F. E., F. T. Johnson, and P. E. Ruppert. "Advanced Panel-Type Influence Coefficient Methods Applied to Subsonic and Supersonic Flows." Aerodynamic Analysis Requiring Advanced Computers. NASA SP-347, Part II, 1975, pp. 939-984.
4. Liepmann, H. W. and A. Roshko. Elements of Gasdynamics. 6th ed. New York: John Wiley and Sons, Inc., 1965, Chapter 8.
5. Jameson, A. Transonic Flow Calculations for Airfoils and Bodies of Revolution. Grumman Aerospace Corporation Aerodynamics Report 390-71-1.
6. Jonas, F. M. "A Singular Perturbation Method for Arbitrary Configurations in Subsonic Potential Flow." Dissertation, AFIT/DS/AA/80-3.
7. Chin, W. C. "Goethert's Rule with an Improved Boundary Condition." AIAA Journal, Vol. 15, No. 10, October 1977, pp. 1516-1518.
8. Shapiro, A. H. The Dynamics and Thermodynamics of Compressible Fluid Flow. Vol. 1. New York: The Ronald Press Co., 1953, Chapter 10.

9. Lighthill, M. J. "A New Approach to Thin Airfoil Theory." Aero Quart, No. 3, 1951, pp. 193-210.
10. Van Dyke, M. Second-Order Subsonic Airfoil Theory Including Edge Effects. NACA Report 1274, 1956.
11. Jones, R. T. "Leading-Edge Singularities in Thin-Airfoil Theory." Journal of Aero Sci, No. 17, May 1950, pp. 307-310.
12. Heslet, M. A. and H. Lomax. "Supersonic and Transonic Small Perturbation Theory." In General Theory of High Speed Aerodynamics, Vol. 6, High Speed Aerodynamics and Jet Propulsion. W. R. Sears, ed. New Jersey: Princeton University Press, 1954, pp. 143-148.
13. Olsen, J. J. "Subsonic and Transonic Flow Over Sharp- and Round-Nosed Nonlifting Airfoils." Dissertation, The Ohio State University, 1976.

A NUMERICAL INVESTIGATION OF THE EFFECTS OF  
FIN PLANFORM PARAMETERS ON THE SUBSONIC CRUISE PERFORMANCE  
OF A SUPERSONIC APROW WING CONFIGURATION

G.T. Matsuyama\* and C.E. Lan\*\*

Abstract

A numerical investigation was conducted to assess the aerodynamic effects of independently varying the leading edge sweep, taper ratio, and aspect ratio of vertical outboard fins mounted on a 71.2-degree sweep arrow wing. This investigation used the Quasi-Vortex-Lattice Method to supplement information from wind tunnel tests of the basic wing configuration and was performed for a Mach number of .85 and a lift coefficient of 0.263. The results indicate that adding the fin to the basic wing configuration always decreases the wing root bending moment and increases wing aerodynamic efficiency, except when the fin leading edge sweep angle is less than approximately 40 degrees and is mounted with its root chord intersecting the wing leading edge. If the fin is shifted aft at a constant spanwise position the root bending moment decreases.

1. Introduction

Because of the potential for achieving greater lift-to-drag ratio (L/D) or aerodynamic efficiency, aeronautical engineers and aircraft designers are devoting increased research to arrow wing configurations rather than delta wing configurations for use in supersonic transport aircraft (Ref. 1). The achievement of an increased lift to drag ratio is important since it would mean that a particular aircraft design would provide a greater range potential.

For example, an arrow wing with vertical fins mounted inboard of the wingtips has become a subject for recent investigations by NASA. After preliminary testing this design appears to be advantageous because of its increased L/D ratio. The addition of the fins not only helps to increase L/D, but they also contribute significantly to the directional stability of the aircraft. An example of an arrow wing model without fins is shown in Figure 1. A similar arrow wing-body model with a span of 40 inches has been tested in the Boeing Transonic Wind Tunnel and the NASA-Ames Unitary Wind Tunnel at Mach numbers from 0.40 to 2.50 (Ref. 2). In addition, tests at the Boeing facility have been conducted with a fin planform and relative size as illustrated in Figures 2 and 3 (Ref. 3). However, there has been no information published regarding the effects of the fin planform parameters (sweep, taper ratio, aspect ratio) on the subsonic cruise performance of an arrow wing. Thus, the purpose of the research described in this paper was to determine the effects of fin planform parameters on the subsonic cruise performance of an arrow wing configuration.

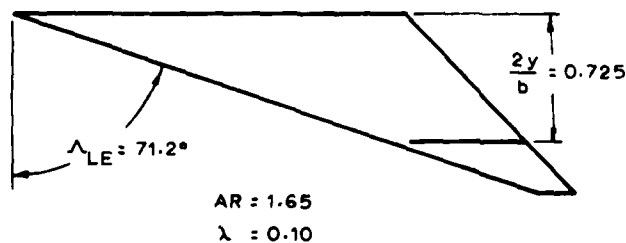


Figure 1. Basic Arrow Wing Planform and Fin Location

\*Lt. Col., USAF, Tenure Associate Professor of Aeronautics, DFAN

\*\*Professor of Aerospace Engineering, University of Kansas, Lawrence, Kansas

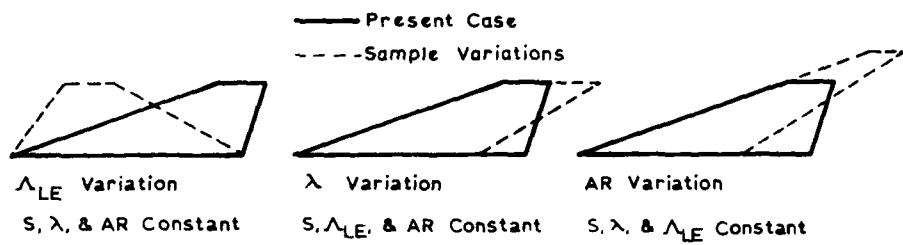


Figure 2. Basic Fin Planform with Parameter Variations

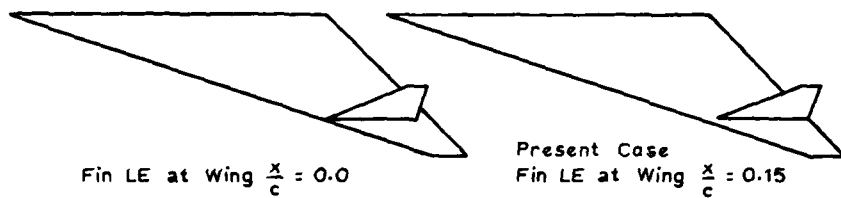


Figure 3. Fin Mounted with Leading Edges and Trailing Edges Aligned

### II. Scope of Investigation

The investigation was focused on determining the effects of changing leading edge sweep angle, wing taper ratio, and the aspect ratio of the fin planform, and determining the resulting aerodynamic performance for a given arrow-wing configuration. Each of these parameters were independently varied while the other two parameters and the fin planform area were held constant. In addition, the investigation was conducted with two different chordwise fin locations on the arrow wing. The fin was mounted at a spanwise location of  $y/(b/2) = 0.725$  for both cases where the expression  $b/2$  represents the semi-span of the wing. In the first fin position, the leading edge of the fin touched the leading edge of the wing, i.e.,  $x/c = 0.0$  where  $c$  represents the wing chord. In the second fin position, the fin was set back from the wing's leading edge at  $x/c = .15$ . The fin leading edge sweep was varied from 0 to 80 degrees, the taper ratio from 0.0266 to 1.0, and the aspect ratio from 0.734 to 8.0. For taper ratio and aspect ratio variations the smaller number represents the limit where the fin root chord is equal to the local wing chord. The basic arrow wing of Figure 1 was used for this investigation, while typical fin planform variations are shown in Figure 2. Figure 3 shows the two fin positions investigated. Figures 1, 2, and 3 also depict the baseline finned-wing configuration as the "present case."

### III. Method of Analysis

The entire analysis was performed using the Quasi-Vortex4.attice Method (QVLM) described in Ref. 4 and in the Appendix. The QVLM is a numerical method (panel method) based on linearized potential flow theory which assumes that a fluid (air) is frictionless and irrotational. Furthermore, the fluid disturbances created by a body are assumed to be small in comparison to the free stream velocity. In using the QVLM the

wing planform is first divided into chordwise and spanwise regions or panels. Then, horseshoe vortices are placed in each panel to model the aerodynamic effects of the wing on the flow field. The QVLM uses a spanwise constant vortex distribution on each panel. However, it differs from other vortex lattice methods (VLM) in the manner in which the chordwise vortex distributions are allowed to vary (Ref. 4 and Appendix). Since the method assumes a frictionless fluid flow about a body, only the effects on lift and pitching moment are examined to determine changes in aerodynamic efficiency.

#### IV. Computer Program Modification

The QVLM exists as a Fortran computer code on the Honeywell 66/60 at the University of Kansas. This code is a 2100-line program which handles straight tapered and double delta planforms with or without winglets and/or flaps. Camber coordinates may be input, and linear twist is allowed. For purposes of this investigation, the program was modified to allow for a vertical fin mounted inboard of the wingtip, and experimental data for a cambered and twisted arrow wing (Ref. 2 and 3) was used as a benchmark for program verification. Camber for the flexible wing is specified by

$$\frac{z}{c} = \underbrace{A \left(\frac{x}{c}\right)^3 + B \left(\frac{x}{c}\right)^2 + C \left(\frac{x}{c}\right)}_{\text{basic camber}} + D + \underbrace{\frac{57.3}{6} \left[1 - \sec \left\{ \frac{6}{57.3} \frac{x}{c} \right\} \right] \bar{y}}_{\text{aeroelastic camber}} \quad (1)$$

where  $\bar{y} = 2y/b$

$$A = 0.11 (1 - 2\bar{y}) + 0.03$$

$$B = -0.0825 (1 - 2\bar{y}) - G(\bar{y}) - 0.101$$

$$C = 0.0275 (1 - 2\bar{y}) + 0.0075 - A - B$$

$$D = -0.0075 (1 - 2\bar{y}) - 0.0075$$

$G(\bar{y})$  is the twist distribution in radians

For this investigation only the basic camber in Eqn. (1) was included since the wind tunnel models were made of rigid steel (Ref. 2).

Twist information was only available in graphic form as shown in Figure 4. A seventh order polynomial was fitted to the twist distribution with reasonable accuracy. It should be noted that the twist axis is located at  $x/c = 0.75$  of the wing. The resulting twisted and cambered planform is shown in Figure 5, where the curvature has been exaggerated by a factor of 8 for clarity.

Numerous computer runs were made with the modified program to verify this computer code against wind tunnel data. Cambered and twisted wings, as well as flat wings, were investigated. Both configurations were tested with the fin on and off. A study was also conducted to determine the minimum number of control points necessary for reasonable accuracy. Since computer processor time varies with the square of the total number of control points per halfspan, cost considerations dictated that the analysis be conducted with the

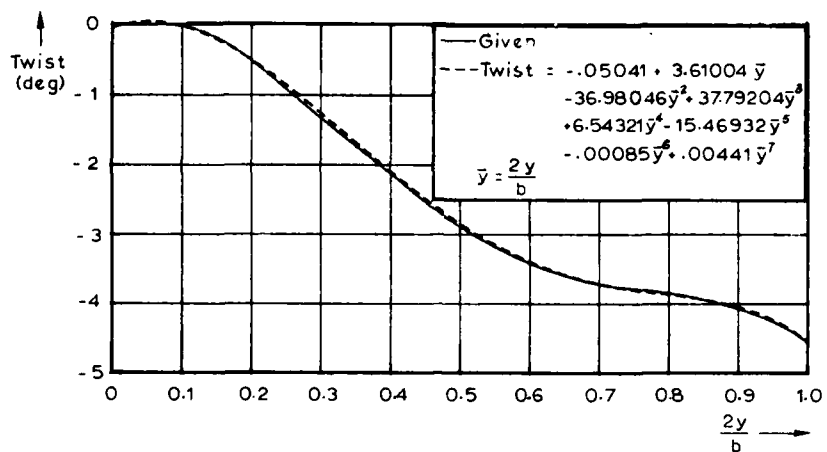


Figure 4. Span-Wise Twist Distribution of the Arrow Wing

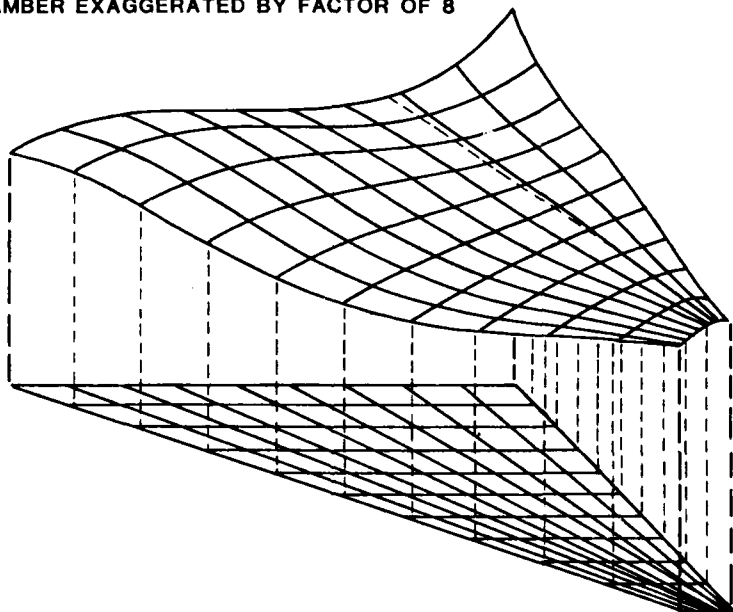
**CAMBER EXAGGERATED BY FACTOR OF 8**

Figure 5. Arrow Wing with Twist and Camber (curvature exaggerated by a factor of 8 for clarity)  
minimum number of points required for reasonable accuracy.

**V. Computer Program Verification**

Table 1 shows the seven control point distributions that were investigated. For the twisted, cambered wing with fin on, both distributions 1 and 4 were used to investigate the lift coefficient and the span loading. Figure 6 shows lift curve behavior, and Figure 7 shows span loading characteristics.  $C_N$ , the normal force coefficient, is compared to  $C_L$ , the lift coefficient, where the two forces reflect differences only because they are measured in reference frames which differ in orientation by the angle of attack,  $\alpha$ .  $C_N$  and  $C_L$  are similar for low values of  $\alpha$ . Figure 8 shows lift curve behavior for a flat wing with fin on as

Table 1  
CONTROL POINT DISTRIBUTIONS

Distribution	No. of Strips Inboard of Fin	No. of Strips Outboard of Fin	No. of Strips on Fin	No. of Vortices Per Strip	No. of Elements Per Halfspan
1	7	5	5	5	85
2	8	6	6	5	100
3	8	7	7	5	110
4	8	6	6	6	120
5	7	5	5	9	153
6	8	7	7	7	154
7	8	6	6	8	160

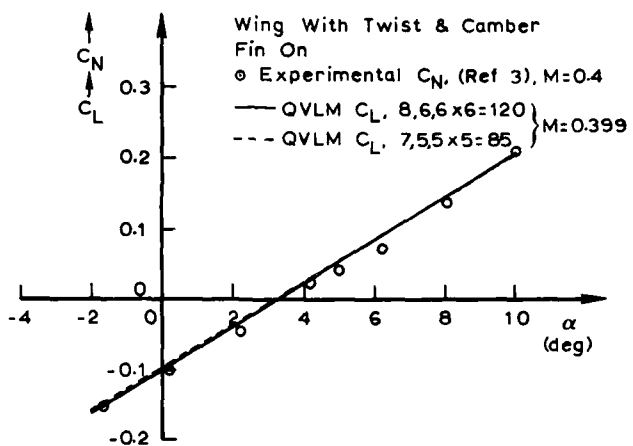


Figure 6. Lift Curve of the Twisted and Cambered Arrow Wing with Fin On at Low Mach Numbers

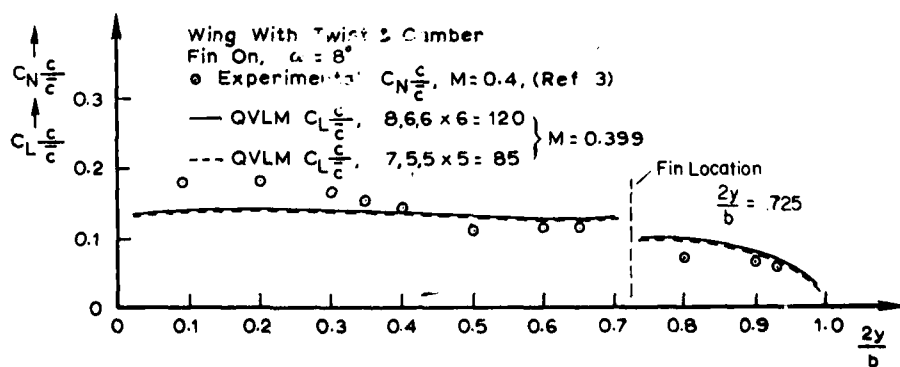


Figure 7. Span Loading of the Twisted and Cambered Arrow Wing with Fin On at Low Mach Numbers

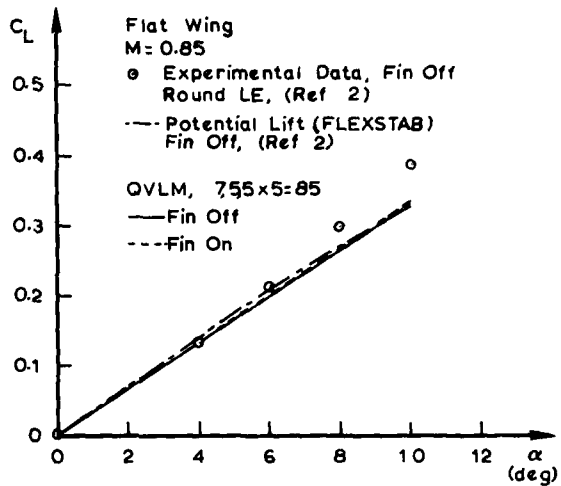


Figure 8. Lift Curve of the Flat Arrow Wing with Fin On and Off Versus a Potential Flow Model and Experimental Data at  $M = 0.85$

well as with fin off using distribution 1. These results show good agreement with results from another potential flow model (FLEXTAB) and experimental data (Ref. 2).

Because the OVLM utilizes a linear, attached flow algorithm, the fin parameter effects would be additive to either the flat or cambered and twisted wing. Thus, a flat wing model was used to investigate these fin effects. Computer runs were then made with distributions 1, 2, 3, 5, 6, and 7 identified in Table 1 using a flat wing with a fin at a Mach number of 0.85 and an angle of attack of 6 degrees. The results of spanwise sectional lift characteristics and bending moment characteristics are shown in Figures 9 and 10, and overall wing lift coefficients are tabulated in Table 2. Discontinuities in the curves of Figures 7, 9, and 10 occur at the wing semi-span location  $y/(b/2)$  due to the presence of the fin.

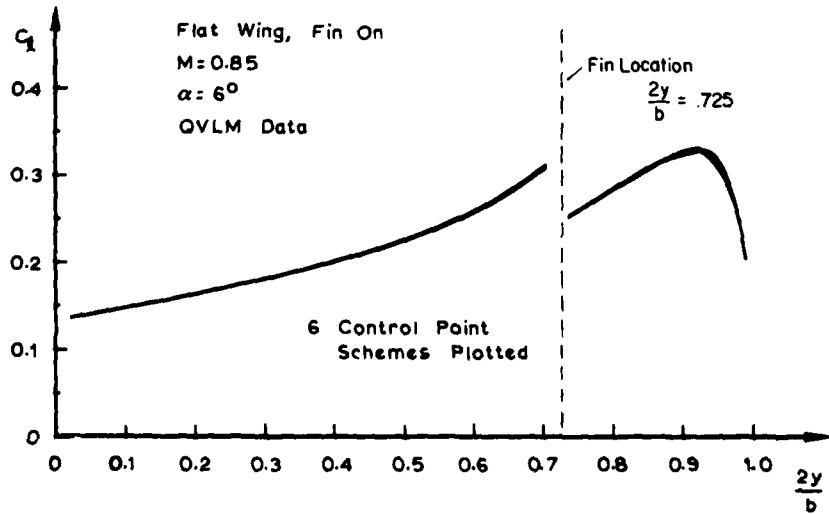


Figure 9. Span-wise Sectional Lift Coefficients for Six Control Point Distributions

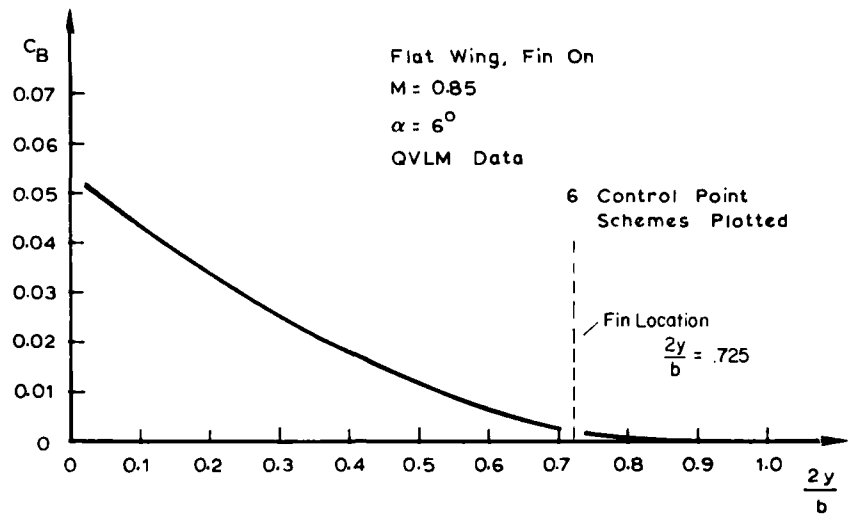


Figure 10. Spanwise Bending Moment Coefficients for Six Control Point Distributions

Table 2  
 COEFFICIENT CHARACTERISTICS FOR SIX CONTROL POINT DISTRIBUTIONS  
 AT  $M = 0.85$ ,  $\alpha = 6$  DEGREES, AND FIN ON

VALUES			
Distribution	$C_L$	$C_{D1}$	$C_B$
1 (7,5,5, x 5 = 85)	.19762	.00753	.053994
2 (8,6,6, x 5 = 100)	.19785	.00754	.054071
3 (8,7,7, x 5 = 110)	.19808	.00752	.054188
5 (7,5,5, x 9 = 153)	.19828	.00772	.054168
6 (8,7,7, x 7 = 154)	.19913	.07762	.054529
7 (8,6,6, x 8 = 160)	.19900	.00765	.054422
<b>Average</b>	<b>.19833</b>	<b>.00760</b>	<b>.054229</b>
VARIATIONS VERSUS AVERAGE VALUES			
Distribution	$\Delta C_L(\%)$	$\Delta C_{D1}(\%)$	$\Delta C_B(\%)$
1 (7,5,5, x 5 = 85)	-.36	-1.05	-.43
2 (8,6,6, x 5 = 100)	-.24	-.79	-.29
3 (8,7,7, x 5 = 110)	-.13	-1.05	-.08
5 (7,5,5, x 9 = 153)	-.03	1.58	-.11
6 (8,7,7, x 7 = 154)	.40	.26	.55
7 (8,6,6, x 8 = 160)	.34	.66	.36

From these results, distribution 1 was chosen for the fin effects investigation. Note that this represents a reduction in computer processor time by a factor of 1.67 when compared with the 110 element scheme, and a factor of 3.5 when compared with the 160 element scheme. (Typical processor time with 85 control points is 33 seconds on the Honeywell 66/60.)

#### VI. Numerical Results and Discussion of Fin Effects

The analysis was performed for a flat wing at an angle of attack of 8 degrees and a Mach number of 0.85 using distribution 1. This yielded a lift coefficient of 0.263. The baseline wing efficiency factor,  $\epsilon_b$ , and root bending moment coefficient,  $C_{B_b}$ , for a flat wing with fin off under these conditions was obtained as  $\epsilon_b = 0.9604$  and  $C_{B_b} = 0.0738$  respectively.

For the fin leading edge sweep investigation, eight cases were run with the fin leading edge at  $x/c = 0.15$  of the wing, and seven cases were run with the fin at  $x/c = 0.0$  of the wing. Results of this analysis are shown in Figure 11, where the "present case" data point reflects the configuration depicted earlier in Figures 1, 2, and 3. These results show that the addition of the fin increased the wing efficiency and decreased the wing root bending moment for all fin leading edge sweep angles between 0 and 80 degrees when the fin was mounted with its leading edge at  $x/c \approx 0.15$  of the wing. Mounting the fin at the wing leading edge degraded both wing efficiency and wing root bending moment. The present configuration with  $\Lambda_{LE} = 71.2$  degrees of the fin yields the lowest wing root bending moment. The increase in wing efficiency associated with the aft-fin configuration is most likely due to the increased leading edge suction on the fin from the strong sidewash produced by the tip vortices.

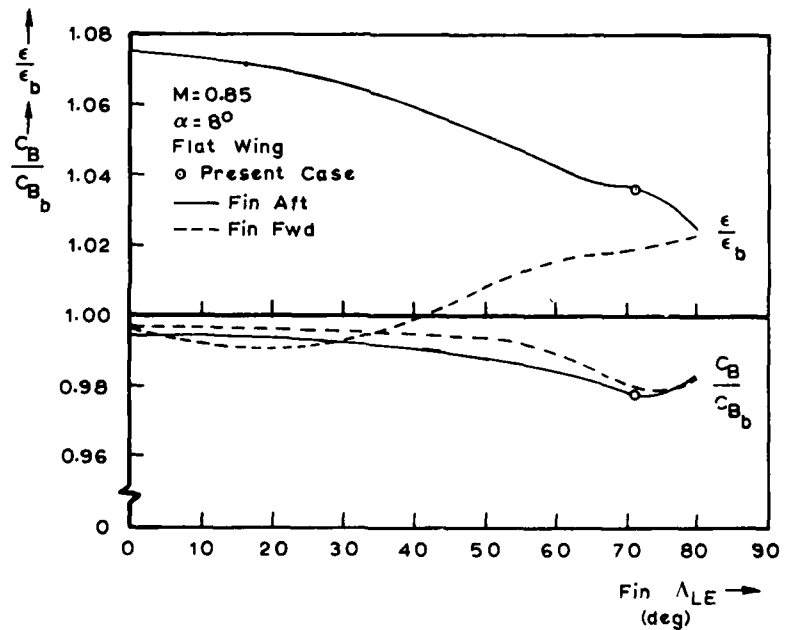


Figure 11. Effect of Fin Leading Edge Sweep Variation on Arrow Wing Efficiency and Root Bending Moment

The fin taper ratio investigation was performed using 11 cases at both the forward and aft fin positions. Results of this investigation appear in Figure 12. Of the three fin parameters investigated, the fin taper ratio had the least effect on both wing efficiency and wing root bending moment. Again, the aft fin position displayed both higher wing efficiencies and lower wing bending moments than the forward-mounted case.

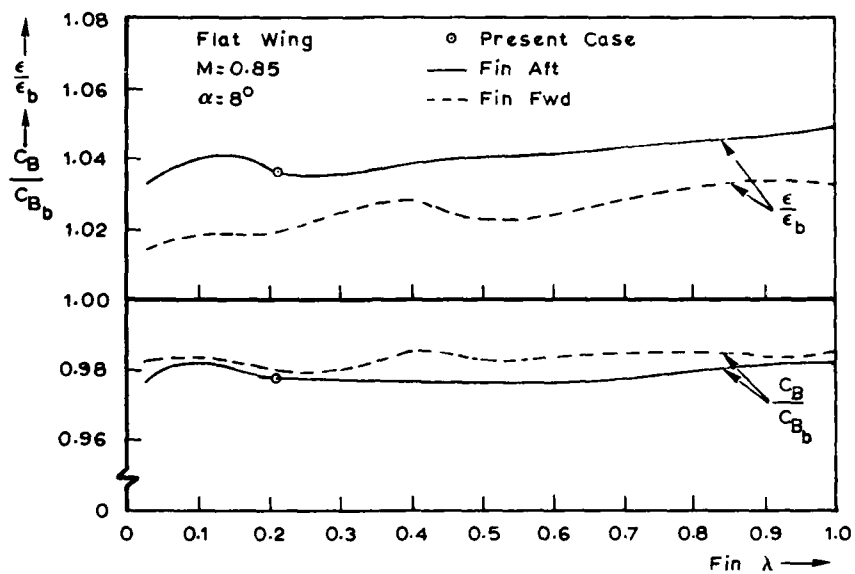


Figure 12. Effect of Fin Taper Ratio Variation on Arrow Wing Efficiency and Root Bending Moment

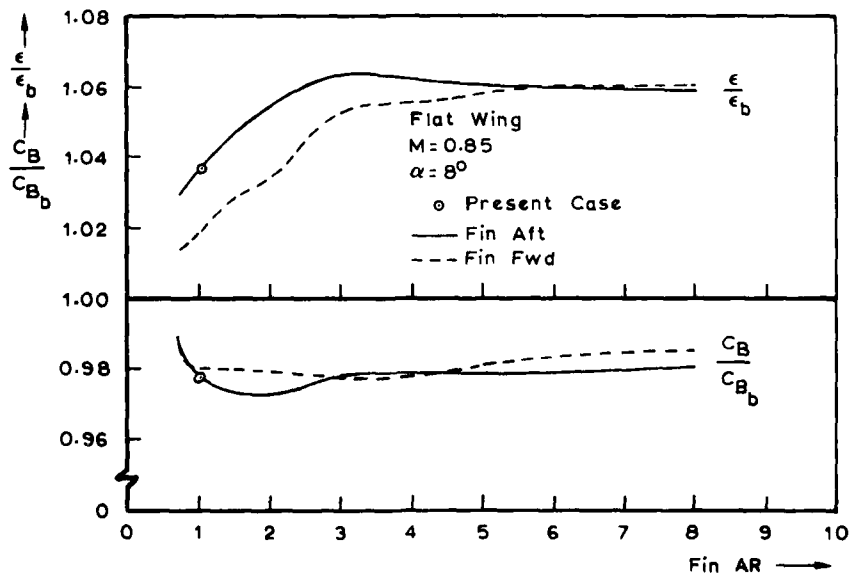


Figure 13. Effect of Aspect Ratio Variation on Arrow Wing Efficiency and Root Bending Moment

The slight nonlinearities at a fin taper ratio ( $\lambda$ ) of 0.12 for the aft-mounted case and  $\lambda = 0.4$  in Figure 12 for the forward-mounted case were first thought to be anomalies resulting from an interference pattern between the fin and vortex control points. Subsequent investigations involving different control point schemes confirmed their existence, and thus they remain unexplained.

Fin aspect ratio variations were investigated by examining 10 cases at both the forward and aft fin positions. Results of this investigation are depicted in Figure 13. Again, the aft-mounted fin exhibited higher wing efficiencies and lower wing bending moments. Of the three parameters investigated, variation of the fin aspect ratio in the range of  $0.73 \leq AR \leq 4.0$ , resulted in the greatest rate of increase in wing efficiency. For the case investigated, increasing the fin aspect ratio from 1.017 to 1.5 will result in an increase in wing efficiency and a decrease in wing bending moment.

#### VII. Conclusions

The effect of varying fin planform parameters on the subsonic cruise performance of an arrow wing was investigated using the QVLM. In general, mounting the fin aft at the 15-percent wing chord position is more advantageous than mounting it at the leading edge. In the aft position, the presence of the fin always improved wing efficiency and decreased the root bending moment of the wing as compared to an unfinned wing. The present configuration is nearly optimal for the cruise condition investigated. Within the constraints of the variations investigated, the present fin leading edge sweep of 71.2 degrees provides the lowest wing root bending moment, while fin taper ratio appears to have little effect on either wing efficiency or wing bending moment. Increasing the fin aspect ratio to 1.5 will increase the wing efficiency and decrease the wing root bending moment.

#### Symbols

AR	aspect ratio
$a_{ik}$	two-dimensional influence coefficient matrix
C	leading edge singularity parameter
c	local chord
$\bar{c}$	mean aerodynamic chord
$C_B$	spanwise bending moment, usually at the wing root
$C_{B_b}$	wing root bending moment, fin off
$c_l$	sectional lift coefficient
$C_L$	wing lift coefficient
$C_N$	normal force coefficient, two- or three-dimensional
$D_{ik}$	three-dimensional influence coefficient matrix
$\frac{\partial z_c}{\partial x}$	camber slope

M Mach number  
N number of vortices, control points, or vortex strips  
S wing planform area (reference area) or leading edge suction force  
w upwash, normalized with respect to free-stream velocity  
x chordwise coordinate of a control point, normalized with respect to local chord  
x/c chordwise coordinate, normalized with respect to local chord  
z/c vertical coordinate, normalized with respect to local chord  
2y/b spanwise coordinate, normalized with respect to wing semi-span  
α angle of attack  
ε wing efficiency factor, fin on  
ε<sub>b</sub> wing efficiency factor, fin off  
γ vortex density, normalized with respect to free stream velocity  
Λ<sub>LE</sub> leading edge sweep angle  
λ taper ratio  
θ polar coordinate of a control point  
θ' polar coordinate of a vortex element  
ξ chordwise coordinate of a vortex element, normalized with respect to local chord

References

1. Wright, B. R., F. Bruckman, and N. A. Radovich. "Arrow Wings for Supersonic Cruise Aircraft." Journal of Aircraft, Vol. 15, No. 12, December 1978, pp. 829-836.
2. Bobbitt, P. J. and M. E. Manro. "Theoretical and Experimental Pressure Distributions for a 71.2 Degree Swept Arrow-Wing Configuration at Subsonic, Transonic, and Supersonic Speeds." Paper presented at the NASA Supersonic Cruise Aircraft Research (SCAR) Conference, November 9-12, 1976. NASA CP-001, 1977, pp. 35-122.
3. Boeing Commercial Airplane Company. Unpublished experimental data from the Boeing Transonic Wind Tunnel Facility, October 1978.
4. Lan, C. E. "A Quasi-Vortex-Lattice Method in Thin Wing Theory." Journal of Aircraft, Vol. 11, No. 9, September 1974, pp. 518-527.
5. Lan, C. E. "Some Applications of the Quasi-Vortex-Lattice Method in Steady and Unsteady Aerodynamics." NASA SP-405, Paper No. 21, May 1976.
6. Bisplinghoff, R. L., H. Ashley, and R. L. Halfman. Aeroelasticity. Reading, PA: Addison Wesley Publishing Co., Inc., November 1957.

## Appendix

## The Quasi-Vortex-Lattice Method (QVLM)

To understand what a vortex-lattice method is, let us examine some fundamental concepts of thin airfoil theory (linearized potential flow). This theory postulates that the camber line of a lifting surface (two-dimensional flow) is replaced with a vortex distribution represented by  $\bar{Y}(\xi)$ , which models the effect of the airfoil on the flow field. In order to determine the unknown vortex distribution,  $\bar{Y}(\xi)$ , it is necessary to apply a boundary condition, i.e., the surface boundary condition which specifies that the velocity normal to the surface is zero at the camber line. A further approximation places the vortex distribution on the chordline. The surface boundary condition from which we determine the unknown  $\bar{Y}(\xi)$  (which requires the velocity normal to the camber line to be zero) is usually given as

$$\frac{\partial z_c}{\partial x} = \alpha - w \quad (A1)$$

where  $\frac{\partial z_c}{\partial x}$  = slope of the camber line

$\alpha$  = free stream angle of attack

$w$  = downwash

The downwash then can be represented as

$$w(x) = \frac{1}{2\pi} \int_0^1 \frac{\bar{Y}(\xi) d\xi}{x - \xi} \quad (A2)$$

where  $\bar{Y}(\xi)$  = vortex density  $Y$  at a chordwise element location,  $\xi$ , and normalized as  $\bar{Y} = Y/V_\infty$ ,

$\xi$  = chordwise location of the vortex element, and

$x$  = chordwise location of the point of observation (control location) to satisfy the surface boundary condition,

and the equation requiring solution is a singular integral equation given as

$$\frac{1}{2\pi} \int_0^1 \frac{\bar{Y}(\xi) d\xi}{x - \xi} = \alpha - \frac{\partial z_c}{\partial x} \quad (A3)$$

This equation is singular in the integrand because the denominator goes to zero when  $x = \xi$ , and thus the integral is undefined (Cauchy singularity). The unknown is  $\bar{Y}(\xi)$  where the bar notation has been dropped. Solutions of Eqn. (A3) can be obtained numerically by both QVLM and VLM. However, the inversion of Eqn. (A3) for  $\bar{Y}(x)$  may be obtained analytically by applying Cartemann's formula or Söhngen's inversion formula (Ref. 6) which results in

$$Y(x) = -\frac{2}{\pi} \sqrt{\frac{1-x}{x}} \int_0^1 \left[ \alpha - \frac{\partial z_c}{\partial x}(\xi) \right] \sqrt{\frac{\xi}{1-\xi}} \frac{d\xi}{x-\xi} + \frac{c}{\sqrt{x(1-x)}} \quad (A4)$$

Application of the Kutta condition at the trailing edge requires that the constant of integration be zero, or

$$\gamma(1) = 0 \rightarrow C = 0 \quad (A5)$$

However, the remaining terms indicate that the Cauchy singularity as well as square root singularities at the leading edge ( $x = 0$ ) and the trailing edge ( $x = 1$ ) are still present in the solution of  $\gamma(x)$ . Also, evaluation of the integral for general camber lines ( $\partial z_c / \partial x$  in the integrand) is usually difficult (see Eqn. (1) for the camber expression and Figure 5 to further appreciate the complexity of the present investigation). Therefore, numerical paneling methods are usually employed to solve Eqn. (A3) because of the difficulty involved in analytically integrating Eqn. (A4) for complex shapes.

Early VLMs addressed overall aerodynamic characteristics of the airfoil such as  $c_L$  and  $c_m$  but could not predict chordwise pressure distributions accurately. Also, the square root singularity at the leading edge (See Eqn. A4) precluded leading edge suction effects from being accurately determined. The QVLM, on the other hand, eliminates both the leading- and trailing-edge singularities as well as the Cauchy singularity. This method is briefly outlined here, showing how these singularities are eliminated. This removes the need to correct the results for regions where our solutions are undefined and therefore the modeled flow field corresponds more closely to the real flow field about a body.

Using the transformations

$$x = \frac{1}{2} (1 - \cos\theta) \quad (A6)$$

and

$$\xi = \frac{1}{2} (1 - \cos\theta') \quad (A7)$$

Eqn. (A2) becomes

$$w(\theta) = -\frac{1}{2\pi} \int_0^\pi \frac{\gamma(\theta') \sin\theta' d\theta'}{\cos\theta - \cos\theta'} \quad (A8)$$

which may be expanded into two integrals by adding and subtracting the integral of  $\gamma(\theta) \sin\theta / 2\pi (\cos\theta - \cos\theta')$  or:

$$w(\theta) = -\frac{1}{2\pi} \int_0^\pi \frac{\gamma(\theta') \sin\theta' - \gamma(\theta) \sin\theta}{\cos\theta - \cos\theta'} d\theta' - \frac{\gamma(\theta) \sin\theta}{2\pi} \int_0^\pi \frac{d\theta'}{\cos\theta - \cos\theta'} \quad (A9)$$

The second integral in Eqn. (A5) is zero by Glauert's formula, and the equation therefore becomes simply

$$w(\theta) = -\frac{1}{2\pi} \int_0^\pi \frac{\gamma(\theta') \sin\theta' - \gamma(\theta) \sin\theta}{\cos\theta - \cos\theta'} d\theta' \quad (A10)$$

Significantly, this downwash integral has neither the Cauchy singularity in the case where  $\theta = \theta'$ , nor the square root singularities at the leading or trailing edge. The latter singularities are resolved by the presence of  $\sin\theta$ . Hence, the integrand is finite everywhere on the interval  $0 \leq \theta \leq \pi$ , and the integral may therefore be represented as a finite sum using the midpoint trapezoidal rule. Letting

$$g(\theta) = \gamma(\theta) \sin\theta \quad (A11)$$

the midpoint trapezoidal rule allows the following formulation of the integral expression:

$$\begin{aligned} w(\theta) &= -\frac{1}{2\pi} \int_0^\pi \frac{g(\theta') - g(\theta)}{\cos\theta - \cos\theta'} d\theta' \\ &\approx -\frac{1}{2\pi} \left(\frac{\pi}{N}\right) \sum_{k=1}^N \left[ \frac{g\left((2k-1)\frac{\pi}{2N}\right)}{\cos\theta - \cos\left((2k-1)\frac{\pi}{2N}\right)} - \frac{g(\theta)}{\cos\theta - \cos\left((2k-1)\frac{\pi}{2N}\right)} \right] \end{aligned} \quad (A12)$$

Noting that the  $g(\theta)$  in the numerator of the second term of Eqn. (A12) is constant with respect to the summation, the theory of Chebychev polynomials is applied to fix control point locations (i.e.,  $\theta$  values) such that the second term vanishes. The result is summarized by

$$w(x_i) = \frac{1}{2N} \sum_{k=1}^N \frac{\gamma_k x_k^{\frac{1}{2}} (1 - x_k)^{\frac{1}{2}}}{x_i - x_k} + \begin{cases} NC, & i = 0 \\ 0, & i \neq 0 \end{cases} \quad (A13)$$

where

$x_k$  = vortex locations

$$= \frac{1}{2} \left[ 1 - \cos \left\{ \frac{(2k-1)\pi}{2N} \right\} \right], \quad k = 1, 2, \dots, N \quad (A14)$$

$x_i$  = control point locations

$$= \frac{1}{2} \left[ 1 - \cos \left\{ \frac{i\pi}{N} \right\} \right], \quad i = 0, 1, 2, \dots, N \quad (A15)$$

and  $C$  is the leading edge singularity parameter defined as

$$C = \lim_{x \rightarrow 0} \gamma(x) x^{\frac{1}{2}} \quad (A16)$$

This semicircle system of vortex and control points (points where the surface boundary condition is satisfied) is depicted in Figure A1 for the case where  $N = 4$ . When put into matrix form, the system of equations may be solved as

$$\{w_i\}_{Nx1} = [a_{ik}]_{NxN} \{Y_k\}_{Nx1} \quad (A17)$$

where

$$w_i = a_i - \frac{\partial z_c}{\partial x} \Big|_i \quad (A18)$$

and

$$a_{ik} = \frac{1}{2N} \frac{x_k^{1/2} (1 - x_k)^{1/2}}{x_i - x_k} \quad (A19)$$

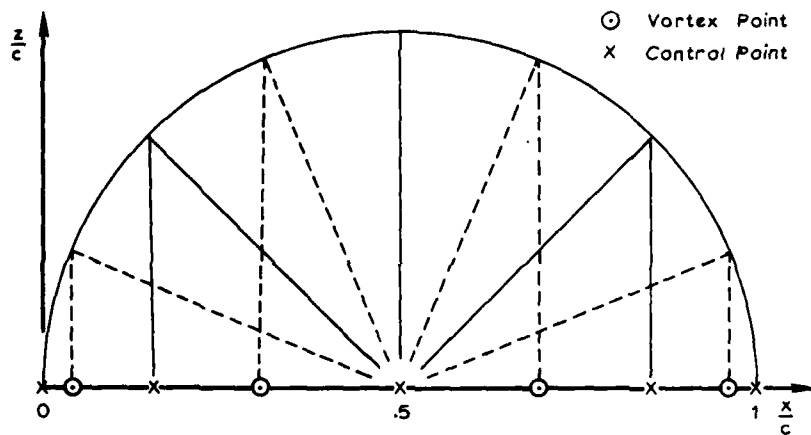


Figure A1. An Example of Vortex and Control Point Locations  
When  $N = 4$

The unknown  $Y_k$ 's can then readily be determined by solving Eqn. (A17). Once they have been determined, the leading edge singularity parameter becomes

$$C = \frac{w(x_0)}{N} + \frac{1}{2N^2} \sum_{k=1}^N Y_k \left[ \frac{1 - x_k}{x_k} \right]^{1/2} \quad (A20)$$

and the leading edge suction force may then be obtained as

$$S = \pi \rho \frac{C^2}{4} \quad (A21)$$

The simplicity of this method belies its elegance. Unlike early conventional vortex lattice methods based on the three-quarter chord theorem, this method (with a continuous loading scheme) yields a chordwise pressure distribution and leading edge suction term in accordance with linear aerodynamic theory.

The two-dimensional flow model is readily extended to a three-dimensional flow model with the assumption that the vortex distribution is stepwise continuous in the spanwise direction only. For the present problem of a wing with a fin, the semicircle method was applied to two sections of the wing and also over the fin in order to divide the planform into vortex strips as shown in Figure A2. Here, the vortex density  $\gamma_k$  at a finite number of points on the planform is determined from the wing tangency condition:

$$\left\{ w(x_i, y_i) \right\}_{N \times 1} = [D_{ik}]_{N \times N} \left\{ \gamma_k \right\}_{N \times 1} \quad (A22)$$

where  $D_{ik}$  equals the downwash influence coefficient matrix, and where  $N$  is the total number of control points distributed over a half-span planform (from Eqn. (A19)). After the inversion of Eqn. (A22) to determine the  $\gamma_k$ 's, sectional coefficients are obtained by assuming that the vortex distribution lies along the camber line. These are then integrated over the wing span to obtain total lift and moment coefficients, as well as leading edge thrust coefficients and induced drag coefficients.

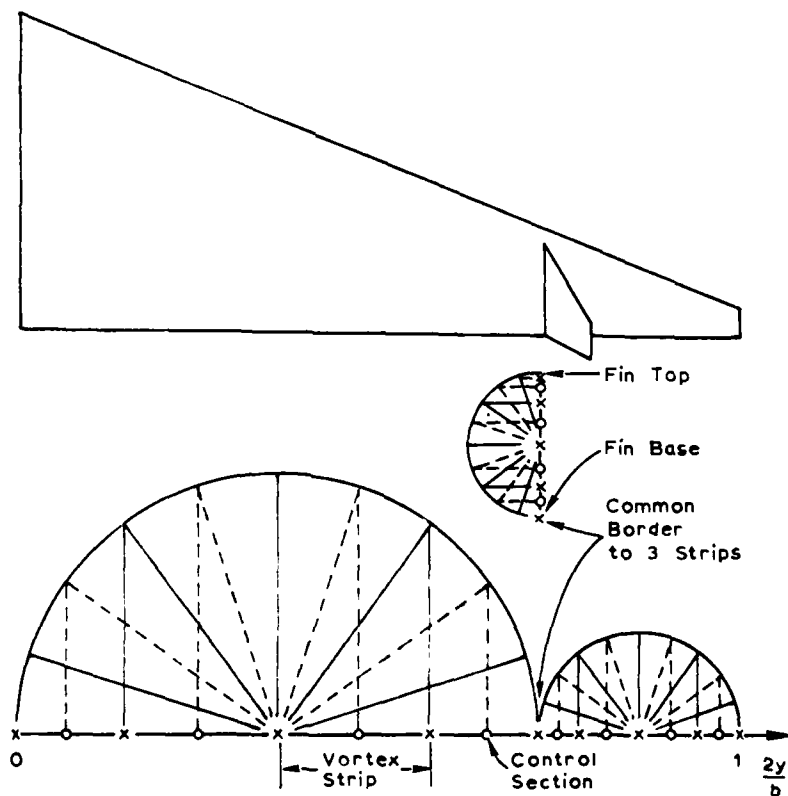


Figure A2. Span-Wise Vortex Strip and Control Point Locations for Arrow Wing with Fin

This method has been used with notable success (Ref. 5). For the present investigation, an existing computer program was modified to allow a vertical fin to be mounted inboard of the wingtip and to incorporate the camber and twist of the arrow wing. The method was extended to compressible flow by applying the Prandtl-Glauert compressibility correction.

**SECTION II**

**Propulsion**

AN IMPROVED METHOD FOR CALCULATION OF STATIC THRUST  
FOR THE USAFA J-85/13 TURBOJET ENGINE

M.K. Reagan\*, P.D. Thornley\*\*, and A.M. Higgins\*\*\*

Abstract

This paper investigates the reasons why there has been a 25-percent difference between the calculated and measured thrusts obtained when testing the General Electric J-85/13 turbojet engine installed in the propulsion test cell at the United States Air Force Academy. Previously, the loss of compressor bleed air was neglected in the theoretical thrust calculation. In the present analysis the mass flow out of the engine exhaust nozzle was measured which allowed the flow of air through the compressor bleed valves to be determined. Using this new method, resultant calculated thrust values are now within  $\pm 2$  percent of actual measured values for engine speeds up to 95 percent of the engine's maximum RPM. At 100 percent engine RPM, the difference between calculated and measured thrust increases to nine percent. Further study is recommended to more accurately determine the total and static pressures and gas properties at the exit nozzle of the J-85/13 engine at 100 percent RPM to reduce the differential between calculated and measured thrust.

I. Introduction

The General Electric J-85 turbojet engine is the primary powerplant for the Northrop T-38 trainer and F-5 fighter aircraft in the United States Air Force inventory. A particular model of this engine, the J-85/13, is installed in the propulsion test cell at the United States Air Force Academy and is used as an instructional aid for students studying aircraft propulsion. The primary use of the engine is to help a beginning student understand the basic principles of propulsion. To accomplish this, the student observes the engine during operation, records various engine temperatures and pressures, and then uses the measured values to predict such engine performance data as thrust and air mass flows. Until recently the difference between the student's theoretically predicted value of thrust and the value of measured thrust has been on the order of 20 to 25 percent. This magnitude of error was considered unacceptable and, in fact, often led the students to question either the instrumentation in the test cell or the validity of the basic equations used to calculate the engine's thrust. We therefore set out to determine the reasons for this wide difference between theoretical or predicted thrust of the J-85 engine and the thrust value actually measured. Our approach not only was to examine the various data readings for accuracy (e.g., measured thrust), but also to question the various assumptions used in deriving the equation used to calculate engine thrust. Previously, we had assumed that the air mass flow entering the compressor face added to the fuel mass flow equalled the gas mass flow through the engine exit, i.e., we assumed that the mass flow through the compressor bleed valves ( $\dot{m}_{CBV}$ ) and air leakage ( $\dot{m}_{LOSSES}$ ) were minimal and could be neglected. Upon closer analysis of the actual engine performance, however, we discovered that these assumptions were erroneous. Indeed, in order to properly analyze the engine, these mass flows had to be accounted for. Therefore, we redeveloped the equation for calculating engine thrust and took these leakages of air into account.

---

\*2nd Lieutenant, USAF, Research Assistant, DFAN

\*\*Captain, USAF, Assistant Professor of Aeronautics, DFAN

\*\*\*Major, USAF, Associate Professor of Aeronautics, DFAN

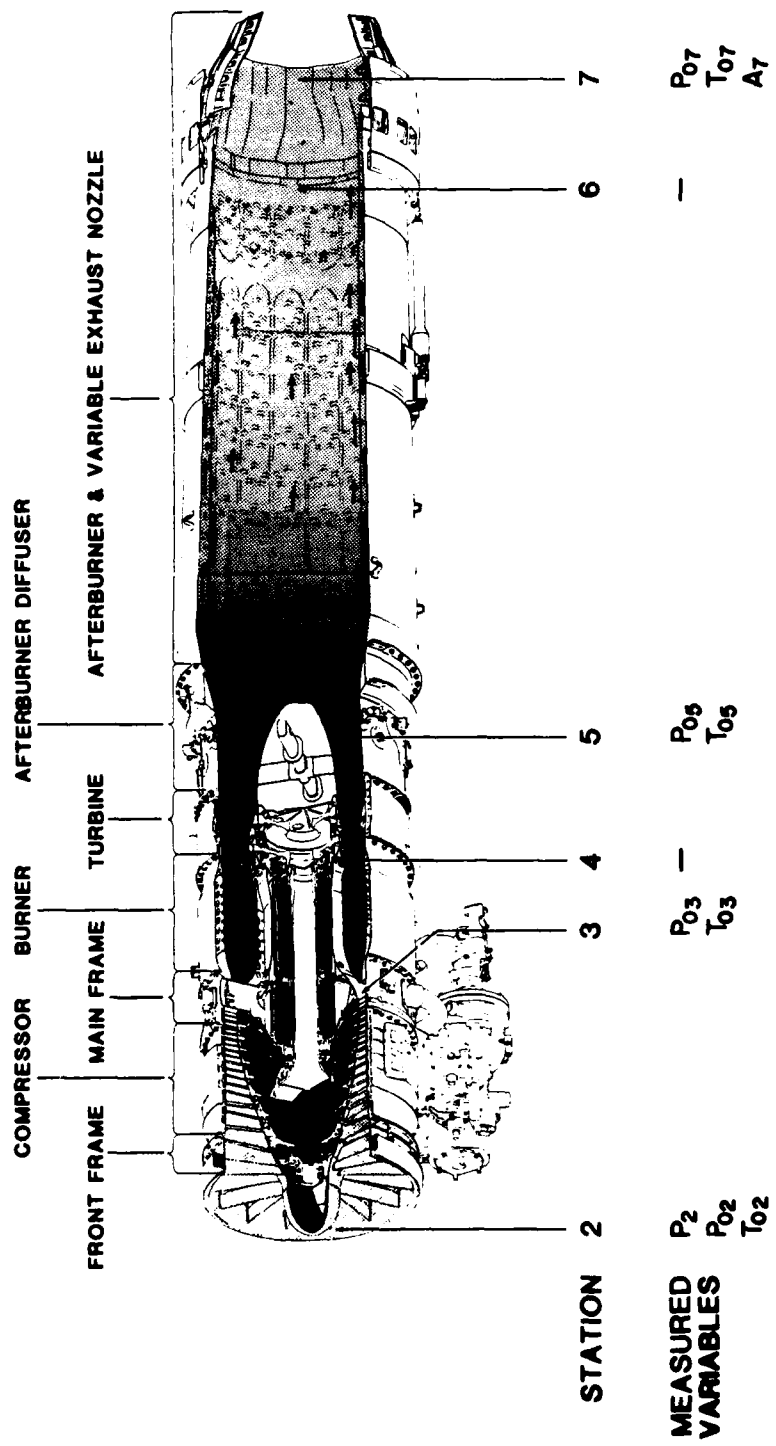


Figure 1. J-84 Engine Schematic and Station Location

### II. Test Apparatus

The General Electric J-85 afterburning engine is a compact, single-crystal, transonic, afterburning engine. It incorporates an eight-stage, high-lift, axial flow compressor coupled directly to a two-stage annular-type combustion system, variable inlet guide vanes, and compressor inlet flow control valves. The engine consists of the following sections: front frame, compressor, main frame, combustor, turbine, diffuser, afterburner, variable exhaust nozzle, and engine accessories (Figure 1). In addition to the engine itself, two more parts deserve description. A bell-mouth nozzle is connected to the front frame of the engine. The purpose of the nozzle is to provide a steady, one-dimensional flow of air into the compressor. Attached to the nozzle is a protective mesh screen which prevents foreign objects from being ingested into the engine and causing serious structural damage. A photograph of the engine front frame with bell-mouth nozzle and screen attached is shown in Figure 2.

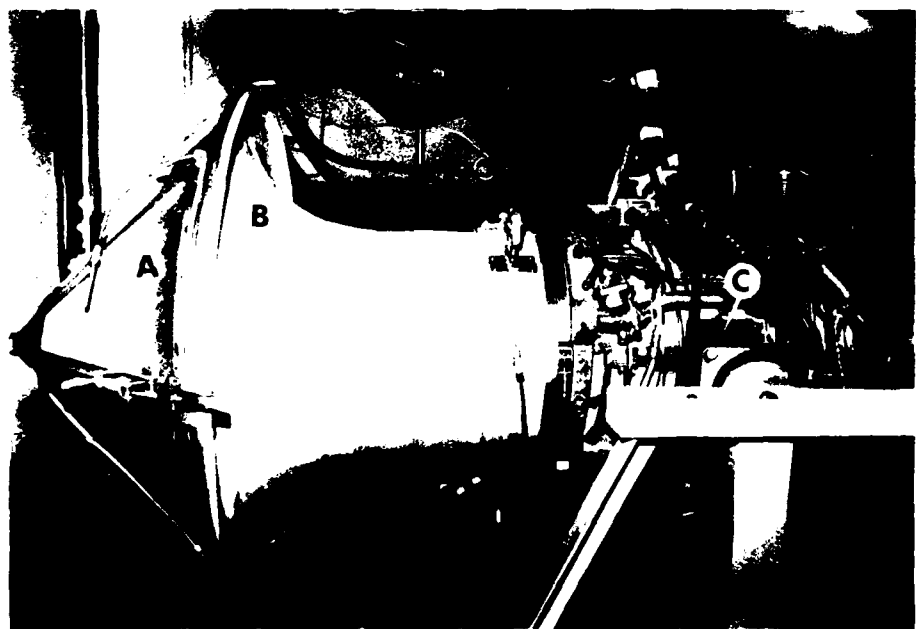


Figure 2. Engine Inlet Showing Screen (A), Bell-Mouth Inlet (B), and Compressor Bleed Dams (C).

The test cell is equipped to measure various engine performance parameters. The parameters are listed in Table 1. Notice that the turbine inlet temperature,  $T_{05}$ , is not measured. This is due to the high temperatures encountered at the burner exit which cause frequent turn-off of the thermocouple protection and the uncertainty of measuring an average gas temperature without using a large number of thermocouples.

### III. Development of Turbojet Thrust Equation

To derive the thrust of a jet engine, we begin with the basic equation for idealized thrust, the thrust derived from the momentum equation (Ref. 2):

$$F = \dot{m}_7 U_7 - \dot{m}_0 U_0 + (P_7 - P_0) A_7 \quad (1)$$

Here  $F$  is the engine thrust,  $\dot{m}_7 U_7$  is the momentum flux out of the engine,  $\dot{m}_0 U_0$  is the momentum flux into the engine,  $P_7$  is the static pressure at the engine exit (nozzle),  $P_0$  is the atmospheric pressure, and  $A_7$  is the nozzle area. Assuming that the static pressure at the exit equals the atmospheric pressure (i.e.,  $P_0 = P_7$ ) so that the flow is perfectly expanded and maximum thrust is realized, we obtain a simpler form of Eqn. (1):

$$F = \dot{m}_7 U_7 - \dot{m}_0 U_0 \quad (2)$$

Expanding the  $U_0$  terms into the product of Mach number and speed of sound so that  $U_0 = M_0 a_0$ , we may write:

$$F = \dot{m}_7 U_7 - \dot{m}_0 M_0 a_0 \quad (3)$$

Table 1  
TEST CELL MEASUREMENTS

PARAMETER	SYMBOL	DIMENSIONS
Engine thrust	$F$	lbf
Fuel flow	$\dot{m}_f$	lbm/hr
Atmospheric pressure	$P_{atm}$	in Hg
Static pressure drop across screen mesh	$\Delta P$	in H <sub>2</sub> O
Total pressure drop across mesh screen	$\Delta P_0$	in H <sub>2</sub> O
Total pressure at compressor exit (gauge)	$P_{03}$	psig
Total pressure at turbine exit (gauge)	$P_{04}$	psig
Total pressure at nozzle exit (gauge)	$P_{07}$	in Hg
Total temperature at compressor face	$T_{02}$	°F
Total temperature at compressor exit	$T_{03}$	°F
Total temperature at turbine exit	$T_{05}$	°F
Total temperature at nozzle exit	$T_{07}$	°F
Percent of maximum engine RPM	% RPM	%
Actual engine RPM	RPM	revolutions per minute

Because we are working with a static engine, the Mach number of the air ahead of the engine inlet is approximately zero and the thrust equation can then be reduced to the following expression:

$$F = \dot{m}_7 U_7 \quad (4)$$

Usually the mass flow rate out of the engine exhaust nozzle,  $\dot{m}_7$ , and the exhaust velocity,  $U_7$ , are not measured quantities in aircraft operations, so Eqn. (4) is manipulated by substituting other measured variables for  $\dot{m}_7$  and  $U_7$ . Gates has done this (Ref. 2) and Eqn. (5) results.

$$F = \sqrt{\frac{2 \gamma_c R}{\gamma_c - 1}} (\dot{m}_2 + \dot{m}_f - \dot{m}_{CBV} - \dot{m}_{LOSSES}) \left\{ \frac{C_{p_t}}{C_{p_c}} T_{o_4} \tau_\lambda T_t \left[ 1 - \left( \frac{P_{o_7}}{P_7} \right) \frac{1 - \gamma_t}{\gamma_t} \right] \right\}^{1/2} \quad (5)$$

This is the form of the engine thrust equation that students in the autopropulsion courses at the USAF Academy usually use and it permits them to immediately determine the effects of changing various engine parameters or environmental conditions. For example, increasing the engine throttle setting increases the temperature at the engine's combustor exit,  $T_{o_4}$ , and therefore  $\tau_\lambda$  ( $\tau_\lambda = T_{o_4}/T_0$ ), which directly increases the thrust of the engine. We have chosen to simplify Eqn. (5) slightly by canceling like terms and obtained Eqn. (6). We did this because we wanted to eliminate  $T_{o_4}$  which was not possible for us to measure.

$$F = \sqrt{\frac{2 \gamma_c R}{\gamma_c - 1}} (\dot{m}_2 + \dot{m}_f - \dot{m}_{CBV} - \dot{m}_{LOSSES}) \left\{ \frac{C_{p_t}}{C_{p_c}} T_{o_5} \left[ 1 - \left( \frac{P_{o_7}}{P_7} \right) \frac{1 - \gamma_t}{\gamma_t} \right] \right\}^{1/2} \quad (6)$$

In previous years we assumed that the air mass flow rate out of the compressor bleed valve doors,  $\dot{m}_{CBV}$ , as well as the air loss rate from the engine through leakage,  $\dot{m}_{LOSSES}$ , were negligible and the  $\dot{m}_7$  term could be expressed simply as:

$$\dot{m}_7 = \dot{m}_2 + \dot{m}_f \quad (7)$$

However, this assumption neglects the effect of compressor bleed air on thrust which is not negligible. In fact, when the bleed valve doors are open, as much as 25 percent of the entrance mass flow can be bled from the engine. This loss will significantly affect the total engine thrust.

During the engine test runs we observed the compressor bleed valves and concluded that they were fully closed at 100 percent RPM. If we assume that  $\dot{m}_{LOSSES}$  are negligible at 100 percent RPM, then Eqn. (7) can, in fact, be used to accurately determine the air mass flow at the exit. However, Eqn. (7) is only valid at RPM's where the compressor bleed valves are fully closed, and losses are neglected. At all other operating conditions we must use the following equation to calculate the air mass flow at the engine exit:

$$\dot{m}_7 = \dot{m}_2 + \dot{m}_f - \dot{m}_{CBV} - \dot{m}_{LOSSES}$$

We see from Eqn. (8) that in order to calculate engine thrust, we must measure  $\dot{m}_{CBY}$ ,  $\dot{m}_f$ , and  $\dot{m}_2$  and assume a value for  $\dot{m}_{LOSSES}$ . The alternative is to measure  $\dot{m}$ , directly. We chose the latter method because the test cell is presently equipped to measure total temperature and pressure at the nozzle exit and it is not equipped to measure  $\dot{m}_{CBY}$ . A brief discussion of how the exit mass flow and velocity was calculated is presented here primarily as a review for the student.

#### IV. Procedure for Calculating Gas Mass Flow Rate and Velocity at Nozzle Exit

The test cell is equipped to measure total temperature and total pressure at the engine nozzle exit. With the assumption that the static pressure equals atmospheric pressure at this point, we may solve for the mass flow and velocity directly. Recall that the gas mass flow rate is the product of air density,  $\rho_7$ , velocity,  $U_7$ , and the nozzle area,  $A_7$ , or:

$$\dot{m}_7 = \rho_7 A_7 U_7 \quad (9)$$

At this point in the analysis, let us assume we know the area of the nozzle exit at any engine RPM. The static temperature of the gas at the nozzle exit,  $T_7$ , can be found using:

$$\frac{T_{07}}{T_7} = \frac{P_{07}}{P_7} \frac{\gamma_t - 1}{\gamma_t} \quad (10)$$

where  $T_{07}$  and  $P_{07}$  are the total temperature and total pressure of the gas at the exit and  $P_7$  is the static pressure at the exit. We assumed  $\gamma_t$  to be equal to 1.35. Remember that we have measured  $T_{07}$  and  $P_{07}$ , and assumed  $P_7$  to be equal to atmospheric pressure. After finding  $T_7$ , we can solve for the density of the exhaust gas directly by assuming it is a perfect gas. Thus,

$$\rho_7 = \frac{P_7}{R_7 T_7} \quad (11)$$

We therefore have  $P_7$  and  $A_7$ , and we need only  $U_7$  to calculate the mass flow rate from Eqn. (9). We can find the nozzle exit velocity,  $U_7$ , since we can determine the speed of sound at the exit from Eqn. (12),

$$a_7 = \sqrt{\gamma_t R_7 T_7} \quad (12)$$

The Mach number of the air flow at the nozzle exit is calculated using:

$$\left( \frac{P_{07}}{P_7} \right) \frac{(\gamma_t - 1)}{\gamma_t} = 1 + \frac{\gamma_t - 1}{2} M_7^2 \quad (13)$$

Then with the Mach number and speed of sound known at this exit, the velocity can be calculated directly from Eqn. (14):

$$U_7 = M_7 a_7$$

(14)

Therefore, if we measure the total temperature and pressure at the engine nozzle exit and we assume that the static pressure at the exit equals atmospheric pressure, the gas mass flow, velocity, and finally thrust of the engine can be calculated if we can determine the nozzle exit area,  $A_7$ .

In a similar manner, we can calculate the mass flow and velocity at the compressor face. To do this we use pressure probes installed directly in front of the engine compressor to measure total and static air pressures. At the point where these measurements are made, the cross-sectional area of the J-85 duct is 1.396 square feet. We also assume that the inlet is adiabatic so that the total temperature of the air remains constant through the inlet.

#### V. Determination of Parameters in the Thrust Equation

The values of each of the parameters in the thrust equation, Eqn. (6), were determined as follows:

##### A. Gas Properties Upstream of the Engine's Combustor: $C_{p_c}$ , $\gamma_c$

Both the specific heat at constant pressure,  $C_{p_c}$ , and the ratio of specific heats,  $\gamma_c$ , are gas properties and are assumed to be constant in this analysis. The gas upstream of the combustor is air. We use  $C_{p_c}$  in the calculation of the gas constant,  $R_7$ , and  $\gamma_c$  in the isentropic equations relating temperature and pressure. We assume the following values for these gas properties:  $C_{p_c} = .240 \text{ BTU/lbm } ^\circ\text{R}$  and  $\gamma_c = 1.40$ .

##### B. Gas Properties Downstream of the Engine's Combustor: $C_{p_t}$ , $\gamma_t$

The gas in this case is a combusted product of air and JP-4 fuel. No work has been done to determine the exact values of these variables. In this analysis we assumed  $C_{p_t} = 0.262 \text{ BTU/lbm } ^\circ\text{R}$  and  $\gamma_t = 1.35$  for all engine RPM settings (exhaust temperatures). These values of  $C_{p_t}$  and  $\gamma_t$  are averages based on the temperature range over which the J-85 operates.

##### C. Static Pressure at the Nozzle Exit, $P_7$

We assume the static pressure at the exit is equal to atmospheric pressure. This results in perfectly expanded flow which will maximize the thrust. The test cell presently is not set up to measure  $P_7$ .

##### D. Total Pressure at the Nozzle Exit, $P_{07}$

The total pressure at the exit is an average value of three Pitot tubes placed in the exit stream. The present location of the probes is a result of a total pressure map which was done in the summer of 1980 (Ref. 3).

b. Total Temperature at the Nozzle Exit,  $T_{07}$ 

The total temperature at the exit is an average value taken from four thermocouples placed at various depths in the exit stream. We placed the thermocouples approximately six inches behind the nozzle exit plane. We will assume the total temperature does not vary appreciably over this distance. The immersion depth into the exit stream was arbitrary.

F. Nozzle Exhaust Area,  $A_7$ 

As we explained earlier, in order to calculate engine thrust we must know the nozzle exit area at all engine operating conditions. How we measure this quantity is explained in the next section.

## VI. Procedure for Measurement of Nozzle Exit Area and Total Temperature

Since the nozzle exit opening varies with engine RPM, we needed some method to determine the area of this opening in order to calculate  $\dot{m}_7$ .

We decided that a linear transducer mounted on the exit nozzle could give us an output voltage that we could relate to the exit area. The variable exhaust nozzle (VEN) movement is controlled by three separate actuator rods. A linear movement of the rods causes the VEN leaves to fold over each other (Ref. 1). The operation is similar to the shutter leaves of a camera. Just as the shutter leaves form the camera aperture, the VEN leaves form the exit area. If we can determine this area, we can plot it as a function of the linear displacement of the actuator rods.

We used a Model 7DCDT-3000/FV linear transducer and its input was set at  $6.5 \pm .01$  volts. A calibration showed the transducer to be linear throughout the range of its travel arm (Figure 3). We attached the case of the transducer to the stationary casting of one of the actuator rods. The travel arm of the transducer was attached to the movable nozzle (Figure 4). As the actuator rods moved, the size of the nozzle varied and this resulted in an output voltage that was dependent on nozzle area. We fed the output of the transducer to a digital voltmeter. To determine the actual nozzle area that corresponded to the various actuator rod positions we manually operated the actuator rods which varied the nozzle area, and at each rod position, we placed heavy butcher's paper against the exit and applied pressure. This left an imprint of the nozzle opening on the paper, and we darkened the imprint with pencil to make it more visible. We determined the area of these imprints with a planimeter and recorded the corresponding output voltage. We performed this same operation at different nozzle openings and generated the curve shown in Figure 5 where output voltage is expressed in volts and nozzle area is in square feet. We did a least squares fit of these two equations and generated a second order equation that relates transducer output (V) to nozzle exit area ( $A_7$ ) (Ref. 4). The equation is shown below:

$$A_7 = .001983V^2 - 0.13237V + 0.9656$$

(157)

The value of this equation is that one simply has to know an output voltage from the transducer in order to calculate a nozzle exit area,  $A_7$ .

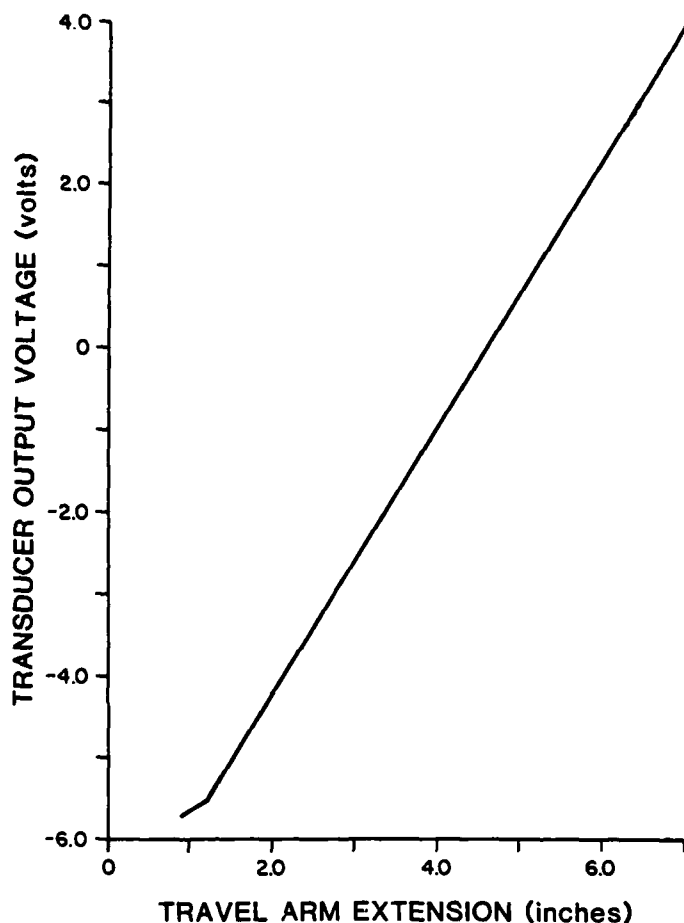


Figure 3. Nozzle Transducer Calibration



Figure 4. Transducer (A) Attached to Nozzle Actuator Rod (B). Also Shown Are Actuator Rod Travel Arm (C), Transducer Travel Arm (D), and Moveable Nozzle-Control Ring (E)

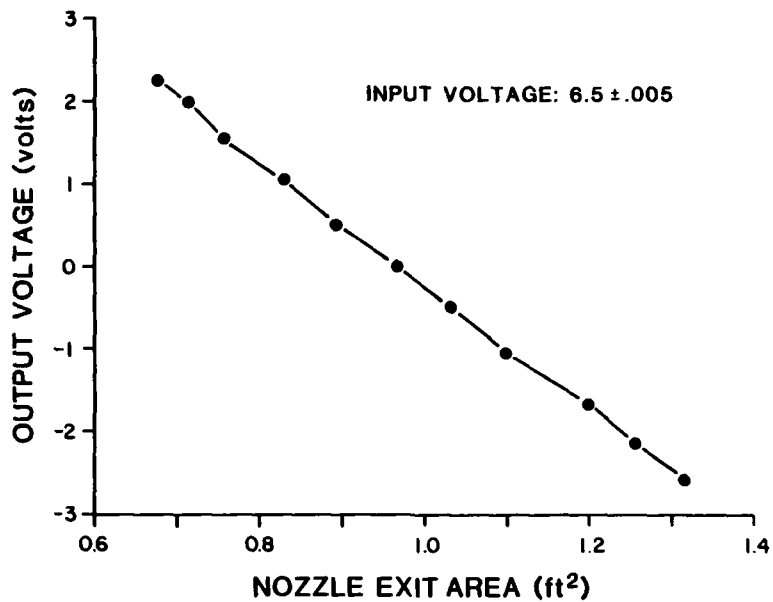


Figure 5. Nozzle Exit Area Calibration

The second area that needed attention was  $T_{07}$ . Previously, a single thermocouple measured this variable. We suspected the thermocouple to be placed in a region of the exhaust where the temperature was hotter than the average gas temperature. To solve this problem we placed four separate thermocouples in the exhaust and recorded the average of the four. While operating the engine, we noticed the four thermocouples were reading a temperature consistently lower than that recorded by the single thermocouple previously used. In the analysis of thrust we used the average temperature recorded by the four.

Being fairly confident of measurements of  $A_7$ ,  $T_{07}$ , and  $P_{07}$ , we were ready to take data from an operating engine. Prior to running the engine, we recorded the atmospheric pressure and temperature. Table 2 shows data taken from two engine runs, each from 70 to 100 percent of the engine's maximum RPM. The engine RPM settings were determined by multiplying the maximum rated engine RPM by the percent RPM desired and then setting the throttle so that the calculated RPM value was obtained on the actual RPM indicator located on the control panel. This procedure simply allowed us to accurately return to the same engine operating point in subsequent engine tests.

#### VII. Data Reduction

We used data from the 1 July 1981 test run, which is listed in Table 2, for the following analysis. Calculations were made using average values of two engine runs. For example, the thrust value at 70 percent RPM was the average of 238 lbf and 258 lbf or 246 lbf.

We calculated thrust using both Eqn. (4) and Eqn. (6). In Eqn. (6) we had some doubt as to the accuracy of the turbine exit temperature,  $T_{05}$ . We first calculated thrust using the measured  $T_{05}$ . Then we

Table 2  
J-85/13 ENGINE TEST RUN DATA

% RPM	Actual RPM	$\dot{m}_f$ lbm/hr	$\Delta P_o$ in $H_2O$	$P_o_3$ psig	$P_o_5$ in Hg	$P_o_7$ in Hg	$T_o_2$ °F	$T_o_3$ °F	$T_o_5$ °F	$T_o_7$ °F	F 1bf	Output Voltage (volts)
70	11579	542	11.8	1.0	18.0	2.5	1.4	84	286	724	774	238 -1.96
80	13234	685	18.4	1.5	26.5	4.9	3.1	84	348	720	776	438 -0.835
90	14888	1168	29.5	2.5	47.0	15.0	11.4	66	411	855	887	1150 +0.93
100	16542	1968	39.2	3.2	64.5	26.3	19.7	62	514	1235	1202	1902 +1.39
70	11579	542	12.0	1.0	18.4	2.7	1.5	82	282	718	776	258 -1.90
80	13234	685	18.5	1.5	26.5	4.8	3.0	82	344	718	777	434 -0.86
90	14888	1162	29.3	2.4	46.6	14.8	11.1	64	409	852	825	1144 +0.91
100	16542	1970	39.3	3.1	64.7	26.4	20.0	62	516	1235	1200	1908 +1.33

TEST RUN DATE: 1 July 1981

 $P_{atm}$ : 23.22 inches Hg $T_{atm}$ : 70 °F

assumed an adiabatic nozzle and afterburner casing, replaced  $T_{05}$  with the temperature read by the four thermocouples at the nozzle exit,  $T_{07}$ , and recalculated the thrust. The results, along with the percent error, are shown in Table 3. The percent error was calculated by dividing the measured value of thrust into the difference between the measured and calculated values of engine thrust.

Table 3  
REDUCED DATA FROM 1 JULY 1981 TEST RUN

	PERCENT ENGINE RPM			
	70	80	90	100
Measured Thrust, $F_{meas.}$ (1bf)	248	436	1147	1905
Calculated Thrust Using Eqn. (6) & $T_{05}$ , $F_{calc.s}$	246.4	444.7	1156.1	1738.6
Calculated Thrust Using Eqn. (6) & $T_{07}$ , $F_{calc.s}$	246.4	444.7	1156.1	1738.6
Calculated Thrust Using Eqn. (4), $F_{calc.}$	246.4	444.6	1156.1	1738.6
Percent Error	-0.648	+1.99	+0.792	-8.74

#### VIII. Discussion of Test Results

We immediately notice from the results in Table 3 that the thrusts calculated with the different temperatures,  $T_{05}$  and  $T_{07}$ , are exactly the same. If we examine the thrust equation that we used, Eqn. (6), and remember how the gas mass flow rate at nozzle exit,  $\dot{m}_7$ , was calculated, we can see why this is so.

The sum of the various mass flows in Eqn. (6) is just the mass flow of gas out of the exhaust nozzle as shown by Eqn. (8). We used  $\dot{m}_7$  in lieu of these other mass flows when we calculated the thrust using Eqn. (6). Thus we effectively substituted Eqns. (9), (10), (11), (12), (13), and (14) into Eqn. (6). If these equations are substituted in Eqn. (6) and we notice that

$$\frac{\gamma_c R}{\gamma_c - 1} = C_p c \quad (16)$$

and

$$\frac{T_7^{1/2}}{R_7 T_7} a_7 \sqrt{\frac{c_{p7}}{\gamma_t - 1}} = \frac{\gamma_t}{\gamma_t - 1} \quad (17)$$

we arrive at

$$F = \frac{2\gamma_t P_7 A_7}{(\gamma_t - 1)} \left[ \left( \frac{P_{07}}{P_7} \right)^{\frac{\gamma_t - 1}{\gamma_t}} - 1 \right] \quad (18)$$

Thus we have arrived at a form of the thrust equation that is independent of the gas temperature at the nozzle exit. This form then eliminates the need to measure either the static or total temperatures at the exit.

In a similar manner we can substitute for  $\dot{m}_7$  in Eqn. (4) and again find that the equation for thrust of the engine is Eqn. (18). Therefore, because of the technique we used to solve for  $\dot{m}_7$ , both Eqn. (4) and Eqn. (6) give us the same result for thrust of the engine.

We therefore used Eqn. (4) and the values of  $\dot{m}_7$  and  $U_7$  that were calculated at the various RPM settings to calculate thrust values. The results are shown in Table 4.

We see from the reduced data in Table 4 that the percent error between calculated and actual thrust is insignificant (i.e., below two percent) up to approximately 90 to 95 percent RPM. However, at 100 percent RPM, the calculated thrust is almost nine percent below the actual. If we look at Eqn. (18), we see that the thrust is a function of exit total pressure, exit static pressure, exit area, and the specific heat ratio. We are confident of the exit nozzle area calibration. This leaves the specific heat ratio,  $\gamma_t$ , and the pressures at the exit as the parameters to be considered in more detail. A sensitivity analysis shows that a one-percent error in  $\gamma_t$  leads to an almost three-percent error in thrust. Our assumption of  $\gamma_t = 1.35$  is based on an average of several values of  $\gamma_t$  that depend on the turbine exit temperature (Ref. 5). A slight error in  $\gamma_t$  at 100 percent RPM would account for some error.

We measured values of the total pressure at the nozzle exit with a simple Pitot tube and assumed the static pressure to be equal to the atmospheric pressure (perfectly expanded flow). Using these values we then calculated the flow Mach number. This calculation indicated the exit flow is near sonic ( $M = .995$ ). We suspect that the flow is not perfectly expanded at 100 percent RPM and that the Pitot tube may be behind a curved shock wave (Ref. 6). The total pressure change through the shock should be insignificant but the static pressure assumption of expanded flow could result in a significant error in calculated thrust. Unfortunately, in these tests we did not measure the static pressure at the nozzle exhaust or the Pitot tube location and therefore we cannot quantify the magnitude of these effects.

To avoid this problem at 100 percent RPM, we can calculate the thrust using Eqn. (4), but instead of calculating an exit mass flow based on uncertain pressures, temperatures and areas, we can use Eqn. (6) and

Table 4  
REDUCED DATA FROM 1 JULY 1981 TEST RUN

	PERCENT ENGINE RPM			
	70	80	90	100
$\dot{m}_7$ (lbm/sec)	15.82	20.07	28.75	31.21
$U_7$ (ft/sec)	501.6	713.6	1294.8	1794.0
$F_{\text{calc.}}$ (lbf)	246.4	444.7	1156.1	1738.6
$F_{\text{meas.}}$ (lbf)	248.0	436.0	1147.0	1905.0
Percent Error	-0.65	+1.99	+0.79	-8.73

assume  $\dot{m}_7$  equal to the sum of entrance and fuel mass flows. We will assume the losses to be negligible. By doing this, the difference between the calculated thrust and the measured thrust can be reduced to below four percent.

Although this method will predict the thrust more accurately at 100 percent RPM, we are still left with the problem of explaining the high error using the other method.

We believe the error between calculated and measured thrust at 100 percent RPM is due to an error in either the measured pressures or the selected value of the specific heat ratio,  $\gamma_t$ . At this RPM we are uncertain of the accuracy of the pressure measurements because of the presence of sonic flow. We are also uncertain of the specific heat ratio because of the increased temperatures.

One result which surprised us was the value of the turbine exit temperature,  $T_{05}$ . If we look at the 1 July data sheet, we see that  $T_{07}$  is consistently higher than  $T_{05}$ , up to approximately 70 percent RPM. From here up to 100 percent RPM,  $T_{05}$  is the higher. Since the afterburner casing is not adiabatic, there should be a temperature difference between  $T_{05}$  and  $T_{07}$ . However,  $T_{05}$  should always be higher than  $T_{07}$ , not vice-versa. At approximately 90 to 95 percent RPM, both  $T_{05}$  and  $T_{07}$  read the same temperature to within 5 degrees Farenheit. At other RPM readings, the difference is greater. We suspect that the location of the  $T_{05}$

thermocouples is the cause of this discrepancy.

At some point between 90 and 95 percent RPM, the turbine exhaust pattern is such that the thermocouples are immersed so as to read an average temperature. At other RPM, this exhaust pattern changes and, hence, the thermocouples read something other than the average temperature. This would account for the difference between  $T_{05}$  and  $T_{07}$  as seen on the data sheet.

#### IX. Conclusions

An obvious conclusion is that the mass flow through the compressor bleed valve must be included in the thrust analysis. By accounting for this bleed mass flow we were able to calculate the thrust of the J-85 engine to within  $\pm 2$  percent at all engine RPM up to approximately 90 to 95 percent RPM. At 100 percent RPM the calculated thrust is approximately nine percent below what is measured.

We cast the thrust equation in a form that was independent of temperature at the nozzle exit and thus eliminated the need to accurately measure the average exit total temperature of the nozzle. Analysis of the resulting equation leads us to believe the remaining thrust error is due to an improper selection of the specific heat ratio,  $Y_t$ , or incorrect total or static pressure measurements. We can predict the thrust at 100 percent RPM to within four percent if we assume the exit mass flow to be equal to the entrance plus fuel mass flows. We remind the reader here that previous errors were on the order of 25 percent.

#### X. Recommendations

We recommend further study in the following areas in order to reduce the error at 100 percent RPM.

1. Perform a total pressure and temperature map of the airstream at the nozzle exit plane. This will allow us to place Pitot tubes and thermocouples in the exit stream at locations that will provide accurate measurements at all RPM.
2. Accurately determine values for  $Y_t$  and  $C_{p_t}$  at all engine operating conditions.
3. Measure the static pressure at the exit plane. This will determine if the assumption of perfectly expanded flow is valid at 100 percent RPM.
4. Calibrate all the test cell instruments to determine if we are introducing any nonlinearities in the equipment which would introduce error into the data.

#### Symbols

$a_0$	freestream speed of sound
$a_7$	nozzle exit speed of sound
$A_2$	compressor frontal area
$A_7$	nozzle exit area
$C_{p_c}$	specific heat at constant pressure ahead of the compressor

$C_p_t$	specific heat at constant pressure downstream of the burner
$\dot{m}_0$	freestream mass flow rate
$\dot{m}_2$	mass flow rate into the compressor
$\dot{m}_7$	mass flow rate out of the nozzle
$M_0$	freestream Mach number
$M_7$	nozzle exit Mach number
$\dot{m}_{CBV}$	mass flow rate through the compressor bleed valves
$\dot{m}_{LOSSES}$	mass flow rate of cooling and leakage air that is not accounted for
$P_0$	atmospheric pressure
$P_7$	nozzle exit static pressure
$P_{07}$	nozzle exit total pressure
psi	pounds per square inch
R	gas constant (for air) at engine inlet
$R_7$	gas constant at nozzle exit
$T_{05}$	total temperature at turbine exit
$T_7$	static temperature at nozzle exit
$T_{07}$	total temperature at nozzle exit
$U_0$	freestream velocity
$U_7$	nozzle exit velocity
VEN	variable exhaust nozzle
$\gamma_c$	specific heat ratio (for air) upstream of burner
$\gamma_t$	specific heat ratio downstream of burner
$\rho_7$	nozzle exit density
$\tau_\lambda$	ratio of total temperature at combustor exit, $T_{04}$ , to ambient temperature $T_0$
$\tau_t$	ratio of turbine exit total temperature to turbine inlet total temperature

References

1. Technical Manual. Intermediate Maintenance Turbojet Engine - Model J85-GE-13. T.O. 23-3000-1, March 1968.
2. Gates, G. C. "Notes on Rockets and Airbreathing Engines." Transcripts from lectures presented at the Air Force Academy during the fall semester, 1975.
3. Rudd, N. W., A. J. Simon, and V. B. Yasay. "The J-85: A Total Pressure Profile and Thrust Analysis." Unpublished Aeronautics Laboratory (Aero 450) Research Report, July 1980.
4. Holman, J. P. and W. J. Gajda, Jr.. Experimental Methods for Engineers. 3rd ed. San Francisco: McGraw-Hill, Inc., 1978.

USAFA-TR-81-11

5. Jones, R. N. "Aircraft Gas Turbine Engine Analysis." Unpublished paper, Department of Aeronautics, USAF Academy, Colorado, 1972.
6. Shapiro, A. H. The Dynamics and Thermodynamics of Compressible Fluid Flow, Vol. 1. New York: The Ronald Press Company, 1953, pp. 153-154.

**SECTION III**

**Instrumentation and Hardware**

PRESSURE MEASUREMENT USING A HIGH-SPEED DATA ACQUISITION  
AND ON-LINE CALIBRATION SYSTEM\*

J.A. Wright\*\* and W.A. Buzzell\*\*\*

## Abstract

This paper discusses the development of a high speed, accurate pressure measuring system for use in the USAF Academy trisonic wind tunnel. The system consists of three major components: (1) seven manometers which provide precise reference pressure levels for calibration of the pressure transducers; (2) Scanivalves which permit flexibility in measuring a large number of pressures very rapidly; and (3) a computer system with associated hardware and software for experiment control, data acquisition, and data reduction. The paper describes the system's components and briefly discusses two experiments that have used this system. The complete system, which has been in operation for nine months, has reduced the time required for wind tunnel experiments and has increased the accuracy of pressure measurements.

1. Introduction

The USAF Academy trisonic wind tunnel is a blowdown facility that uses previously charged reservoirs to provide the tunnel's air supply rather than using a fan. The tunnel has a one-foot square test section and is capable of generating flows with Mach numbers ranging from 0.14 to 4.38. The subsonic and transonic air flow Mach numbers ( $0.14 \leq M \leq 1.33$ ) are obtained with a variable porosity test section which allows continuous variation of air flow Mach number in this range. Fixed, interchangeable nozzle blocks are used to establish the Mach number increments between  $M = 1.44$  and  $M = 4.38$ . (The air flow regulation techniques are discussed in Ref. 1.) The air storage capacity of the reservoirs is 54 cubic feet at 600 psin and 100 degrees Farenheit. This gives a useable test duration of two minutes at  $M = 1.2$  to over seven minutes at  $M = 4.38$ . The total pressure in the test section is regulated with an automatic control valve, while the tunnel exhaust pressure is the local atmospheric pressure. Figure 1 is a schematic drawing of the USAF

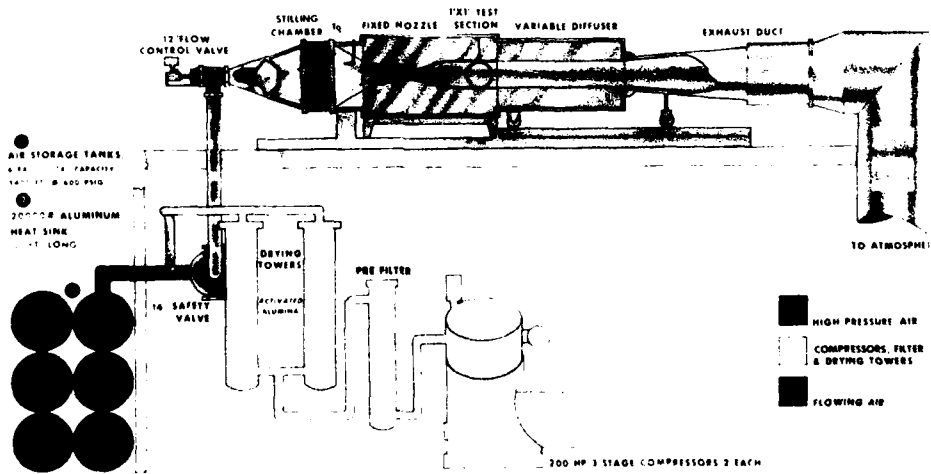


Figure 1. Schematic of USAF Academy Wind Tunnel Less Trisonic Test Section

\*This paper was presented to the 55th Meeting of the Supersonic Tunnel Association at the National Aerospace Laboratory NLR, Amsterdam, The Netherlands, April 1981.

\*\*Major, USAF, Assistant Professor of Aeronautics, DFAN

\*\*\*Captain, USAF, Instructor of Aeronautics, DFAN

Academy trisonic wind tunnel components.

Since its completion in 1958, the trisonic facility has undergone several major design improvements. These changes are summarized in Table 1. The main purpose of the modifications was to improve the quality of the air flow in the wind tunnel, resulting in better aeronautical data. The success of the modifications

Table 1  
FLOW QUALITY IMPROVEMENTS TO THE TRISONIC TUNNEL

•1962	HEAT SINK INSTALLED IN STORAGE TANK AREA
•1963	CONIC DIFFUSER ADDED
•1964	TRISONIC CART ADDED
•1978	DIFFUSER MODIFIED TO IMPROVE FLOW QUALITY
•1979	AUTOMATIC TOTAL PRESSURE CONTROLLER ADDED

has provided an expanded capability to conduct investigations into areas such as the calibration of multi-port flow probes and measurement of various flow properties in turbulent boundary layer flows. In addition to maintaining a well-conditioned air flow in the wind tunnel, we must also be able to measure pressures at various points in the tunnel or on a test model precisely and rapidly. These measurements must be made quickly to maximize data-gathering during the limited test run time and to minimize tunnel operating costs.

Because of these requirements, a multi-port pressure scanning system capable of continuous pressure transducer recalibration was developed. Included in this system is a digital computer, along with various peripherals and software, that provides experimental control, data acquisition and reduction, and display.

## II. System Description

### A. Pressure Measurement System

The first task of our system is to acquire the desired pressures and convert them into electronic signals. To obtain these multiple pressure measurements during experiments, we use a scanning-type pressure device or Scanivalve. The Scanivalve system allows the rapid, sequential measurement of multiple pressures (static or total) using only one transducer. It achieves this capability by allowing the transducer to "scan" or rotate between pressure ports, each of which is separately connected via tubing to a test measurement location. A schematic of a typical Scanivalve configuration is shown in Figure 2. For our application the use of the Scanivalve has several inherent advantages. First, the Scanivalve design readily lends itself to computer control via a separate stepper-control unit. This unit allows the computer program to control the stepping rate of the Scanivalve motor and thereby the settling or dwell time of the transducer at each pressure measurement port. Changes in the dwell time that may be required by different experimental configurations are easily accomplished by changes in the controlling program. Second, the Scanivalve units we use allow us, when needed, to locate these units inside the test models to be placed in

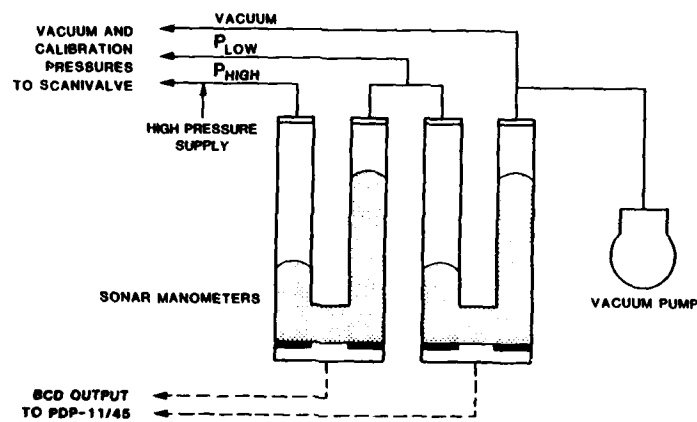


Figure 2. Schematic of Pressure Calibration Components

the wind tunnel. This reduces tubing lengths and thus the potential for frequency response problems. This is especially critical for small tubing sizes or multi-diameter tubing connections. Finally, the cost of setting up a pressure measurement system for each of the varied experiments that we may conduct in a semester's time frame has been reduced, since only one pressure transducer per Scanivalve is required.

#### B. Pressure Calibration System

Once the desired pressures have been acquired and converted to electronic signals, we must relate the signal level to the appropriate pressure reading, i.e., calibrate the pressure transducer. We use Wallace and Tiernan precision sonar manometers to accomplish this calibration.

The sonar manometer achieves its accuracy by measuring the difference in the height between the two legs of the U-tube mercury-filled manometer by means of sonar echoes through the mercury. A schematic of the calibration system components is shown in Figure 3. One piezoelectric transducer mounted at the bottom of each leg of the sonar manometer pictured on the left side of Figure 2 transmits an ultrasonic pulse through the mercury to the surface and receives the echo from that surface. By transmitting the sonic pulse simultaneously in both legs, the difference in time between reception of the echoes from the surface of the mercury in the two legs can be related to the height difference. By holding the temperature of the mercury constant (and therefore the speed of sound in the mercury) and by using a specified time reference for the sonic pulse, we measure the pressure differential between the two pressures ( $\Delta P = P_{HIGH} - P_{LOW}$ ). Since these pressures also were alternately impressed on the pressure transducer, we have two voltage levels and, therefore, a voltage difference that corresponds to the measured pressure differential. Consequently, we have achieved a pressure calibration for the pressure transducer, i.e., PSI per millivolt. A mercury-in-glass thermostat provides the thermal reference and the variation of the temperature in the sonar manometer system is specified as  $\pm 0.5$  degrees Farenheit. This variation in temperature yields a

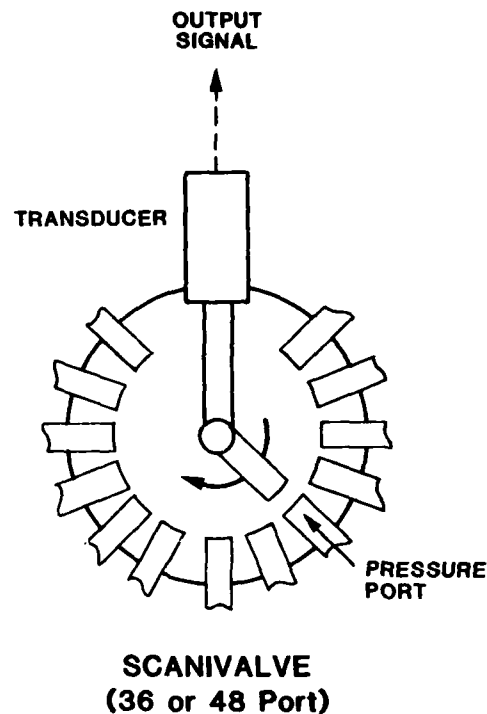


Figure 3. Schematic of a Typical Scanivalve Configuration

calibration accuracy of  $\pm 0.002$  PSI for a full scale pressure range of 15 PSI.

In our calibration system we use three reference pressures: (1) the high reference pressure,  $P_{HIGH}$ , is set higher than the expected highest test pressure; (2) the low reference pressure,  $P_{LOW}$ , is set lower than the lowest expected test pressure and may be below atmospheric pressure; and (3) the vacuum is used to achieve the low reference pressure and it also provides a vacuum reading to "unload" the transducer (to be discussed later). Our method of selecting the  $P_{HIGH}$  and  $P_{LOW}$  provides a pressure calibration that is applicable to the complete range of test procedures.

The sonar manometers have another quality that is very useful when they are used in conjunction with a digital computer: their output is a digital signal. The digital signal allows direct interface with the computer, thus eliminating the requirement for an analog to digital converter.

#### C. Experimental Design

When developing the data sampling schedule for an experiment, we adhere to the following methodology as closely as possible in order to maximize the accuracy and repeatability in making multiple pressure measurements:

(1) Reference pressures for the sonar manometers are chosen to bracket the expected pressure measurement range. This provides a high and low calibration to the Scanivalve. These calibration pressures are sampled each time a sequential reading of test pressures is made by the Scanivalve transducer. We have,

therefore, essentially eliminated the problem of transducer "drift", thus insuring a more accurate pressure measurement capability.

(2) The vacuum pressure used in the low-reference sonar manometer is sampled between all key pressure measurements, such as the high and low reference, tunnel total and static pressures, and between groups of similar pressures on the test model (i.e., static and total). This procedure "unloads" the transducer sensing element so that these important pressures always will be measured by the sensing element from the same deflected state, thus reducing transducer hysteresis.

(3) When an estimate of the pressure distribution over a test model can be made, the pressures to be measured are indexed on the Scanivalve, if possible, from the lowest to the highest pressure. This is done in addition to the vacuum sampling described in (2), since the number of total Scanivalve ports is usually limited, and, therefore, placement of a vacuum port after each pressure measurement is not practical. However, by allowing the transducer sensing element to move in the same direction for each reading (i.e., low to high), transducer hysteresis again can be minimized.

(4) If an experiment requires the use of small tubing sizes or multi-diameter connections for a pressure measurement, a computer program is available which checks the frequency response of the proposed system. The program analytically predicts the natural frequency response of a pressure measurement system based on inputs of tubing length, diameter, and transducer sensing volume. It has the capability of analyzing a system consisting of multiple tubing lengths and diameters. This program is valuable for insuring that the tubing lengths and diameters chosen for use between the pressure measurement location and the Scanivalve will not adversely affect the measurement accuracy.

Use of the methodology described above has contributed significantly to the improved accuracy of pressure measurements taken during recent tests. Combining this methodology with the use of the sonar manometer reference, we predict an accuracy of  $\pm .005$  PSI in the measurement of differential pressures.

#### D. Computer Hardware/Software

A Digital Equipment Corporation (DEC) PDP-11/45 computer provides the experimental control as well as the data acquisition, reduction, and display. To accomplish these functions, various peripherals and software have been added to supplement the mainframe computer:

(1) A Diva Disk System is used as the mass storage device for the PDP-11/45. The disk system is a high-speed, fast-access device which is capable of storing up to 40 megabytes of formatted data.

(2) A Laboratory Peripheral System (LPS-11) is used to convert the analog signals from the various types of sensors into a digital form suitable for computer use. This system is also used to control various devices via the digital-to-analog process located inside the LPS-11.

(3) Tektronix 4025 and 4051 CRTs, used as the control/graphics display terminals, generate, compile, and run various acquisition and reduction computer programs. Control of data acquisition and on-line

reduction is performed via the 4025. Both are used to display preliminary plots when this type of output is selected.

(4) A Decwriter III is a teletypewriter used as the system list device for hard-copy printout. A Tektronix 4662 Digital plotter is also available for hard-copy ink plots.

A schematic of the PDP-11/45 computing system is shown in Figure 4.

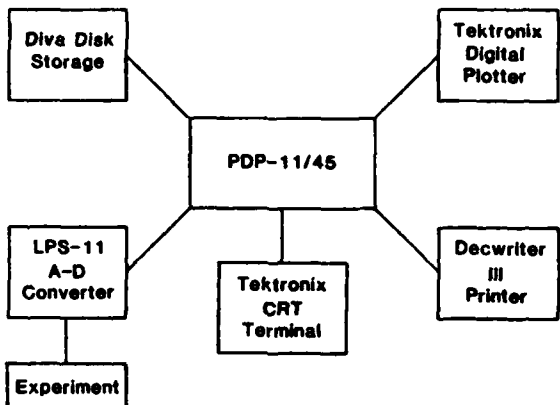


Figure 4. PDP-11/45 and Associated Hardware

#### E. Summary of System Description

Figure 5 shows all the elements of the pressure measurement system that have been discussed. The experimental layout shown is for a test model requiring multiple static pressure measurements and a computer-controlled, total pressure traverse mechanism. These multiple static and total pressure measurements are shown in Figure 5 as  $P_n$  to  $P_1$ , and they would be arranged for sampling according to the methodology discussed in Section II.

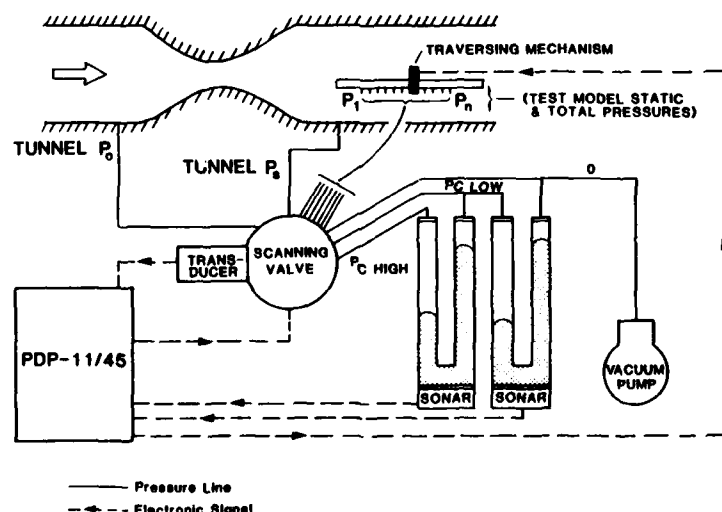


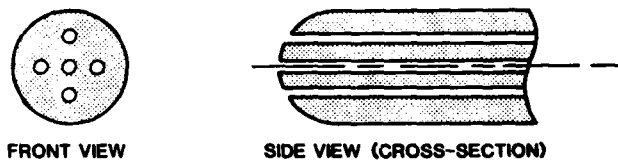
Figure 5. Overall System Schematic

III. Examples Utilizing the Pressure Measurement System

To demonstrate the use and flexibility of our system, two experimental projects recently undertaken in the USAF Academy trisonic wind tunnel are presented as examples.

**A. Five-Hole Pitot-Static Probe Calibration**

Calibration of multi-port pressure probes represent a large portion of the work currently being performed in the USAF Academy trisonic tunnel. The particular probe described here is a five-port, analytically designed, blunt-nose probe shown in Figure 6. The task was to measure the pressures at each port as angle of attack, roll angle, and Mach number were varied, and then to convert these pressures into calibration coefficients and plot the results. The importance of creating these calibration coefficients is to allow the probe to be used in other tunnels to make pressure measurements based on the calibration coefficients formed in this test. Table 2 summarizes the test matrix and variables.



FRONT VIEW

SIDE VIEW (CROSS-SECTION)

TEST VARIABLES

INDEPENDENT	DEPENDENT
•Mach number	•Total pressure coefficient
•Angle of attack (AOA)	•Static pressure coefficient
•Roll angle	•Sideslip pressure coefficient
	•AOA pressure coefficient

Figure 6. Schematic of Five-Hole Probe

Table 2  
TEST MATRIX: FIVE-HOLE PROBE

		ROLL ANGLE			
		0°	7.5°	15°	30°
MACH NUMBER	.37	Run 1	2	3	4
	.61	5	6	7	8
	.91	9	10	11	12

**•ONE TEST RUN:** 0, +5°, +10°, +20° AOA (7 AOA settings)  
 5 pressure measurements/AOA setting  
 70 seconds elapse time

**•TEST TOTAL:** 84 data points  
 420 pressure measurements  
 14 minutes tunnel run time

The instrumentation for measuring the probe air pressures was arranged according to the methodology described in Section II. Probe calibration computer software routines for both data acquisition and reduction were previously developed and were modified to meet the specific requirements of this test. In particular, the data acquisition program was set to sample the five probe pressures. The model angle of attack, roll angle, and Mach number were adjusted by the operator. Additionally, the Scanivalve transducer dwell time was adjusted by an additional minor change to the control program software. Data plotting routines incorporated into the reduction software allow real time review of the data via the CRT terminal.

The set-up time for the test required approximately one day; data acquisition required four days.

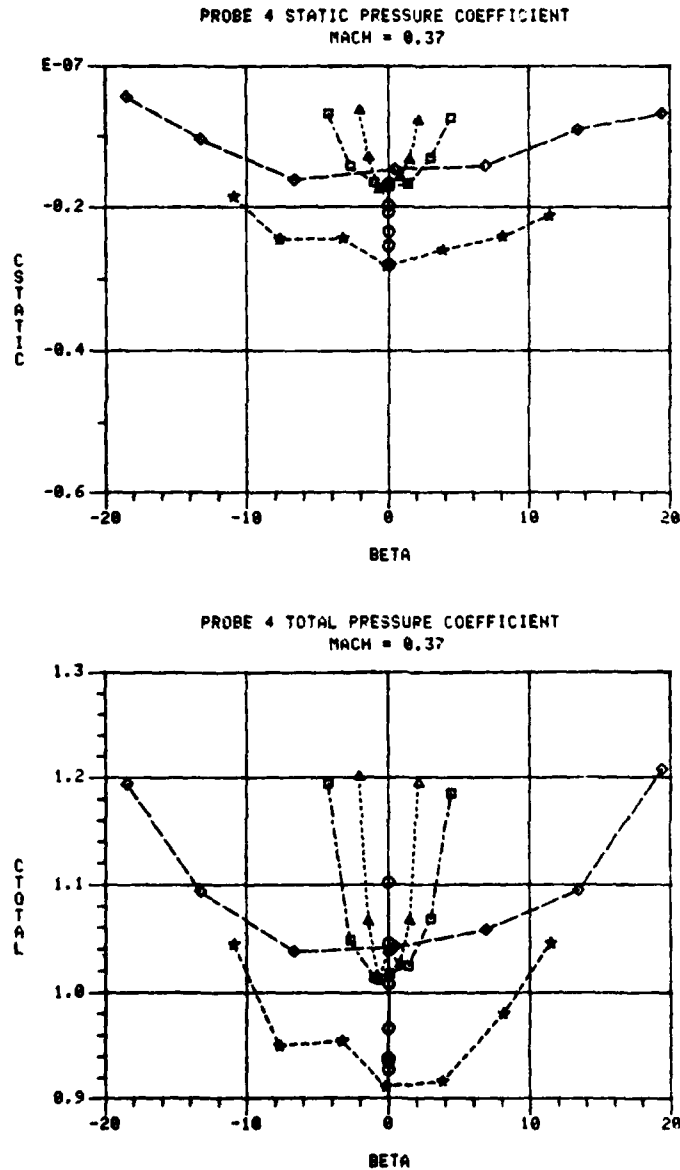


Figure 7. Sample Data Plots, Five-Hole Probe

including the production of hard-copy printout and plots. The need for a four-day test time was due to the necessity of charging the air reservoirs between data runs. Figures 7 and 8 show the four data coefficients plotted against sideslip angle (beta) and angle of attack (alpha) for a single Mach number. These plots represent a sample of a data set for a typical run sequence. The sample data set required only five minutes for generation, including the time from tunnel start-up until the final plot was produced.

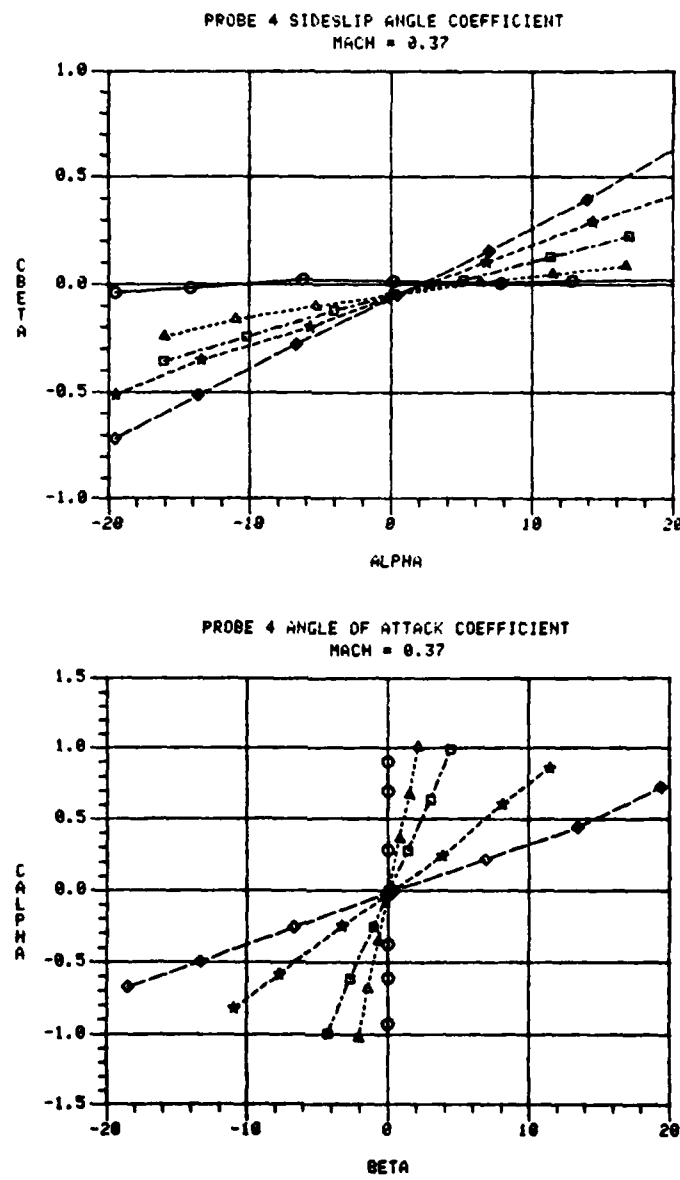
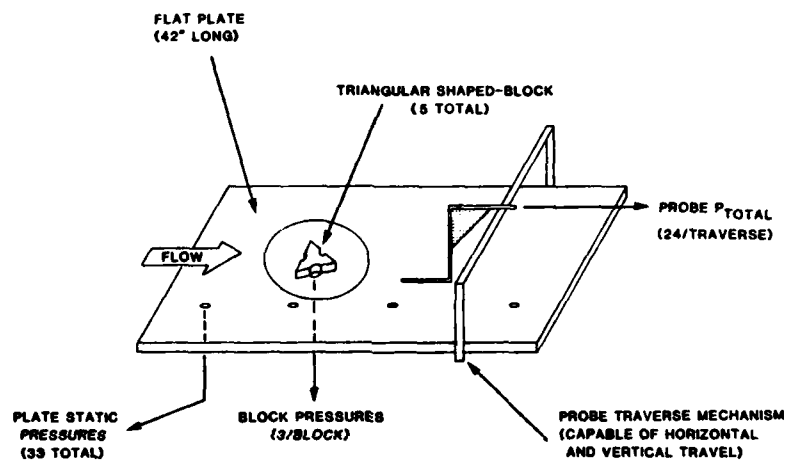


Figure 8. Sample Data Plots, Five-Hole Probe

#### B. Skin Friction Measurement Project

The second example represents a more complex research effort currently underway in the Department

of Aeronautics. The objective of the program is the development of a pressure measurement device (shaped-block) for determining the skin friction coefficient in turbulent boundary layer flow. Figure 9 shows the key elements of the project. The shaped-block design under evaluation is a three-port, triangular design and is tested at five locations on a 42-inch-long flat plate which is placed horizontally in the one-foot by one-foot test section of the tunnel. To accurately determine the velocity distribution near the surface of the plate, a total pressure probe with a .004-inch by .008-inch opening is used to traverse the boundary layer via a computer-controlled stepping motor.



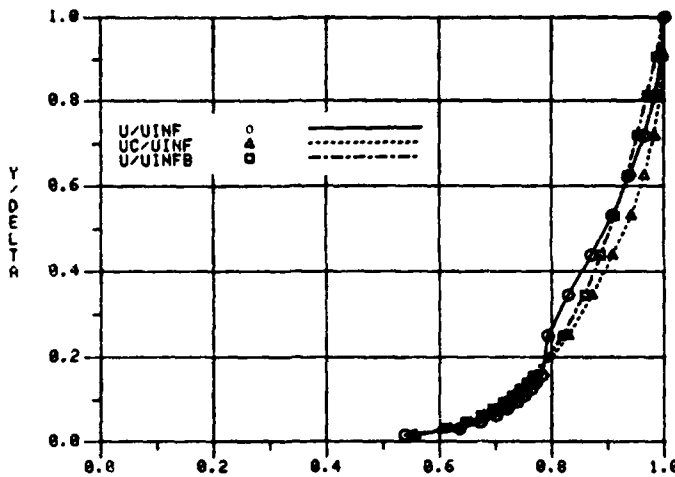
- Pressure Measurements/Run Sequence: 390
- Elapse Time/Run Sequence: 140 seconds

Figure 9. Key Elements of the Skin Friction Project

Table 3 lists the variables measured during each test run. A total of 390 pressure measurements are made in a typical test run by two 36-port T-type Scanivalves located inside the flat plate. Time duration for a typical test run is 140 seconds. The entire sequence, including Scanivalve sampling of all test pressures and total pressure probe horizontal and vertical movement, is controlled by the computer data

Table 3  
TEST VARIABLES: SKIN FRICTION PROJECT

INDEPENDENT	DEPENDENT
● Shaped-block dimensions	● Skin friction coefficient
● Shaped-block locations	● Boundary layer velocity distribution
● Mach number	● Boundary layer thickness
● Shaped-block flow angle	● Shaped-block pressure difference
● Flat plate angle	



RUN #155, MACH .53, STATION 3, SB ANGLE 0, PLATE ANGLE -5, BLOCK .020

Figure 10. Sample Data Plot, Skin Friction Project

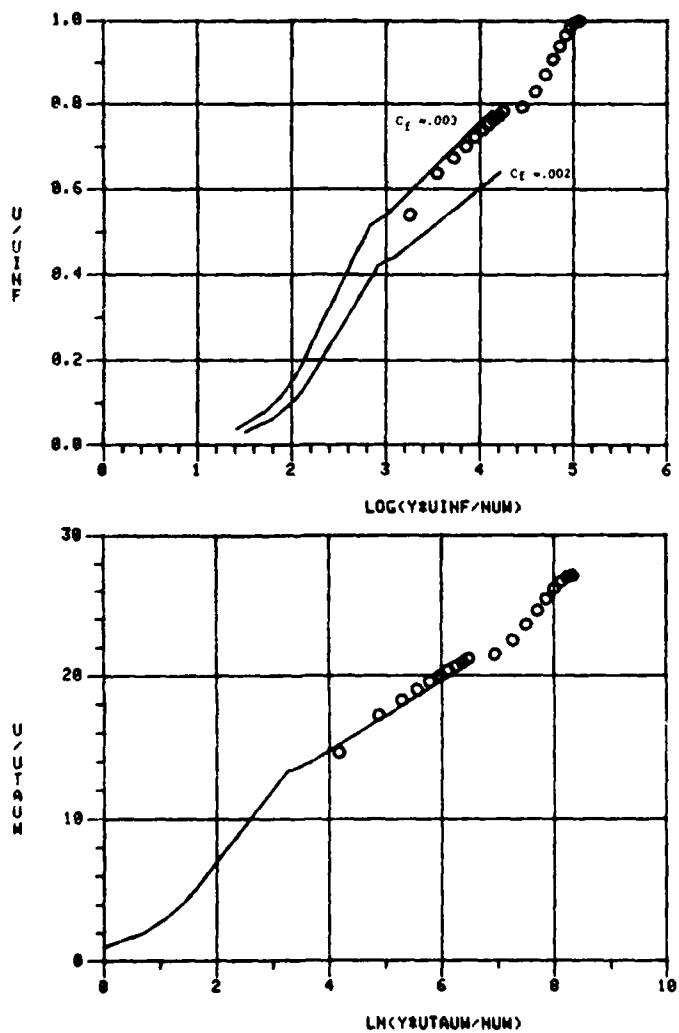


Figure 11. Sample Data Plots, Skin Friction Project

acquisition program. Data reduction and presentation is available in real time to allow flexibility in adjusting the test matrix. Sample data plots are shown in Figures 10 and 11. Figure 10 is a sample plot of the turbulent boundary layer thickness ratio ( $Y/\Delta$ ) plotted against three different velocity profiles based on data from the third shaped-block location on the flat plate at a Mach number of .53. In this plot,  $U/U_{\infty}$  is the velocity profile based on the traverse total pressure measurement,  $U_C/U_{\infty}$  is the theoretical calculated velocity distribution, and  $U/U_{\infty}^{FB}$  is the empirically predicted velocity profile based on the Blasius turbulent solution. Excellent data correlation between measured and calculated values was achieved. Figure 11 shows two plots which compare the experimental data with the theoretical solution for the inner region of the turbulent boundary layer. The good correlation achieved between the measured and calculated data has helped to validate both the data acquisition methodology and the accuracy of the pressure measurement system.

#### IV. Summary

The addition of a high-speed pressure data acquisition and on-line calibration system has resulted in an increase in the accuracy and flexibility of the research we are now doing in the trisonic wind tunnel facility. This has meant an increase not only in the number of projects we now are able to complete because of better tunnel time utilization, but we also have realized an improvement in the quality of research now being conducted.

#### References

1. Department of Aeronautics. "Subsonic and Trisonic Wind Tunnel Facilities." Internal Publication, USAFA.
2. Davis, M. W., S. E. Icardi, R. W. Gallington, and J. A. Wright. "Flow Quality Improvements in the USAFA Trisonic Tunnel." STA Paper, presented at the Supersonic Tunnel Association's 51st Meeting, Burbank, CA, April 1979.
3. Gallington, R. W. and J. A. Wright. "An Analog Pressure Controller for a Blowdown Tunnel." STA Paper, presented at the Supersonic Tunnel Association's 53rd Meeting, Palo Alto, CA, March 1980.
4. Brilliant, H. M. "Test Plan, Evaluation of Shaped-Block Skin Friction Gauges in Subsonic Compressible Flow." Department of Aeronautics, USAFA. Prepared for the Air Force Aero-Propulsion Laboratory, July 1980.

**SECTION IV**

**Engineering Education**

CADET PERFORMANCE DURING SUMMER ACADEMICS:  
REPEAT VERSUS NON-REPEAT STUDENTS

J.H. Russell\*

Abstract

This study analyzes the performance of cadets enrolled in the following United States Air Force Academy engineering core courses during the 1981 summer semester: Engineering Fundamentals (Engr 110), Mechanics and Materials in Engineering Design (Mech 210), Fundamentals of Aeronautics (Aero 311), and Introductory Engineering Thermodynamics (Aero 312). The paper analyzes and describes data comparing the performance of students taking the courses for the first time with those who had previously failed the course or dropped it in lieu of failure. Subjective performance comparisons of these two student groups are also described.

The results of the study indicate that the performance of cadets taking any of these engineering courses for the first time compared quite favorably with the performance of cadets who study the material a second time.

I. Introduction

The decision to allow students to take an engineering course such as Aero 311 or Aero 312 for the first time during the compressed Air Force Academy summer semester is a difficult one. Traditionally at the Academy an argument has been made against enrolling first-time students in engineering courses during the summer semester because it is said that there are too many concepts to learn and there is too little time in which to learn them. On the assumption that new students will have extraordinary difficulty in a particular summer course, proponents of this argument also feel that first-time students will "hold back" class progress.

Additionally, some people believe that students who repeat courses might have an unfair advantage over first-time students since they have some familiarity with course material. Another advantage that a repeat student might have is the knowledge that failure during a Class Committee-directed summer semester means possible elimination from the Air Force Academy. This fact alone may spur enhanced performance from the typical repeat student. Of course, both of these seeming advantages for a repeat student in the summer term would also be advantageous for a repeat student during the regular academic year.

On the other hand, there are persons at the Academy who have argued that students who take an engineering course for the first time during the summer semester are not at a disadvantage. Supporters of this view believe that the typical first-time student has a better academic record than does one taking the course for the second time. Proponents of this argument also feel that because the typical first-time student is a better student, he or she is better able to adapt to the rigorous summer semester schedule.

The purpose of this study was to provide quantitative and qualitative comparisons of the performance of both first-time and repeat enrollees in engineering core courses taught during the 1981 Air Force Academy summer semester in the hope that factual data could be used to resolve the debate over which students should be permitted to enroll in the summer semester courses.

---

\*Captain, USAF, Instructor of Aeronautics, DFAN

### II. Research Procedures

To gather data for the study we analyzed the performance of students enrolled in four engineering core courses offered during the summer semester of 1981 and we divided those students into two groups, repeat and non-repeat students. Repeat students consisted of those cadets who had previously failed a particular course or had dropped the course at mid-semester and thus had already been exposed to some of the course material. The non-repeat students group was composed of those cadets for whom the summer semester represented their first formal exposure to course material.

Performance data was collected for each group and compared to each cadet's Academy cumulative grade point average (GPA). In addition, for each cadet a statistical measure of course grade deviation from cumulative GPA was determined. For example, a cadet whose deviation was +1.00 would have earned a course grade that was one letter grade higher than predicted by his or her cumulative GPA. Also, in each course the average course grade was computed, as well as the student's course grade deviation from his or her cumulative GPA. The qualitative evaluation of the performance of repeat and non-repeat students was based only on the subjective comments of the individual instructors of the Aero 311 and Aero 312 courses.

### III. Quantitative Results

In general, the data seemed to indicate that repeat and non-repeat students performed equally well during the summer semester. In practically all courses offered during the summer semester the performance of both groups exceeded the expected results based on student cumulative GPAs. In only one group did the average course grade that was achieved fall short of the anticipated course grade (see Table 1). But the limited number of individuals in this particular group made any accurate generalization about their performance difficult. In all the other groups, however, the final course grades achieved by the summer students averaged the same or better than the anticipated results.

Table 1 shows the large number of individuals enrolled in the summer courses who had entering cumulative GPAs below 2.00. Their motivation to do well and avoid possible dismissal from the Academy was evidenced by their performance average which was almost one letter grade higher than predicted by their cumulative GPAs.

Table 2 shows both groups to have averaged better than their cumulative GPAs would have indicated.

Table 3 demonstrates that both repeat and non-repeat students did better than predicted by their previous academic records. In the course from which this data was taken, Aero 311, the non-repeat students actually performed better than did the repeat students, both in terms of their course grades and in deviation from their cumulative GPAs. As a side note to this table, the Aero 311 course final exam was quite similar to one given during the previous semester of the formal academic year. And, in fact, the course progress was not "held back" at all by the presence of non-repeat students. This is clearly shown by the final exam scores for the two semesters. The spring semester final exam had a mean score of 72.5

CADET PERFORMANCE DURING SUMMER ACADEMICS:  
REPEAT VERSUS NON-REPEAT STUDENTS

J.H. Russell\*

Abstract

This study analyzes the performance of cadets enrolled in the following United States Air Force Academy engineering core courses during the 1981 summer semester: Engineering Fundamentals (Engr 110), Mechanics and Materials in Engineering Design (Mech 210), Fundamentals of Aeronautics (Aero 311), and Introductory Engineering Thermodynamics (Aero 312). The paper analyzes and describes data comparing the performance of students taking the courses for the first time with those who had previously failed the course or dropped it in lieu of failure. Subjective performance comparisons of these two student groups are also described.

The results of the study indicate that the performance of cadets taking any of these engineering courses for the first time compared quite favorably with the performance of cadets who study the material a second time.

I. Introduction

The decision to allow students to take an engineering course such as Aero 311 or Aero 312 for the first time during the compressed Air Force Academy summer semester is a difficult one. Traditionally at the Academy an argument has been made against enrolling first-time students in engineering courses during the summer semester because it is said that there are too many concepts to learn and there is too little time in which to learn them. On the assumption that new students will have extraordinary difficulty in a particular summer course, proponents of this argument also feel that first-time students will "hold back" class progress.

Additionally, some people believe that students who repeat courses might have an unfair advantage over first-time students since they have some familiarity with course material. Another advantage that a repeat student might have is the knowledge that failure during a Class Committee-directed summer semester means possible elimination from the Air Force Academy. This fact alone may spur enhanced performance from the typical repeat student. Of course, both of these seeming advantages for a repeat student in the summer term would also be advantageous for a repeat student during the regular academic year.

On the other hand, there are persons at the Academy who have argued that students who take an engineering course for the first time during the summer semester are not at a disadvantage. Supporters of this view believe that the typical first-time student has a better academic record than does one taking the course for the second time. Proponents of this argument also feel that because the typical first-time student is a better student, he or she is better able to adapt to the rigorous summer semester schedule.

The purpose of this study was to provide quantitative and qualitative comparisons of the performance of both first-time and repeat enrollees in engineering core courses taught during the 1981 Air Force Academy summer semester in the hope that factual data could be used to resolve the debate over which students should be permitted to enroll in the summer semester courses.

---

\*Captain, USAF, Instructor of Aeronautics, DFAN

Table 1  
STUDENT PERFORMANCE IN ENGR 110 DURING 1981 SUMMER SEMESTER

REPEAT (17 Students)			NON-REPEAT (2 Students)		
Cum GPA <sup>1</sup>	Course Grade <sup>2</sup>	Deviation <sup>3</sup>	Cum GPA	Course Grade	Deviation
2.34	C	-.34	2.35	B	+.65
1.99	C	+.01	2.77	C	-.77
1.74	B	+.12			
1.91	C	+.09			
2.44	B	+.56			
1.86	B	+.14			
1.99	B	+.01			
2.15	C	-.15			
1.93	A	+.07			
2.09	A	+.91			
1.90	C	+.10			
2.10	C	-.10			
1.86	A	+.14			
2.00	C	0			
2.24	A	+.76			
2.00	A	+.00			
1.80	A	+.20			
Average					
2.02	2.94	+.92	2.56	2.50	-.06
NOTES:					
<ol style="list-style-type: none"> <li>1. Cum GPA valid through spring semester 1981.</li> <li>2. Course letter grades are assigned numerical values as follows: A = 4, B = 3, C = 2, D = 1.</li> <li>3. Deviation of course grade from Cum GPA, i.e., Deviation = Course Grade - Cum GPA.</li> </ol>					

Table 2  
STUDENT PERFORMANCE IN MECH 210 DURING 1981 SUMMER SEMESTER

REPEAT (9 Students)			NON-REPEAT (13 Students)		
Cum GPA	Course Grade	Deviation	Cum GPA	Course Grade	Deviation
2.08	C	-.08	2.86	B	+.14
2.20	B	+.80	2.43	C	-.43
2.21	C	-.21	2.10	C	-.10
2.11	A	+.89	2.39	B	+.61
2.12	A	+.88	1.93	C	+.07
2.23	C	-.23	2.18	C	-.18
3.05	C	-1.05	2.97	B	+.03
2.03	B	+.97	2.70	B	+.30
1.94	B	+.06	3.10	A	+.90
			2.22	C	-.22
			2.22	B	+.78
			2.16	C	-.16
			1.96	C	+.04
Average					
2.22	2.78	+.56	2.40	2.54	+.14

Table 3  
STUDENT PERFORMANCE IN AERO 311 DURING 1981 SUMMER SEMESTER

REPEAT (8 Students)			NON-REPEAT (10 Students)		
Cum GPA	Course Grade	Deviation	Cum GPA	Course Grade	Deviation
2.62	C	-.62	2.55	B	+.45
2.00	B	+1.00	2.70	A	+1.30
2.26	C	-.26	2.05	D	-1.05
2.19	C	-.19	1.99	C	+.01
2.79	B	+.21	2.34	B	+.66
2.18	C	-.18	2.53	A	+1.47
2.80	B	+.20	2.41	B	+.59
2.27	A	+1.73	2.45	A	+1.55
			3.89	A	+.11
			2.23	A	+1.77
Average					
2.39	2.63	+.24	2.51	3.20	+.69

percent, while a similar exam given during the summer semester had a higher mean score of 76.2 percent.

Table 4 shows that Aero 312 repeat students averaged about one-half letter grade better than their cumulative GPAs, while non-repeat students performed about as predicted by their cumulative GPAs.

#### IV. Qualitative Results

A performance analysis of the summer semester students must also include some subjective comments by the instructors involved in teaching and by the students themselves. The Aero 311 and 312 instructors found their students, both repeat and non-repeat groups, to be much more responsive during the summer semester. Daily preparation, as measured by class participation and quiz scores, appeared to be more thorough than during the regular academic year. To a slight degree, both instructors found the class participation to be

Table 4  
STUDENT PERFORMANCE IN AERO 312 DURING 1981 SUMMER SEMESTER

REPEAT (9 Students)			NON-REPEAT (12 Students)		
Cum GPA	Course Grade	Deviation	Cum GPA	Course Grade	Deviation
2.45	B	+.55	2.24	C	-.24
3.16	A	+.84	2.47	C	-.47
2.28	B	+.72	2.11	D	-1.11
2.54	B	+.46	3.32	A	+.68
2.04	B	+.96	1.99	C	+.01
2.59	B	+.41	2.52	C	-.52
2.27	C	-.27	3.95	A	+.05
2.26	B	+.74	2.68	A	+1.32
2.44	B	+.56	2.30	C	-.30
			2.38	C	-.38
			2.95	B	+.05
			2.05	B	+.95
Average					
2.45	3.0	+.55	2.58	2.58	0

at a higher level for the non-repeat students than for the repeat students. Student comments on the desirability of taking engineering courses such as Aero 311 and 312 during the summer semester were quite favorable. Both repeat and non-repeat student groups responded on their end-of-course critiques that the continuity afforded by a rapid succession of lessons made the engineering concepts easier to understand. Both groups commented that their relative lack of other activities aided greatly in their course performance.

V. Conclusions

As a result of this study, several conclusions can be supported by the data collected. First, the average non-repeat student does not harm his or her GPA by voluntary enrollment in summer engineering courses. The presence of first-time students in the summer engineering core courses offered at the Air Force Academy does not seem to hold back class learning. The continuity provided by the rapid succession of lessons, and the relative lack of activities which compete for a student's attention and detract from course preparation time allows both repeat and non-repeat students to do well.

Secondly, while the engineering concepts taught in these courses are difficult to learn, the students seem to grasp them well, in so far as quantitative methods of measuring performance in class preparation and tests are concerned. These measurement techniques, it should be noted, only determine short-term understanding and retention of course material. In this study we did not attempt to measure the students' long-term retention of the material taught during the summer semester, and thus no generalization regarding that issue can be made.

But on the basis of this preliminary and rudimentary study, it would appear that the Academy should not inhibit the enrollment of any students who wish to take engineering core courses for the first time during the summer semester.

REFLECTIONS OF AN ENGLISH LITERATURE MAJOR ON  
OUR TECHNOLOGICAL SOCIETY\*

J.M. Kempf\*\*

Abstract

For much of the twentieth century artists and intellectuals have been critical of the technological orientation of modern industrial society. Many social analysts argue that the contemporary era is characterized by an increasing estrangement between humanistic and scientific disciplines of knowledge. A teacher with experience in both disciplines argues that we must reverse this situation. To do this, engineers as well as scholars of the humanities must develop a common language that will enable all educated persons to communicate across the artificial barriers that have been erected around specialized domains of knowledge.

As one who has spent a number of years training to join a profession of humanities teachers and scholars and who has several times found himself involuntarily enlisted in the ranks of workers in large technological organizations, I sympathize with the plight of many modern artists who see the seemingly overwhelming inertia of technological society as a threat to the human--and humane--crafts of the arts. Indeed, it seems a threat to culture as we know it. But my experiences in technological organizations have also made me aware of the fact that the purported conflict between the arts, or humanistic knowledge, and the sciences may be an exaggerated and certainly unnecessary, not to mention destructive, concept. Let me try to explain why I think this is true.

While recently thinking about this subject, I was reminded of something I heard Saul Bellow say several years ago. Bellow was describing Joyce's Ulysses and the impact it had on him as a young writer because of its insight into a crucial problem facing writers in the modern world. This problem, as Bellow saw it, was that literature has become overwhelmed by the sheer glut of written communication caused by technology. The fact that this situation has been compounded by the electronic revolution since Ulysses is a common theme of modern sociology as well as literature.

My subject really does not deal with English literature as an art such as Bellow himself writes, but rather with English as a skill badly needed for clear communication in a modern, technically oriented society. This skill is particularly vital today because the relationship between the wisdom of the arts and the humanistic tradition of knowledge and the factual information that characterizes the world of modern business and technological enterprises appears to be one of widening distance. Some of the reasons for this situation are historical.

Ever since the English Romantic poet William Blake condemned Isaac Newton to torment because of Newton's purportedly wicked powers of "Urizen," modern literary art and a good deal of literary theory has claimed that the "rationality" of science and technology was the source of modern cultural destruction. This idea fostered the notion of a split between two cultures, the scientific and the literary or

---

\*This paper is a slightly revised version of remarks delivered to the First Southwest Regional Convention of the National Council of Teachers of English, Las Vegas Hilton Hotel, October 18, 1980.

\*\*Captain, USAF, Instructor of English, DFENG

humanistic. For several decades academics have been at work analyzing the profound implications of the shift of social power taking place to a "New Class" of technocratic experts and managers that has occurred over a period of decades, but most rapidly in the post World War II era. This subject of shifting social power is a heated one among political scientists, economists, and sociologists.

In contrast to sociological analyses of our rising technically oriented society, modern literary responses have generally attempted to ignore analysis. Modern writers like D.H. Lawrence and W.B. Yeats sought refuge from technical culture in neo-primitive or anti-rational mythologies. For example, during the 1930's the American writer Henry Miller found expression for his feeling of cultural oppression by asserting that a vast conspiracy against the human spirit existed within modern corporate society which was symbolized for Miller by the "Cosmodemonic Telegraph Company of North America," which reached everywhere robbing modern man of freedom and spirit. He argued that the only available response was escape through imaginative creation, that permitted art to transcend mundane, material reality. Failing that he stood and raged:

"What is true interests me scarcely at all, nor what is real; only that interests me which I imagine to be, that which I had stifled every day in order to live.... I wanted to see America destroyed, razed from top to bottom... as atonement for the crimes that were committed against me.... And yet [I] remain powerless to alter my life" (Ref. 1).

Norman Mailer rephrased this theme in 1968 in The Armies of the Night, his analysis of our Vietnam debacle, a war caused, he said, by the lobotomizing effect of technology on American sensibility and by an imperious rationality:

"Technology had driven insanity ... out of all the lost primitive places; one had to find it now wherever fever, force, and machines could come together, in Vegas, at the race track, in pro football.... None of it was enough--one had to find it in Vietnam...."

Mailer summarized his view of the current American cultural dilemma, brought about by what he believed was our worship of technology, when he described the alienated youth of the 1960's:

"There were nightmares beneath the gaiety of these middle class runaways, these Crusaders, going out to attack the hard core of technology land ... [where] nature was a veil whose tissue had been ripped by static, [by] screams of jet motors, the highway grid of the suburbs, smog, defoliation, and pollution of the streams...." (Ref. 2).

More recently, in his own portrait of a ruined writer friend Delmore Schwartz, Saul Bellow wrote of the self-defeating results of the long literary opposition to technological culture. In pondering Schwartz's shabby death, Bellow asked the following rhetorical questions about the role of writers in a modern technical world:

"....were poets like drunkards and misfits or psychopaths, like the wretched, ... destined to sink into weakness.... Having no machines, no transforming knowledge like Boeing, or Sperry Rand or IBM or RCA? Could a poem pick you up in Chicago and land you in New York two hours later? Could it compute a space shot? It had no such powers. And interest was where power was. In ancient times poetry was a Force, the poet had real strength in the material world. Of course, the material world was different then. But what interest could a Humboldt raise? He threw himself into weakness and became a hero of wretchedness. He consented to the monopoly of power and interest held by money, politics, law, rationality, [and] technology...." (Ref. 3).

I have emphasized this literary opposition to modern corporate and technical society because it has become a central issue for academic humanities departments in recent times. The constant discussion of the

"crisis in the humanities" has led to numerous studies seeking ways to find "relevance" in school curriculums to meet the trend of vocationalism among students, to bridge the gap between the humanities and science, and to salvage whole departments from pessimism and self-immolation. The crisis has led to much cynicism among academic humanities teachers and to some who see a vast capitalist conspiracy to turn academic life itself into merely an instrument for training a technical force for big business. Such pessimism and cynicism may be misguided and counter-productive.

In the title story of his collection City Life, Donald Barthelme wrote about the tasteless, cliche-ridden lives of contemporary urban adults. One of the central symbols in this story about the spiritual emptiness of our technological age was a television. What particularly interested me in the symbol was that Barthelme emphasized the television brand name -- Motorola (Ref. 4). Now, by an odd quirk of circumstances, several years ago I found myself recruited out of a graduate program in English literature and asked to accept a job with Motorola Electronics Corporation, a job I never would have pursued on my own, believing as I did, that a person with an English literature degree was about as necessary to a modern electronics company as an old vacuum tube. What I discovered was that, indeed, the company did not necessarily need someone with broad literary knowledge. But it did need someone who could produce clear, intelligible prose. In fact, the company could not get paid without technical reports that were intelligible, and few professional engineers can write such reports.

Similarly, I found that the broad knowledge I possessed, not about technology but about business, world affairs, and the arts, permitted me to provide an important dimension to the corporation and its people. And I found that the engineers working at Motorola were not lobotomized technicians. Several held season tickets to the Chicago Symphony Orchestra and Chicago's Lyric Opera, one raised exotic forms of African violets, another was a former president of the Chicago Rhododendron Society. Many were fervent environmentalists and, though often lacking in wide reading, were eager for conversation with someone who was well read in all kinds of humanistic subjects, from politics to art. One audio engineer, a specialist in microphone design, provided tapes of local Chicago area college musical events to one of the few remaining classical FM radio stations in Chicago.

What I am suggesting here is that if technological organizations in our society have become identified in modern literature as enemies of culture, it is also a fact that human beings constitute those technical organizations and are as interested as anyone in the full range of human subjects that touch their lives. Indeed, the human dimension of society is, or ought to be, modern industry's chief concern, whether it be the psychology that causes abrupt market changes in foreign currency values, labor matters, communication laws, foreign business regulations, and government, politics, and divergent cultures and cultural values. To deal with this human culture, business needs people who can read and write and think about all these subjects and communicate to a variety of audiences. Modern technical businesses in particular absolutely depend on written communication and on employees who can translate the technical jargon of their often

crippled writing into intelligible English prose.

By the time I left Motorola I was supervising a wide range of written corporate and technical communications, such as operating and repair manuals, research and development reports, financial reports, and numerous other types of written work. I had designed and taught a writing course for managers and engineers dealing with international markets, and I had become frustrated because I could not always get the organization to work efficiently. And I discovered that the inefficiency of a great deal of modern institutional life is due, in large part, to indecisiveness about, and lack of expertise in, written communication.

The skills and knowledge that humanities students bring to modern business, then, are hardly irrelevant. They may, in fact, be crucial to the business world's success in the future.

Many economists have recently come to the conclusion that a major cause of the decline in American economic productivity is incoherent written and verbal communication. Think of this assertion for a minute--faulty syntax leads to confusion and therefore has directly weakened our national security! That statement must boggle the minds of some of our current defense analysts. Yet, if one accepts this assertion, it is understandable that management experts place high value on communication skills as a major component of business and government leadership.

My own job experience, as a university teacher, a civil engineering assistant, a worker in the gargantuan bureaucracy of modern government and the military, or as an editor and manager of communications for a large American technological organization, convinces me that humanistic studies, particularly the discipline of English as an academic background when coupled with knowledge of other disciplines, is vital to modern American industry. Who else but a trained writer is impatient with sometimes incoherent bureaucratic and technical written communication? And who else is capable of radically paring wordy communication so that it becomes clear, precise, and economical? Let me give an example from personal experience. Two months into my job at Motorola I had cut approximately 50 percent of a monthly report on research projects that saved management time and many overtime and weekend sessions for a number of people. In the Air Force, I once did a similar job, thereby permitting eight people to do what they were trained to do--fix airplanes. The "editorial" principles of standard English usage, when applied as a "technical skill" to communicate information, cut across all organizations and disciplines. We need to emphasize how this skill trains people, engineers as well as students of the arts, to think clearly, efficiently, and acutely in analyzing all subjects, not just literature. A really good English student ought to be impatient with unnecessary meetings, wasted discussion, unclear forms, or unnecessary activities and instructions and he should be critical of sloppy thinking. This attitude and the associated skills are the essence of management.

Nor is it the case that we should merely think that training in the humanities, in the sense of emphasizing skills such as "editing," is a vocational education. Humanistic perspective and values are also

crucial to the success of modern industry. But humanities departments have insufficiently addressed this issue. For example, the September 1980 Atlantic Monthly contained an article analyzing what is wrong with the American economy. Incidentally, it points to companies like Motorola and the electronics industry as a hope for the future to provide more jobs, labor-saving efficiency, and a liberation of men from dull routine work (Ref. 5). That has always been the hope for technology. But if humanities teachers wish to participate in the modern economic challenge, they must recognize that all technology requires written English instructions on how to repair and operate machines, and industry needs people to clearly communicate to the public the problems which technology creates. There are many positions in America that badly need students who can combine writing skills with knowledge of and interest in physics, electronics, and all other scientific and engineering disciplines. And those disciplines badly need translation into a common cultural language.

What we need today is a new perspective on the relationship between humanistic, and particularly English, "knowledge" and our contemporary social order based on technology. The old antagonistic attitude is self-defeating, and dangerous. For example, in his book English in America, the former editor of the journal College English, Richard Ohmann, begins by opposing English to science. He criticizes academic English scholars for allowing their subject to become narrowly specialized and disconnected, unlike science he says, to generalized theories relating English research to a larger cultural reality. In aping scientific specialization humanities teachers have failed, Ohmann argues, to emphasize the moral insights of literature and to provide a theoretical framework to integrate the subject into our larger cultural context (Ref. 6). Much of what he says is true--but not totally. Technological research is often extraordinarily specialized, boring, and unconnected to wider theory. And it certainly, sometimes critically, lacks a humanistic perspective.

Similarly, in a recent article expanded from remarks made at MIT during the spring of 1980, John Hersey noted that C.P. Snow's famous description of the gap separating the "two cultures" of technical and humanistic education has, even with some curricular reforms at major universities, become wider rather than narrower as Snow had hoped. Hersey places most of the blame for this situation on humanities departments for their avoidance of science (Ref. 7). Much of what he says is true--but not totally.

Furthermore, most discussions of the conflict between science and the humanities ignore the issue of "power" which Saul Bellow, Norman Mailer, and Henry Miller so astutely noted. To deal with it we must insure that students can program a computer and edit a paper on physics as well as analyze a poem. This premise applies to technical as well as humanities students. Such a goal means we need to return to a philosophy of education, and a curriculum, that emphasizes the tradition of liberal arts with the term "liberal" somewhat redefined. Every humanities student should take several courses in physics and the natural sciences, in math, and in basic accounting, and four years of one foreign language as well as literature, history, and philosophy. One of the most valuable skills American business will require in the

future is the skill to speak other languages to deal with our increasingly international culture. Engineers need to contemplate the human dimension of their disciplines too. We need more than ever today a common language that permits us to find a common ground between our increasingly specialized domains of knowledge.

Let me also note that those who blame the current plight of the humanities (or the lack of political influence of humanities departments) on their indifference to technical issues have never edited technical or business prose or read technical journals or textbooks. Fifty years ago the French Surrealists advocated writing prose that was unrevised, disorganized, unintelligible, and irrelevant to social reality. Much business and technical prose has achieved today what Surrealism only dreamed of. The excuse used by engineers that one doesn't have sufficient background to understand technical subjects is usually an excuse for incoherent and elliptical writing on those subjects. Technical writing is often incoherent because it fails to describe completely the premises and reasoning processes behind, or the actual design of, machinery or scientific research and assumes that its intended audience will fill in missing information. The frustration technical people feel in reading their own journals proves that this assumption is fallacious. Thus, "technical expertise" in English, the ability to organize ideas and information coherently, to revise syntax, to choose precise and logical combinations of words, and to subordinate ideas is precisely what is missing in much contemporary scientific and technical writing.

Technical culture does have power today, but it is also dangerously vulnerable. To protect us all from the sometimes blind arrogance, foolhardiness, and short-sighted vision of business and technical organizations whose technology affects public life from places like Love Canal to Three Mile Island, we must translate the jargon of technical subject matter, including legal and medical writing, into a universal language intelligible to all citizens. Such a "job" is crucial to a freely functioning society if it is to make rational decisions about its own future based on all available knowledge. I don't think engineers, trained as they are in the contemporary world, can do this translating work. Lewis Thomas and Barry Commoner do not seem to have many peers in the scientific and engineering professions.

My experience tells me that far from being merely ornamental or a luxury in this world, command of the skills of language is extraordinarily important in terms of power in modern society. For students these skills don't just make better citizens or provide them vocational employment. They allow them to maintain their freedom. Totalitarian regimes always arrest dissident writers first. Presidents and corporate executives have speech-writers as their closest aides. And the most crucial war of our time is the one for our minds, a war fought through propaganda, subliminal advertising, and outright manipulation of information. Let me illustrate.

Recently I read an editorial in a Colorado newspaper that charged John Anderson and President Carter with "appeasement" for believing that diplomacy was the first line of American strategy and for opposing certain costly military weapons systems. Another article by a retired Air Force General urged that America support the new Korean military government because Koreans were not used to democracy and therefore we

should not force it on them, as if our treasure and lives had not been expended there for thirty years for just that reason. And a corporate advertisement several months ago urged America not to allow single interest groups to divide our basic national unity, a unity that was good for the company which got much of its business from the government. But when the Justice Department subsequently filed suit against the company for anti-trust violations due to acquisitions that led to domination of certain technology markets, the company changed its advertising. Today unity is said to be bad. The company's public advertisements now call for nonintervention in free markets by government agencies. Finally, an article I read in the August, 1980, issue of Commentary magazine by a literature professor at Berkeley (Ref. 8), reviewing recent books about the American literary history of the 1930's by Edmund Wilson and Malcolm Cowley, attacked the purported "Marxist ideology" of these eminent men of American letters. The article was particularly disturbing because I have read most of the letters and articles this professor only selectively used as evidence for his accusations, and I was stunned by the extent to which he quoted material out of context or misrepresented other material.

Each of these essays, or the corporate advertisement, severely violates basic principles of rhetoric. These violations include consecutively: ad hominem attacks on politicians that beg the question of issues, sweeping generalizations that ignore history or our own political values, corporate manipulation of language that clouds truth and motives, and academic criticism that is close to being scandalous since the "professional standards of English" demand that we do not quote information out of context, misrepresent a writer's full text, or use post hoc ergo propter hoc argumentation. Indeed, teaching the "techniques" of communicating historical truth through documented research has traditionally been the domain of English departments whose professionals are vested with responsibility to uphold the standards of objective scholarship.

Now, no engineer I know could analyze, let alone be aware of, the "technical" violations of language and the manipulation going on in these articles. Engineers are, in effect, helpless in the war of words for control of our minds. It is in this regard that modern technical society badly needs people informed about the values and lessons of human cultural history and who possess the technical skills of communication and verbal analysis.

Humanists should be experts in human civilization, that arduous accumulation of wisdom, about human nature and society and its fragile balance, that was built from the long search for truth throughout recorded time; and truth requires language for transmission of these truths to successive generations, whether it be the truths of Shakespeare or Newton. It is this expertise that must be marshalled when confronting technology with questions about social design and values and that must be used to help direct technical energies into productive and constructive civilized goals. But to do this, humanists have a responsibility to do more than criticize and bemoan a loss of influence. To direct technical energy into civilized, humanistic activity, humanists must first understand their sometime and now longstanding

antagonist--technology. Modern business and government also need wise, humanistic, and historical perspective to save them from themselves. For the history of modern business, and of authoritarian governments, is that their often short-sighted goals undermine their own long-term success and create a political climate of extremist opposition.

Thus, instead of training in weakness, the study of the humanities creates an educated citizenry capable of analyzing technical inertia as well as propaganda and false statements. Such a citizen is a thinking force of power, the most subversive force on earth and hardly powerless in the face of any kind of information, technical or advertising.

Literature is the discipline best suited to train us to analyze language because it is the best, most complex use of language used to transmit human values. It is not, therefore, contradictory to study literature as the means to discipline and train the human mind or master communicative "skills." Scientists, after all, don't train on quacks or bad technology; they study the best, often the most lucid and elegant technical thinkers and writers like James Clerk Maxwell, Einstein, and Galileo.

Another needed reform of pedagogical attitude concerns humanities teaching itself. We should train our students, including future engineers, so that they will become an audience for art and literature rather than themselves becoming academic literary critics or scholars. Such an attitude is not a retreat, though it may mean there are fewer graduate students studying specialized subjects. Rather, it is a reassertion of the idea that always governed liberal education. We should train good citizens who will have a breadth of historical perspective and an appreciation for civilized values, and an understanding of where technology fits in the overall ideal of a "good and just" society. Such a task requires cooperation among disciplines, not antagonism.

"The whole argument about a dichotomy between art and science may be false. Lewis Mumford once wrote that technology is not inherently inimical to art (Ref. 9). The construction of the violin led to Beethoven! And some Motorola engineers I know don't watch television. They listen to Beethoven--or belong to the Sierra Club.

#### References

1. Miller, H. Tropic of Capricorn. New York: Castle Books, 1961, pp. 10-13.
2. Mailer, N. The Armies of the Night. London: Weidenfeld and Nicolson, 1968, pp. 153 and 192.
3. Bellow, S. Humboldt's Gift. New York: Viking Press, 1975, p. 155.
4. Barthelme, D. "City Life," City Life. New York: Farrar, Straus & Giroux, 1970, pp. 149-168.
5. Fallows, J. "American Industry: What Ails It, How to Save It." The Atlantic Monthly, September 1980, pp. 35-50.
6. Ohmann, R. English in America: A Radical View of the Profession. New York: Oxford University Press, 1976, Chapter 1.

USAFA-TR-81-11

7. Hersey, J. "The Triumph of Numbers." The Atlantic Monthly, October 1980, pp. 78-84.
8. Alter, R. "The Travels of Malcolm Cowley." Commentary, August 1980, pp. 33-40.
9. Mumford, L. Art and Technics. New York: Columbia University Press, 1952.

**SECTION V**

**Aeronautical History**

THE EVOLUTION AND FUTURE OF AEROPROPULSION SYSTEMS\*

Hans von Ohain

Editor's Note

Hans von Ohain independently initiated the development of the turbojet engine in Germany prior to World War II. He directed a research and development program which led to the HeS-3B turbojet engine, which was used to power the Heinkel He-178. The He-178 made the world's first turbojet-powered flight on August 27, 1939. In this paper on the evolution and future of aeropropulsion systems he discusses the beginnings of the turbojet engine in Germany. We are pleased to publish this paper as a companion to the article by Sir Frank Whittle in the May 1961 *Dirigat*. Together these papers detail the development of the first jet aircraft.

I. Introduction

In this discussion about the evolution and future of aeropropulsion systems, I will address four main topics: (A) I will give a very condensed overview of the entire evolution of aeropropulsion systems. (B) Then I will highlight the beginning of jet propulsion, including my activities in the early phases of jet engine development. (C) I will show how the evolution progressed from first generation simple, fixed geometry turbojets to the highly complex, giant jet and fanjet engines of today. (D) Finally, I will discuss future potentialities of aeropropulsion systems.

II. Discussion

A. The Evolution of Aeropropulsion Systems

Since the beginning of powered flight, the evolutions of both the aero-vehicle and aeropropulsion systems are strongly interrelated, and are governed by a few major thrusts, namely: demands for improving reliability, assurance and lifetime improvements in flight performance, such as speed, range, altitude maneuverability; and in more recent times, strongest emphasis on overall economy. Under these thrusts the technologies of aero-vehicle and propulsion systems advanced continuously.

To gain a better insight in the evolution of aeropropulsion systems it is necessary to be aware of the concurrent advancements in aero-vehicle technology. We can observe a continuous trend towards lighter and stronger airframe structures and materials; from wood and fabric to all metal structures to lighter and more heat-resistant materials, and finally to composite materials. At the same time, the aerodynamic quality of the vehicle, characterized by the ratio of "Lift to Drag" (L/D) increased over the years and extended to higher flight speeds. This is illustrated in Figure 1, which I would like to discuss briefly. In order not to lose proper historical perspective, let us recall that at the turn of our century the science of aerodynamics was in its infancy, specifically, the phenomenon of aerodynamic lift was not understood. Therefore, the early pioneers could not benefit from scientific knowledge; they had to conduct

\*Printed courtesy of the Smithsonian Institution Press from The Jet Age: Forty Years of Jet Aviation, Walter Bryant and Donald L. Lewis, eds., c. 1979, Smithsonian Institution, Washington, D.C.

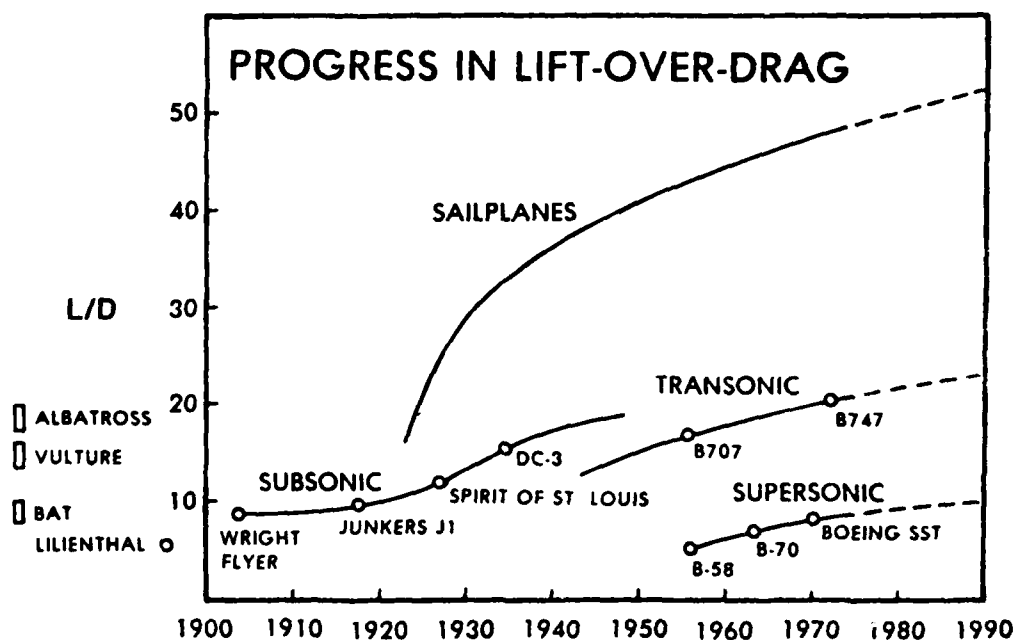


Figure 1. Lift-To-Drag Ratio

their own fundamental investigations. The world's first successful glider vehicle by Lilienthal in the early 1890s had an L/D of about 5; by comparison, birds have an L/D ranging from 5 to 20. The world's first man-controlled powered aircraft, by the Wright brothers in 1903, had an L/D of about 7.5. As the L/D values increased over the years, sail planes advanced most rapidly and are currently attaining the enormously high values of about 50. This was achieved by employing ultra high wing aspect ratios and profiles especially tailored to the low Reynolds and Mach numbers of those airplanes. Powered aircraft advanced to L/D values of about 20 in the late 1940s by continuously improving aerodynamic shapes employing advanced profiles, extremely smooth and accurate surfaces, engine cowls, and retractable landing gears. In the 1940s, this high aerodynamic quality was extended from the subsonic to the transonic flight speed regime by employing the swept wing principle, and later in 1952, the area rule of Whitcomb. In the late 1960s, the Boeing 747 attained in transonic flight an L/D of about 20. In the supersonic flight speed regime L/D improved from 5 in the mid-1950s to the currently considered L/D values of about 10. This progress can be attributed to the application of artificial stability and also to area rule, and advanced supersonic profile shapes which are made possible by advanced structures. The hypersonic speed regime is not fully explored. Current emphasis is placed on wing reentry vehicles and lifting bodies where a high L/D is not of greatest importance. Fundamental investigations have shown that much greater values of L/D than those currently employed are attainable.

To appreciate the technological advancements in propulsion technology, let us again look back at the beginning of our century. Steam and internal combustion engines were then in existence, but were far too

heavy for flight application. The Wright brothers recognized the great future potential of the internal combustion engine and developed both a relatively lightweight engine suitable for flight application and an efficient propeller. Let us now look at the progress of propulsion systems over the years (Figure 2). The Wright brothers' first aeropropulsion system had a shaft power of 12 horsepower, and its ratio of power output to total propulsion system weight including propeller and transmission was about 0.04. Through the

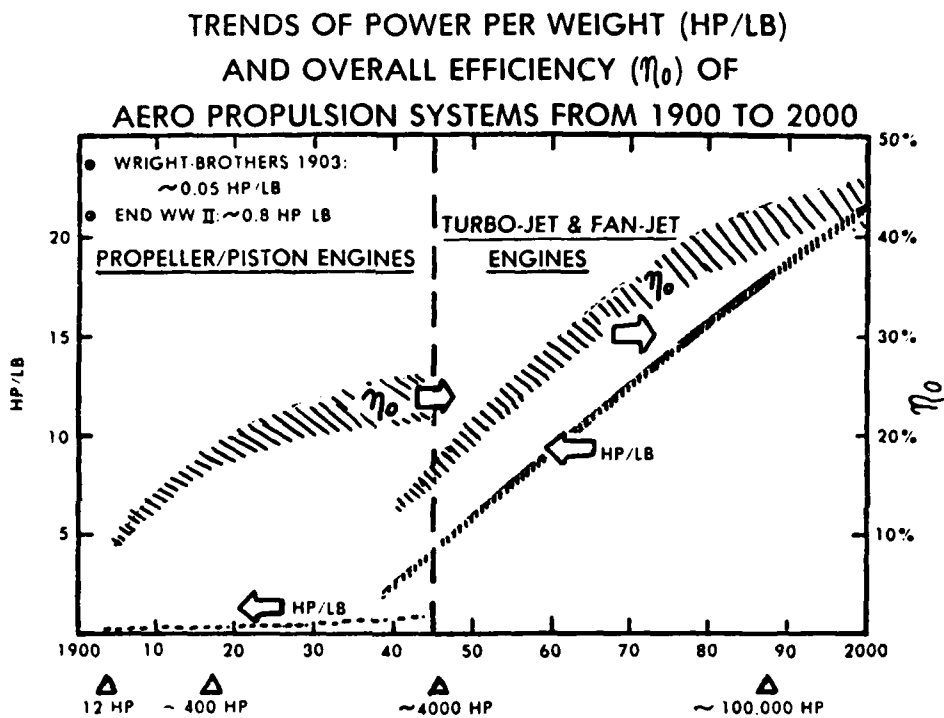


Figure 2. Progress in Propulsion Systems

subsequent four decades the horsepower weight ratio improved by more than an order of magnitude, to about 0.7 hp/lb. The power output of the largest engine amounted to about 4000 hp and the overall efficiency (engine and propeller) reached about 25 percent. In the mid 1930s, the turbojet came into being. This new propulsion system was immediately superior over the reciprocating engine with respect to power-to-weight ratio; however, its overall efficiency was initially lower than that of the reciprocating engine. As can be seen, progress was rapid. In less than four decades the power-to-weight ratio increased more than tenfold and the overall efficiency exceeded that of a diesel propulsion system. The power output of today's largest gas turbine engines reaches nearly 100,000 horsepower.

These truly gigantic technological advancements had an enormous impact on flight performance. The improvements in aerodynamic quality and overall engine efficiency tremendously increased the flight range and total aircraft economy. The lighter vehicle structures and greater engine power/weight ratios had a crucial impact on aircraft maneuverability and flight speed.

The increase in flight speed over the years (Figure 3) may be best suited as a basis for discussing the evolutions of aero-vehicle and aeropropulsion systems. In December 1903, the Wright brothers succeeded

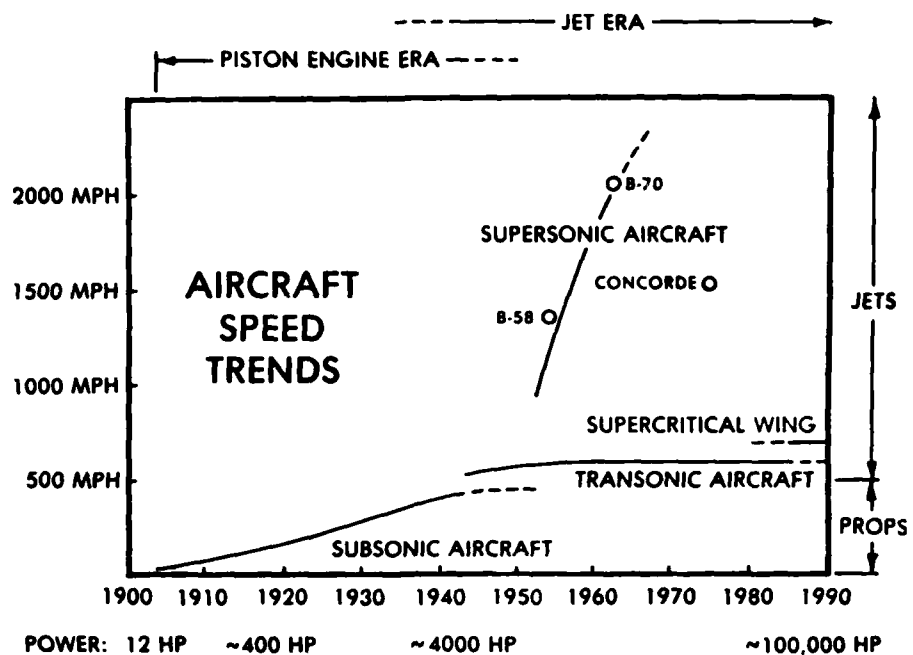


Figure 3. Increase in Flight Speeds

with the first man-controlled powered flight in the world. While the flight speed was only 30 mph, the consequences of the first flights were enormous:

- (1) Worldwide interest in powered flight was stimulated.
- (2) The science of aerodynamics received a strong motivation.
- (3) The U.S. Government became interested in powered flight for potential defense applications.

In 1909 the Wright brothers built the first military aircraft under government contract. During World War I, aircraft technology progressed rapidly. The flight speed reached about 150 mph, and the engine power output 400 horsepower. After the war military interest dropped, but aircraft technology had reached such a degree of maturity that two nonmilitary application fields could emerge, namely:

- (1) Commercial Aviation - Mail and passenger transport. (First all metal monoplane for passenger and mail transport: Junkers F13, 1919.)
- (2) Stunt Flying leading to General Aviation. (Sport and private transportation.)

In the period from 1920 - 1940, the speed increased about 350 mph through evolutionary improvements in vehicle aerodynamics and engine technology, such as supercharger, variable pitch propeller, and improvements in engine design, structures, and materials.

At the end of World War II, the flight speed of propeller aircraft reached about 400 to 450 mph and the power output of the largest reciprocating engines was 4000 horsepower. This constituted about the

performance limit of the propeller/reciprocating engine propulsion system. Today, the propeller/reciprocating engine survives only in smaller, lower speed aircraft used in general aviation.

During the 1930s, jet propulsion emerged which promised far greater flight speeds than attainable with the propeller/piston engine.

The first jet propelled experimental aircraft flew in Summer 1939, and in early 1941 the first prototype jet fighter began flight tests.

In 1944, mass produced jet fighters reached a speed of 620 mph.

In the early 1950s, jet aircraft transgressed the sonic speed. In the mid-1950s, the first supersonic jet bomber (Hustler) appeared, and later the B-70 which reached Mach 3.

Also during the 1950s, through more than 15 years of military development, gas turbine technology had reached such a maturity that commercial applications became attractive:

- (1) Commercial Aircraft, e.g. Comet, Caravelle and Boeing 707.
- (2) Surface Transportation (land, sea).
- (3) Stationary Gas Turbines.

In the early 1960s, the high bypass engine appeared which revolutionized military transportation.

In the end 1960s, based on the military experience with high bypass engines, the second generation of commercial jet aircraft, the "Wide Body Aircraft" with large passenger capacity, such as the Boeing 747, and later the "Tri-Stars," came into being. By that time the entire commercial fleet exclusively used gas turbine engines.

Advantages for the airlines were: (1) overall fan jet efficiency equivalent to diesel; (2) overhaul between about 5 million miles; (3) short turn-around time; (4) passengers enjoy the very quiet and vibration-free flight, the short travel time, and the comfort of smooth stratospheric flight.

By the end of the 1960s essentially the entire business of passenger transportation was diverted from ships and railroads to aircraft.

In the mid 1970s, the third generation of commercial transport, the supersonic Concorde, 1500 mph, appeared with an equivalent power output of about 100,000 horsepower.

In summary, the evolution of aero-vehicle and aeropropulsion systems looks, in hindsight, like a masterplan. The evolution began with piston engine and propeller which constituted the best propulsion system for the initially low flight speeds, and had an outstanding growth potential up to about 450 mph.

In the late 1930s, when flight vehicle technology reached the ability to enter into the transonic flight speed regime (in excess of 500 mph) which was beyond the capability of the propeller/piston engine, the jet engine had just demonstrated its suitability for this flight speed regime. A vigorous jet engine development program could be launched. Soon the jet engine proved to be not only an excellent transonic but also a supersonic propulsion system. This resulted in the truly exploding growth in flight speed.

It is interesting to note that military development preceded commercial applications by about fifteen

to twenty years of both the propeller engine and the gas turbine engine. The reason is that too many generations of improved propulsion systems were required before a commercial utility could be envisioned.

Today, after 75 years of powered flight, the aircraft has outranked all other modes of passenger transportation and also has become one of America's greatest single export articles.

The evolutions of both aero-vehicle and aeropropulsion systems have in no way reached a technological level which is close to the ultimate potential! The evolution will go on for many decades toward capabilities way beyond current feasibility and, perhaps, imagination, which I will discuss later.

#### B. The Beginning of Jet Propulsion

Let us now bring the beginning of jet propulsion in focus.

In the time period around the early 1930s, aircraft performance was in a state of continuous advancements. The flight speed was around 250 mph, sufficiently away from any critical speed limit for airplane or propeller/piston engine; and therefore no immediate need for a radically new propulsion system seemed to exist. However, this situation changed in 1935 when the theoretical possibility of flight speeds near and above the speed of sound was envisioned by a swept-back wing. This historical event is described in Dr. T. von Karman's Memoirs, "The Wind and Beyond." Let me quote:

"The fifth Volta Congress in Rome 1935 was the first serious international scientific congress devoted to the possibilities of supersonic flight. I was one of those who had received a formal invitation to give a paper at the conference from Italy's great Guglielmo Marconi, inventor of the wireless telegraph. All of the world's leading aerodynamicists were invited.

"This meeting was historic because it marked the beginning of the supersonic age. It was the beginning in the sense that the conference opened the door to supersonics a meaningful study in connection with supersonic flight, and secondly because most developments in supersonics occurred rapidly from then on, culminating in 1947 -- a mere eleven years later -- in Captain Charles Yeager's piercing the sound barrier with the X-1 plane in level flight ... In terms of future aircraft development, the most significant paper at the conference proved to be one given by a young man Dr. Adolf Busemann of Germany ... by first publicly suggesting the swept-back wing and showing how its properties might solve many aerodynamic problems at speeds just below and above the speed of sound."

The prospects of the propeller/piston engine as a propulsion system for flight speeds above subsonic speed were by far not as good as those of the aero-vehicle for a number of reasons. One of the major reasons is that the propeller becomes inefficient and very noisy at high subsonic flight speeds; another reason is that the power-to-weight ratio of the reciprocating engine is too small for high subsonic and supersonic flight speeds.

In hindsight, this situation was ideal for launching the development of a radically new propulsion system that promised the capability of flying much faster than the propeller/piston engine. At that time, however, the aircraft engine industry had no understanding of the need for future high speed propulsion systems. As a matter of fact in 1938, when the German Air Ministry tried to sponsor the development of turbojets, the aircraft engine industry was completely negative to such a project.

I cannot claim that I had a clear picture of the imminent need for jet propulsion, nor was I aware of the various turbojet propulsion patents already in existence such as the patent of Guillaume (1921) and the farsighted patent of F. Whittle (1930). My enthusiasm in jet propulsion was based more on the intuition

that a continuous aerothermodynamic propulsion process could be inherently more powerful, smoother, lighter, and more compatible with the aero-vehicle than a propeller/piston engine.

In the Fall of 1933, my thoughts began to focus on a steady aerodynamic flow process in which the energy for compressing the fresh air would be extracted from the expanding exhaust gas. Such a steady flow process promised a far greater air volume handling capability than that of a reciprocating engine and consequently a much greater power concentration and power-to-weight ratio. Also, the air ducted into such a system could be decelerated prior to reaching any Mach number-sensitive engine component. Both of these characteristics are of greatest significance for a high speed propulsion system.

First, I intended to accomplish this process without employing moving machinery by bringing the inflowing fresh air in direct contact with the expanding combustion gas (a kind of ejector process). But after studying specific processes and configurations, it became apparent that such types of processes would have enormous problems with respect to internal losses and adverse heat transfer effects caused by mixing between fresh air and combustor gas. I put this idea aside for future considerations and began to investigate a propulsion process in which compression and expansion were separated, and carried out by a turbo-compressor and turbine respectively. Searching for an extremely lightweight, compact and simple configuration having a minimum development risk, I chose a radial outflow compressor rotor back-to-back with a radial inflow turbine rotor. This configuration also promised correct matching simply by providing equal outer diameters for the straight radial outflow compressor rotor and the straight radial inflow turbine rotor. I was aware of the possibility of employing axial flow compressors and turbines, and I considered an axial flow configuration as very desirable for future developments from a standpoint of small frontal area, but as too complex and expensive for the beginning. In particular, stage matching of a multistage axial flow compressor and matching of axial flow compressor and turbine without component test facilities appeared to me too risky.

During 1934, I conducted rudimentary design and weight studies and made some performance calculations based on a pressure ratio of 3:1 which appeared attainable with a single stage compressor and a turbine inlet temperature of about 1200 to 1400 degrees Farenheit. It appeared that at a high flight speed of about 500 mph, an overall efficiency could be obtained which was around 60 percent of that of an equivalent propeller/piston engine. The corresponding high fuel consumption was somewhat discouraging. However, the weight of such a propulsion system promised to be only a fraction (quarter or less) of that of an equivalent propeller/piston engine system. At that time the propulsion system of a fighter aircraft constituted a much greater weight portion than the fuel, and consequently the above trade between fuel weight and propulsion system weight seemed to be a very favorable one.

All in all, I was encouraged and began patent procedures. My greatest concern was what approach to choose for setting the idea of turbojet propulsion. I felt that in any case a working model would be most important, and so I decided at the end of 1934 to have a model built at my own expense at the auto repair

shop and garage "Bartels & Becker" in Goettingen.

I was well acquainted with this repair shop and with the head mechanic and machinist, Max Hahn, long before I thought of jet engines. I had a small car which I parked there, and in this way I had frequent conversations with Hahn about automobiles and other technical subjects, and I had gained the impression that Max Hahn had an outstanding natural engineering talent and was specifically knowledgeable in manufacturing methods.

So it came that I discussed with Max Hahn the cost and possibilities of building my demonstration model. I showed Max Hahn my sketches; he made many suggestions for simplification and changes to enable manufacturing the model with the machine tools of the auto repair shop. Hahn's ingenuity and practical mind brought the construction of my model within the realm of my financial means. Including combustor, the total price estimate was slightly greater than 1000 marks! The actual price was somewhat greater, mainly due to some changes. It is difficult to convert in a meaningful manner 1000 marks' work of machine-man hours of 1935 into dollars of today. If I would build the same model today, it probably would cost more than \$10,000.

The photos show the back-to-back compressor-turbine rotor (one shroud being removed) (Figure 4); primitive balancing on a lathe of Bartels & Becker's repair shop (Figure 5); and Max Hahn with the complete model engine (Figure 6).



Figure 4. Back-To-Back Compressor-Turbine Rotor

In this time period I worked at my PhD thesis in the Institute of Physics, G.A. University, Goettingen, under Prof. R.W. Pohl. I showed Prof. Pohl my theoretical investigations, the results, conclusions and a program for my working model. Although this was quite an extracurricular activity, completely unrelated to my thesis and to the work of the Institute, Prof. Pohl was open-minded and reacted very positively. Generously, he gave permission for the use of instruments and equipment of the Institute and for conducting experiments in the back of his Institute. I made essential measurements of temperature



Figure 5. The Bartels & Becker Repair Shop

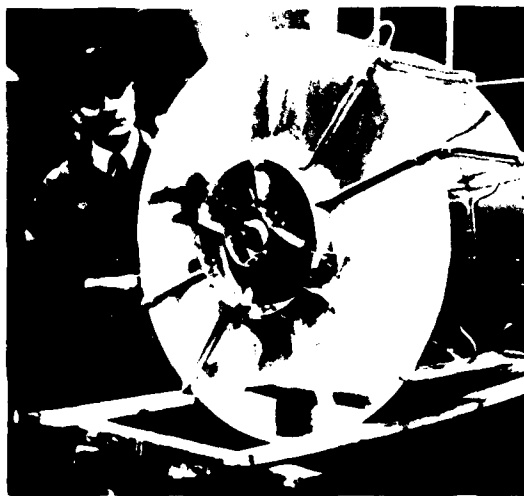


Figure 6. Max Hahn

and pressure distribution and gained valuable experience. Unfortunately, the gasoline combustors were not functioning. It appeared that the combustion did not take place within the combustor, but rather inside the radial turbine rotor extending into the exhaust jet; long yellow flames leaked out of the turbine, and the apparatus resembled more a flame-thrower than a turbine. The malfunctioning of the combustors was substantiated by temperature indications on the metal surfaces and the formation of lampblack depositions. Self-sustained operation could not be achieved, however, the starter engine was greatly unloaded. While the

experimental outcome was very disappointing for me. I cannot forget an evening instance. Max Hahn, who normally was very stern and skeptical, seemed in this instance quite positive and optimistic. He expressed hope and optimism in view of the fact that the drive motor was greatly unloaded and that the flames came out at the right place with seemingly great speed.

These tests indicated to me that the fundamental combustor investigations and systematic developments were necessary which would require time and money exceeding my private means. Again, Prof. Pohl came to my rescue. In a very cordial discussion he declared that he was convinced of the correctness of my considerations and of the great future potentialities of jet propulsion. However, he suggested that industrial support would be necessary. Prof. Pohl was willing to give me a recommendation letter to any company of my own choice. Intuitively, I thought that the engine industry would be negative toward a gas turbine development; and therefore I suggested the Heinkel Corporation, since Heinkel was the sole owner of his airplane company, and his unconventional thinking and enormous interest in the development of high-speed aircraft were generally known.\* Prof. Pohl wrote a letter of recommendation to Heinkel, and thereupon Heinkel invited me to come to his home in Warnemuende. He arranged a conference between me and a group of his leading engineers about my jet engine proposals. The engineers were undecided. The fuel consumption of the jet engine seemed to the group extremely high, but the power-to-weight ratio of a turbojet was considered as potentially better than that of the propeller/piston engine. Heinkel's two top aerodynamic designers, Siegfried and Walter Guenther, emphasized the need for high power output per frontal area (more than 2000 equivalent horsepower per square meter of frontal area). They also acknowledged the importance of abolishing the propeller in view of future high-speed aircraft. I suggested that the jet engine also could be utilized for the generation of direct lift. The back-to-back compressor/turbine configuration could lead to a flat "pancake" type engine suitable for wing installation. The thrust could potentially amount to several times the engine weight. Heinkel's engineers felt that this jet engine application was not attractive; however, since they did not altogether reject the idea of jet propulsion, Heinkel entered into an agreement with me. Upon my insistence he made two separate contracts, namely one royalty agreement and one employment contract (beginning on April 15, 1936). Max Hahn also became employed upon my request, after initial difficulties were resolved.

Heinkel wanted to keep the jet development apart from his aircraft organization with the goal to form a separate gas turbine division in the event that the early phases of jet development were successful. For this purpose he made a clause in my employment contract that I would report and be responsible directly to him for the development of the jet engine. However, for reasons of security this development was called Sonder-Entwicklung, i.e., "Special Development" rather than jet engine development. For the same reason he wanted the location of the "Special Development" to be separated from the rest of his company, and so a

\*I learned later that my belief about a negative attitude of the engine industry toward jet propulsion was very true; even the Air Ministry had great difficulties to persuade the engine industry to accept generous contract offers for jet engine development.

kind of temporary small building with an adjacent semi-open test stand was erected a considerable distance away from the main building complex. This building provided working space for eight people. After the building was finished (early June 1936), Heinkel detailed Max Hahn and Dip. Ing. Wilhelm Gundermann with initially two draftsmen to the Special Development.

Heinkel explained to me that he wanted the jet engine development to remain his own enterprise, not sponsored by the Air Ministry. He was extremely anxious to fly with jet propulsion as soon as possible, and gave me as a technical target an engine thrust of about 600 kilograms. He wanted me to begin immediately with the design of such an engine suitable for flight. Ground testing should begin after a time span of one year, on about June 1937.

It became quite clear to me that my original plan to develop first a well-functioning combustor and then begin with an engine design was impossible in view of the political climate and my rather tenuous position in the corporation and, most of all, the great impatience of Heinkel. On the other hand, it was also clear to me, from previous experience with my first model, that a poorly functioning combustor could result in a nonfunctioning engine which could well mean the end of the turbojet project. In this situation I decided to follow a twofold approach, namely to build very quickly a simple jet engine of minimum risk, which would demonstrate the jet principle in a very convincing and impressive manner, and to begin immediately with a systematic gasoline combustor development. I was convinced that after a successful demonstration of a jet engine I could win the necessary timespan for the development of combustor and flight engine.

The combination radial outflow compressor and radial inflow turbine in my judgment was an ideal configuration for a jet engine of very low development risk. In order to also have a very low risk combustor, I chose gaseous hydrogen as fuel, which was known to have a very high diffusion speed and a very wide fuel-air concentration range in which combustion is possible. I had conceived a hydrogen combustor which I was sure would function very well and would not need time-consuming pre-tests. This hydrogen combustor consisted of a large number of hollow vanes with blunt trailing edges placed within the airduct between compressor stator exit and turbine stator inlet (see Figure 7). The gaseous hydrogen was ducted into the hollow vanes and was injected into the wake downstream from the vanes through a number of small holes along the blunt trailing edge. My greatest attention was devoted to the calculations and layout of the hydrogen combustion engine and to the development of the gasoline combustor. Gundermann and Hahn worked on a design concept using spin-parts riveted to ring flanges. Gundermann particularly made the mechanical calculations of the sheet metal rotors and discs. The Heinkel Corporation was, as an airframe company, well equipped to produce quickly large spin-parts, but was unable to manufacture the ring flanges and the rotor discs. These parts had to be manufactured in a nearby shipyard.

The gasoline combustor development program was as follows:

(1) Installation of a two horsepower Sirocco blower with controllable bypass.

AD-A112 421

AIR FORCE ACADEMY, CO

AIR FORCE ACADEMY AERONAUTICS DIGEST - SPRING/SUMMER 1981. (U)

F/G 20/4

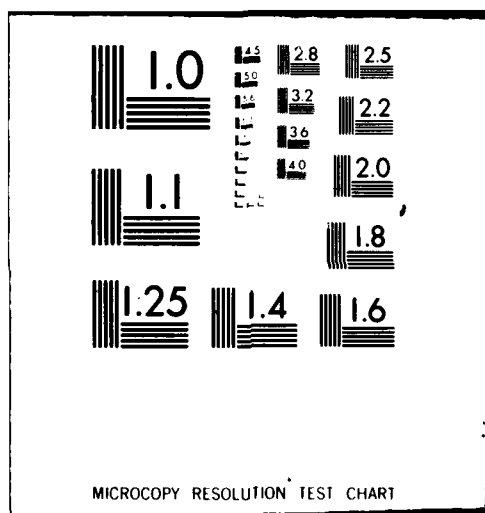
DEC 81 A M HIGGINS, F M JONAS, E J JUMPER

UNCLASSIFIED USAFA-TR-81-11

NL

2 4 2  
2 1 1

END  
DATE FILMED  
4-82  
DTIC

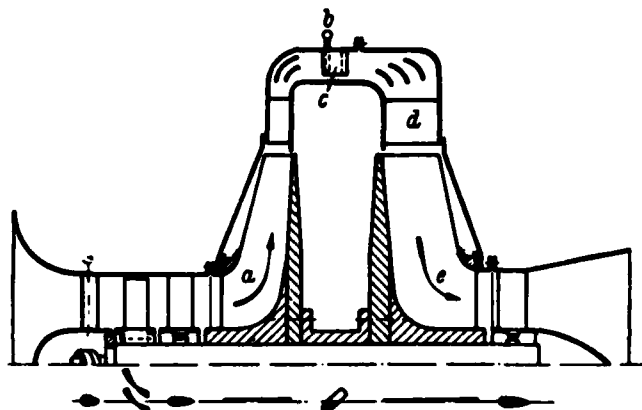


(2) Investigations on segments of annular combustors.

- a. Influence of the shape of the combustion chamber.
- b. Flame holding mechanisms.
- c. Methods of gradual air addition.
- d. Factors influencing combustor volume for given pressure and fuel flow.
- e. How to obtain a low total pressure drop through the combustor.

(3) Gasoline vapor generation and injection into the combustor (generation of high pressure gasoline vapor by an electrically heated pressure boiler).

(4) Combustor utilizing atomized liquid fuel.



(Built in 1936; tested in April 1937)

**Radius of rotor - 1'**

**Thrust - 250#**

**10,000 RPM**

Figure 7. Radial Turbojet (He.S.1) with Hydrogen

During 1936 we made only slow progress in the combustor development program because highest priority was placed upon design and construction of the hydrogen demonstrator engine He.S.1.

The He.S.1 engine was completed and installed in the test bed about the end of February 1937. I am not certain about the exact date of the first run of the hydrogen engine; it may have been in late February or early March.\* During April most of our test runs were completed.

The apparatus fully met expectations. It reached the anticipated performance, it handled very well in acceleration and deceleration, probably because of the relatively small moment of inertia of compressor and

\*Heinkel wrote in his Memoirs that the first run of the hydrogen engine He.S.1 took place in September, 1937. This date is definitely wrong because I remember several comments in which nine months from the beginning to the first run were emphasized. In addition, I recall that water puddles in the vicinity of the jet made the demonstration very impressive. During March and early April we often had night frost, and prior to our first demonstrations to Heinkel's top engineers and important visitors, the test platform cracked the thin ice coverage of the puddles.

turbine rotor and the great stability of the hydrogen combustor over the wide operational range. Most of all, the psychological effect was enormous. Heinkel and his engineers suddenly believed firmly in the feasibility of turbojet propulsion, and my position in the company was now very firm. It also was a considerable morale boost to my co-workers and myself.

It should be noted that Whittle's engine made its first run at the end of April 1957; but in contrast to the Heinkel engine, the Whittle engine already operated with liquid fuel, and the first test run was witnessed and documented. For these reasons a comparison of the dates of the first test runs of Heinkel's hydrogen engine and Whittle's liquid fuel engine is, in my opinion, not meaningful.

After the successful demonstration of the He.S.1, Heinkel exerted a strong pressure for an accelerated flight engine program. We greatly intensified our combustor development efforts, beginning in May 1937; and in less than one year, in early 1938, a combustor with excellent operational characteristics and very low total pressure drop was achieved. These combustors worked best, however, with gasified fuel. The tests with atomized liquid fuel still exhibited some difficulties during starting and low-speed operation which were later overcome. Max Hahn had helped me most effectively in the experimental phases of the combustor development program.

I should mention here that Gundermann, Hahn and I worked as a team where each of us had an idea of strongest technical interest and competence: Hahn in manufacturing techniques and combustion experimentation; Gundermann in stress analysis and mechanical design. He also was head of the group of draftsmen. I gave the overall technical direction, such as utilizing hydrogen for the first test engine and establishing the program for the combustor development. I also made the layouts for the test engines, specifically the thermodynamic analysis and the internal aerodynamics, and became versed in the design techniques of axial flow compressors.

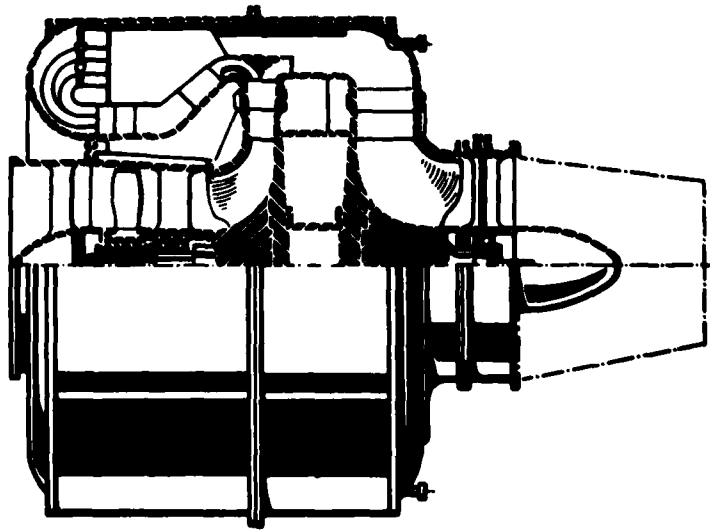


Figure 6. 1937 version

During the last months of 1937, the Guenters began with predesign studies of the first jet propelled aircraft and specified as a necessary thrust 500 kilograms. This aircraft was in many respects an experimental aircraft for demonstration of the principle and characteristics of jet propulsion, but had already provisions for some armament.

In late 1937, while I was working on various layouts of the flight engine, Max Hahn disclosed to me an idea of arranging the combustor in the large unused space in front of the radial flow compressor. He pointed out that this would greatly reduce rotor length and total weight. I thought that this was an excellent idea. I could see many additional mechanical and aerodynamical advantages. So I incorporated Hahn's suggestion in the layout of the flight engine and worked out the aerodynamics of the air ducts and the mixing of the flame gases with the bypass air (Figures 8 and 9).

In view of the initial difficulties I had with Max Hahn's employment, it gave me great satisfaction to notify Heinkel and the Patent Division about Hahn's proposal. The company proceeded with an international patent.\*

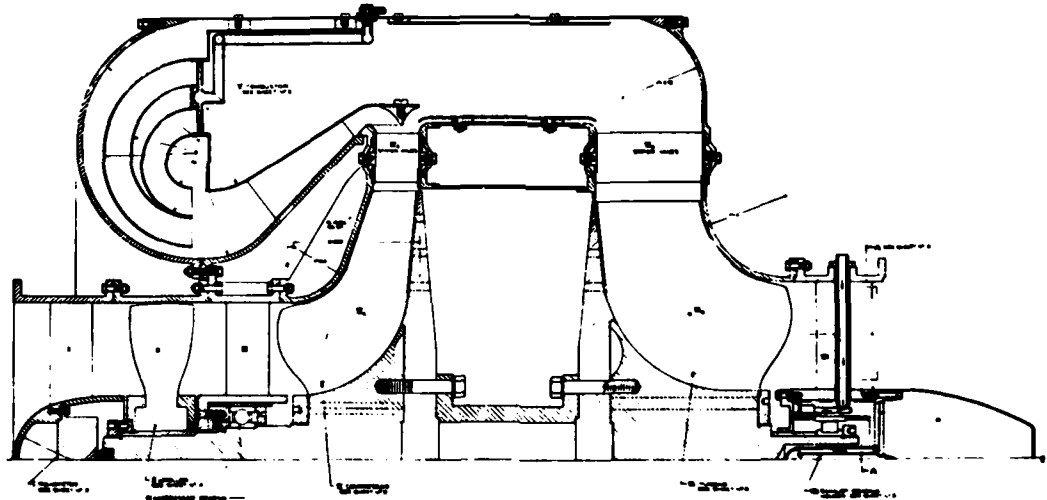


Figure 9. 1937 Design

Aside from the combustor problems a major difficulty of the flight engine lay in the need for achieving a high massflow and high component efficiencies of compressor and turbine. The high massflow was obtained by an unconventionally large ratio of compressor rotor inlet diameter to rotor exit diameter. Normally such a compressor configuration would result in very large inlet losses caused by too high Mach numbers and too large inlet blade curvatures. I tried to reduce these losses by means of an axial inducer stage which gave the inlet flow both a precompression and a prerotation, thereby substantially reducing the mach number and curvature of the rotor inlet blading.

Since the flight engine had to be completed in a very short time (early spring 1939), we had to freeze

\*The Encyclopedia Britannica speaks of a joint patent of Max Hahn and Hans von Ohain. This is incorrect; Hahn was the sole inventor of the "Front Combustor" configuration. The von Ohain patents had been applied for several years prior to Max Hahn's patent application.

the design in about early summer 1938. At that time the combustor with atomized liquid fuel injection was not working entirely satisfactorily; therefore, we used the system with internal fuel gasification for the first flight engines (Figure 10). It was planned to utilize an independent accessory drive for the first flight engines; for later engines, utilization of the atomized liquid fuel injection and a mechanical accessory drive developed by Gundermann was planned.

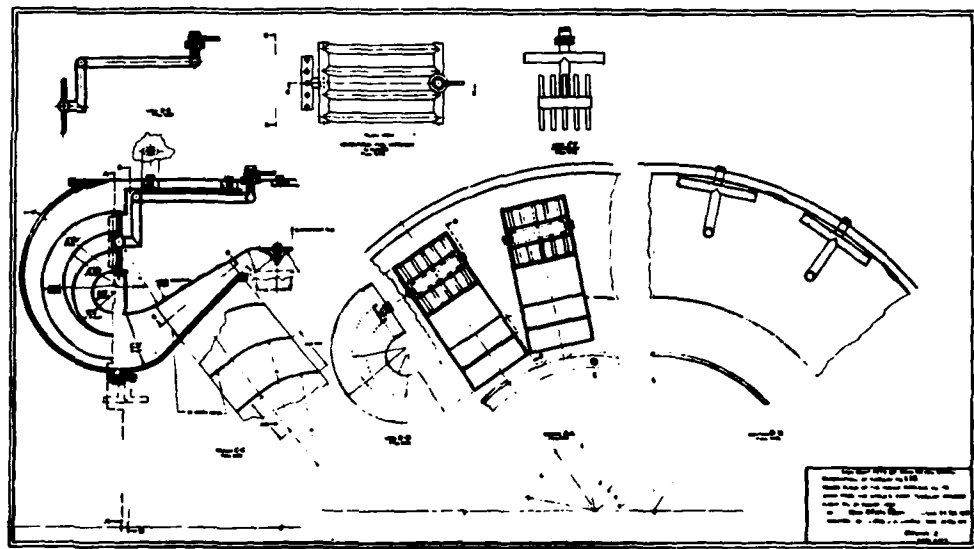


Figure 10. 1938 Design

About early 1938 the detailed design of the He 178 began. Gundermann made essential contributions to the shape of the air inlet, and the air and exhaust gas ducts (Figures 11 to 14).

In late spring of 1939 engine and airframe were completed, but the net thrust was considerably below the anticipated 500 kilograms; therefore, a take-off from the relatively short company air field was not possible. We made a number of internal engine adjustments, specifically in the exchangeable compressor-diffuser and turbine stator. In August the engine performance reached nearly the anticipated values. On August 27, 1939, Heinkel's test pilot, E. Warsitz, made the first successful flight.

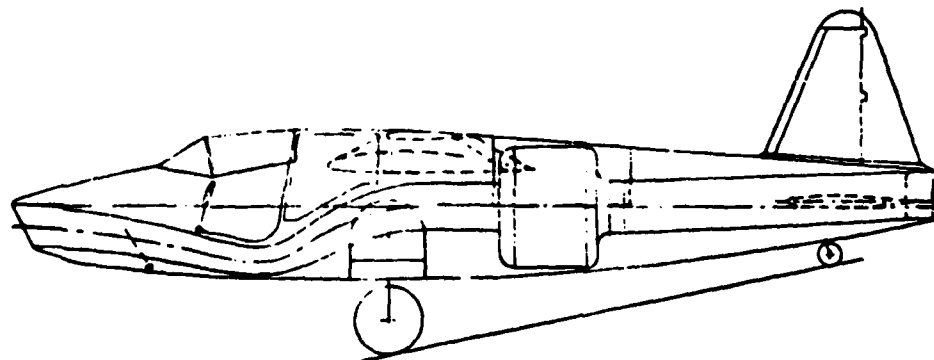


Figure 11. Detailed Design of the 1938 He 178



Figure 12. The Heinkel He 176



Figure 13. The He 178

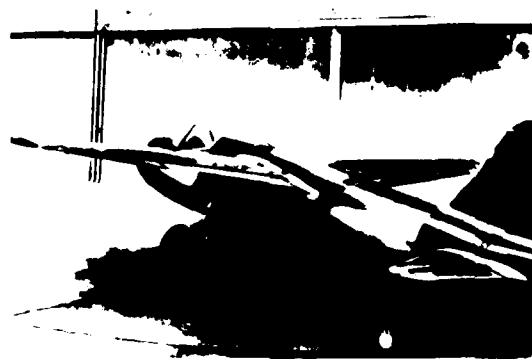


Figure 14. The He 178

Heinkel immediately informed high Air Ministry officials about this flight and invited them for a demonstration which took place in Fall 1939. To Heinkel's disappointment, his visitors were quite indifferent. Nevertheless, a few months later Heinkel's proposal for a jet fighter, the He-280 with two He S8A turbojets installed under the wing, was accepted by the Air Ministry (figures 15, 16, and 17).

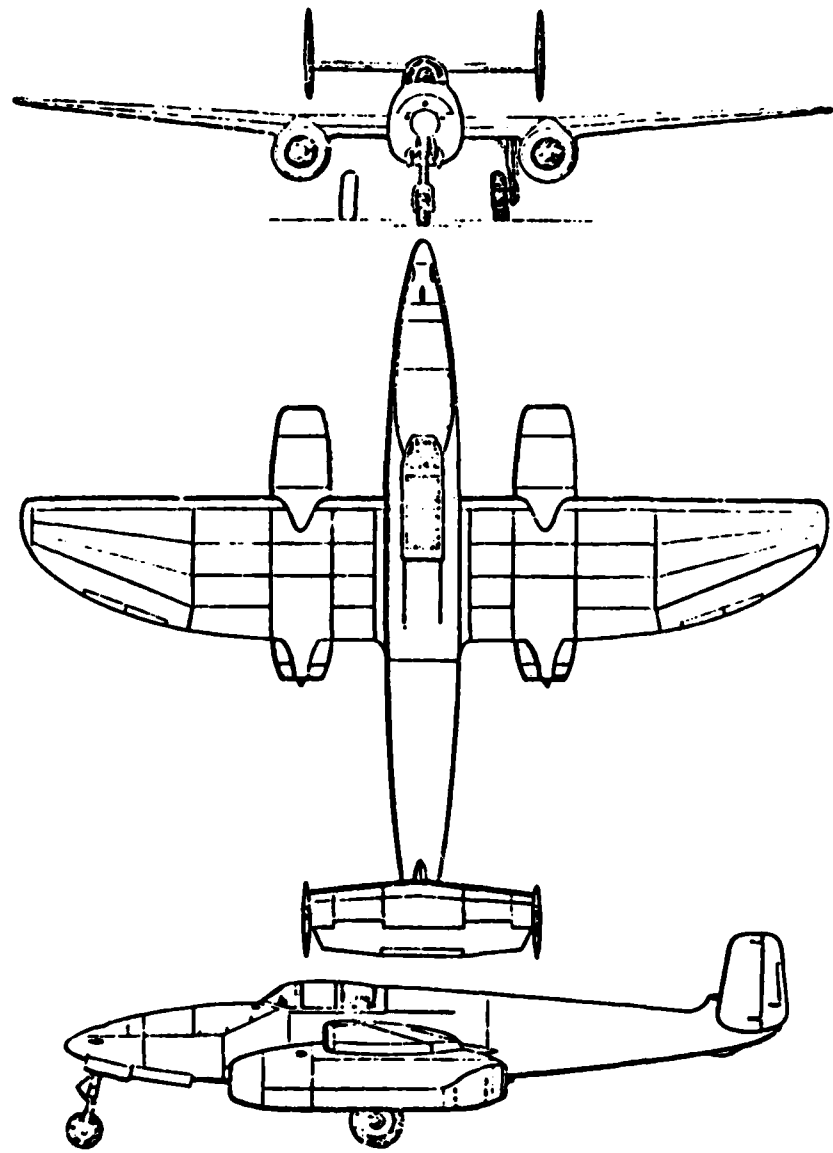


Figure 15. The He-280, the Heinkel Jet Fighter

It is not the purpose of my presentation nor is it possible to give here a complete picture of the German turbojet development; however, a few facts and highlights may be appropriate.

In the early phases of the German turbojet development, from about 1936 to the early 1940s, the higher echelons of the Air Ministry were skeptical or disinterested in turbojet development. In strong contrast to this attitude, the technical group of the Air Ministry headed by Hans Mauch and later by Helmut Schelp were from the beginning strong proponents of this new propulsion system. In fact, Schelp had personally investigated the best application regimes of advanced aeropropulsion systems including the propeller gas turbine, the bypass engine, the pure turbojet and the ramjet, which he presented to the German Academy of Aeronautics in the late 1930s. He used the results of his study for planning and guiding purposes. Both

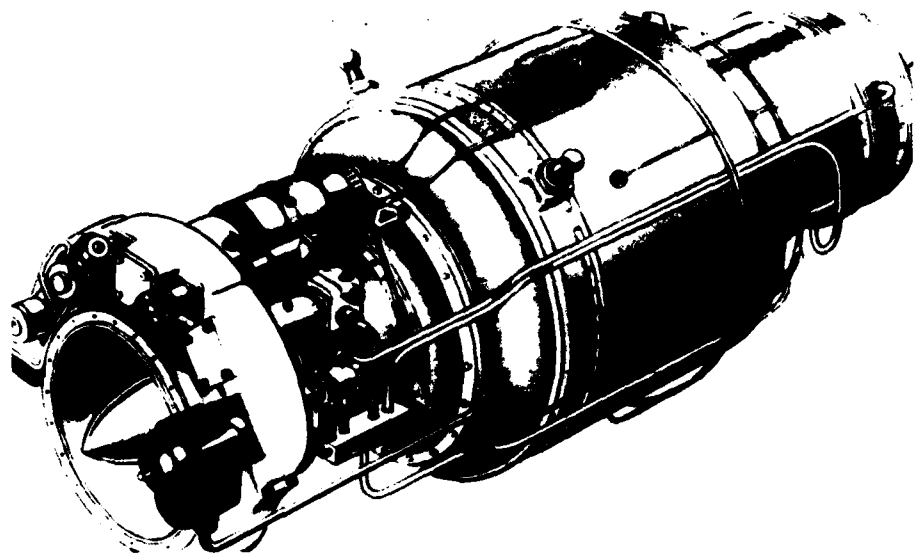


Figure 16. The He S8A

Mauch and Schelp appreciated Heinkel's complete lack of experienced engine designers, facilities, and machine tools. Therefore, Mauch and Schelp approached the German aircraft engine industry in 1938 and offered contracts for study and development of turbojets. The aircraft engine industry, however, did not believe in nor was interested in gas turbine engine developments. After many initial difficulties Mauch and Schelp finally succeeded in their negotiations with Junkers, Bramo, BMW; and these companies accepted jet engine study contracts, while Daimler Benz ultimately refused. The Junkers' development of the 004 engine was headed by Dr. Anselm Franz who was in charge of internal aerodynamics and turbo superchargers, while Dr. Herman Oestrich became head of the 003 development team after Bramo and BMW had merged.

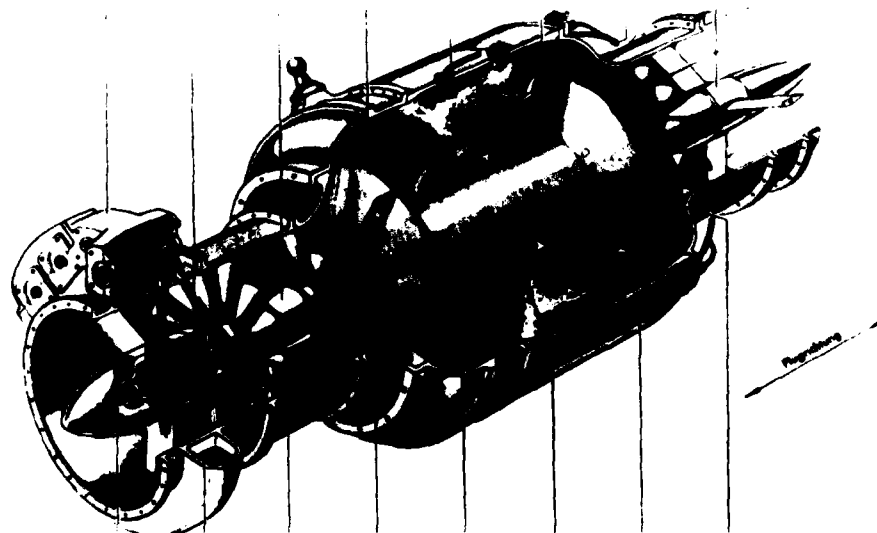


Figure 17. The He S8A

Heinkel's competitors had larger teams with great engine design competence and excellent facilities. Heinkel realized the need for an engine company and made an agreement with the Air Ministry to purchase the Hirth Engine Company -- a side condition was that the He-280 should make its first flight in Spring 1941. The He-280 actually flew for the first time on April 2, 1941, and a few days thereafter Heinkel could acquire the Hirth Company.

In subsequent flight test of the He-280, a top speed of 485 mph was attained at 20,000 foot altitude, but higher speeds (about 550 mph) were expected once the anticipated engine thrust (1600 pounds), would be reached.

During the following two years, nine prototypes of the He-280 were built and tested at military proving grounds, and on various occasions flight demonstrations were made. In one instance a mock combat between the He-280 and a contemporary propeller fighter was arranged where the He-280 displayed clear superiority.

In the Spring of 1942, prospects for preproduction of the He-280 looked favorable, while the Messerschmitt 262 with axial flow turbojet Jumo 004 was plagued with several problems and delays. However, this picture soon changed when the main difficulties with the Me-262 were resolved by early 1943. The Me-262 proved to be superior over the He-280 with respect to both aircraft and engine performance and was chosen for future large-scale production. Therefore, in March 1943, work on the He-280 was terminated. The performance of the Messerschmitt advanced rapidly and in mid 1944 a speed of 624 mph was demonstrated.

By the end of 1944, the BMW engine (003) was chosen for the Heinkel He-162.

For the Heinkel Corporation the most important result of the early flights of the He-280 was the acquisition of the Hirth Company. In 1942 I joined with my team the newly created Heinkel-Hirth Company. The former Hirth Company not only had excellent shops and facilities, but also outstanding scientific as well as practical engineers and support personnel. Integration of the former Hirth and Heinkel teams into a restructured broader organization proceeded very harmoniously. Top engineers of the Hirth group received leading positions in this new organization. One noteworthy example is Dr. Max Bentele, renowned aeromechanical engineer with a national reputation in turbine blade vibrations. Dr. Max Bentele became Chief of the Gas Turbine Component Development Division in the newly-formed Heinkel-Hirth organization.

In Fall 1942, the Heinkel-Hirth Corporation received a government contract to develop a new turbojet, the HeS.011. The technical and performance specifications had been worked out by H. Schelp of the Air Ministry, who then had envisioned the future need for a higher performance engine for new applications as well as a replacement of the Jumo 004 and the BMW 003. Emphasis was placed on a high compression ratio of about 5:1 for greater fuel economy and aircraft range, a thrust of 3000 pounds and no utilization of strategic materials such as nickel which called for a completely air-cooled turbine.

We abandoned the radial outflow compressor and radial inflow turbine, which are living on, however in small gas turbines. Dr. Max Bentele devised a novel air-cooled axial turbine with a most efficient

utilization of cooling air and extremely low manufacturing cost (Figure 18). By the end of 1944 the specified performance had been met and transgressed, and production drawings had largely been completed. Beginning of production was scheduled for early summer 1945.



Figure 18. Air-Cooled Axial Turbine Devised by Max Bentele

In Great Britain the early turbojet development was carried out by essentially one man, Sir Frank Whittle. His first turbojet patent in 1930 of an axial flow compressor followed by a radial inflow compressor represented a very advanced configuration. Although radial flow compressors in large turbojet engines have been abandoned for a long time, they may have an excellent chance for a comeback as the last stage in a multistage axial flow compressor in large fan engines.

Whittle's first test stand engine, having a single U-shape combustor, ran in April 1937, which represented the first liquid fuel aircraft gas turbine test run in the world. Sir Frank Whittle achieved his goals in the face of greatest adversities. His struggle and final success, and the early phases of Great Britain's industrial jet developments are excellently described in his book Jet.

In the United States theoretical investigations on jet propulsion were conducted by the Bureau of Standards in the early 1920s based on a system in which a turbo-compressor was driven by a reciprocating engine (similar to the Caproni Campini system flown on August 28, 1940). The high overall propulsion system weight and the low propulsive efficiency due to the relatively low speed of aircraft at that time made this propulsion system appear unattractive.

In the late 1930s two gas turbine engine developments were undertaken: The turbodyne propeller gas turbine and the pure turbojet of Dr. Nathan C. Price. Both engines had very advanced design features and extreme high pressure ratios, which were too far beyond the state of the art and thus could not succeed.

In Summer 1941, General H. Arnold became aware of the Whittle engine and its aircraft, the Gloster E 28/39, which had made its first flight in May, 1941. General Arnold recognized the enormous future potential of jet propulsion. After an agreement was signed between the American Secretary of War and the British Air Commission, the Whittle engine and drawings were shipped to the United States in late September, 1941. Upon direction of General Arnold, a copy of the Whittle engine was to be built by the General Electric Company in Lynn, Massachusetts, because of the company's great experience in superchargers. At the same time a twin jet airplane powered by the G.E. engines was to be constructed by Bell Aircraft Company in Buffalo. A few months thereafter on March 18, 1942, General Electric built Whittle engine GE1A, ran it on the test stand; and October 3, 1942, the Bell Airacomet (XP-59A) equipped with two GE1A engines flew successfully at Muroc, California and reached flight altitudes up to 10,000 feet. For the United States the Jet Age had begun, and soon after this flight the United States industry was building jet engines of their own design.

In France, turbojet development was essentially dormant during World War II. After the war Dr. Oestrich and his team who had developed the 003 which ultimately had demonstrated outstanding performance characteristics went to France and laid the foundation for France's turbojet industry. The enormous know-how of this group and the advanced turbojet projects they transplanted to France minimized the effects of France's inactivity in aircraft gas turbine development during the war, and in the mid 1950s the French Caravelle and the British Comét were the earliest mass produced passenger jet transports in the world.

In Russia, I believe, the acquisition of Rolls Royce engines has made a great impact on Russian jet technology, but the entire Russian turbojet evolution is not sufficiently known to me to assess this with certainty.

#### C. The Evolution of Aircraft Gas Turbine Engines

The early jet engines were simple and had a ratio of power output to weight far more favorable than piston engines (about two to three times greater), and were capable of greater flight speeds than propeller engines because the compressor elements were shrouded. However, lifetime, reliability, and overall fuel efficiency were substantially below the standards of propeller/piston engines.

Consistent with the initially stated thrusts, the broad goals in the gas turbine development can be briefly stated as follows:

(1) Improvement of Structural Integrity for Greater Endurance, Life Reliability, and Total Life Cycle Cost Reduction. Since the late 1940s, a tremendous effort has been made to combat fatigue by analytical methods, analysis of vibrations, creation of advanced diagnostics techniques, advanced materials and

manufacturing processes. Through these efforts the engine life has increased from 20-40 hours in the mid 1940s to currently 10,000 hours and more.

(2) Improvement of Overall Efficiency (Thermodynamic and Propulsive Efficiency) for Increasing Fuel Economy Range, and Total System Cost. The first step toward higher thermodynamic efficiencies was increasing the turbine and compressor pressure ratio. From pressure ratios of 4:1 in the mid 1940s to 10:1 in the 1950s, 20:1 in the late 1960s, and perhaps 40:1 in the future. Such high pressure ratios necessitate more than one spool compressors, variable stator vanes, better shrouds, seals, and possibly gap control. As a consequence of the increasing number of variable geometry engine components, the control systems became more and more complex and sophisticated.

While the thermodynamic efficiency was continuously improved, the propulsive efficiency had to be increased also in order to attain highest overall efficiencies. For this purpose the ducted fan engine was employed by which the massflow of the jet is increased, while the average jet velocity is decreased, resulting in an improved propulsive efficiency. The first ducted fan engines were built in the mid 1950s with relatively low bypass ratios (1:1 to 2:1). The problems associated with high bypass ratios, around 5:1 and possibly greater, were resolved in the early 1960s with the help and support of the Aero Propulsion Laboratory, Wright Patterson Air Force Base, especially of Cliff Simpson.

(3) Improvements of the Ratios of Thrust-to-Engine Weight and Frontal Area. Improvements in thrust-to-weight ratio have a strong impact on aircraft maneuverability, flight envelope, and speed capability. Unfortunately, the above described improvements in overall efficiency have inherently an adverse effect on the thrust-to-weight ratio of the engine. However, simultaneously with the efficiency improvements, strong efforts had been made to reduce engine weight. This resulted in the trends shown in Figure 2 which indicate that both overall efficiency and power-to-weight ratio increased over the years. The weight reductions were achieved by the following means:

- a. Advanced designs constantly striving towards stronger and lighter structures.
- b. Lighter, stronger, and more heat resistant materials.
- c. Increase in throughflow per frontal area approaching the theoretical limit.
- d. High stage pressure ratio in compressor and turbine to reduce number of stages and thereby total engine weight.
- e. Higher Turbine Inlet Temperature: In the mid 1940s, turbine inlet temperatures were around 1400 degrees Fahrenheit. These temperatures were increased continuously through the following technological advancements: more uniform and suitable combustor exit temperature profiles, improved internal cooling methods, advanced materials and materials treatment, such as directional solidification, and advanced manufacturing techniques. As a result, today's turbine inlet temperatures are nearly doubled.
- f. Increase in Engine Size: In the early 1940s the engine thrust was ranging between 1000 and 2000

pounds. With the advent of the large jet transports and jet bombers in the early 1950s engine thrust rose to more than 10,000 pounds. With supersonic aircraft and still larger transports (C5A and Boeing 747), the thrust of the largest engines is now greater than 50,000 pounds.

g. Constant and Variable Cycle Engines: For aircraft missions with constant speed over most of the mission time, for example a long-range transport with flight Mach number 0.9, the engine would be optimized for this particular flight speed. Efficiency trends of various types of aeropropulsion systems for single speed operation are shown in Figure 19, which I will discuss briefly:

h. For subsonic flight, the propeller-gas turbine with very high pressure ratio is the best propulsion system.

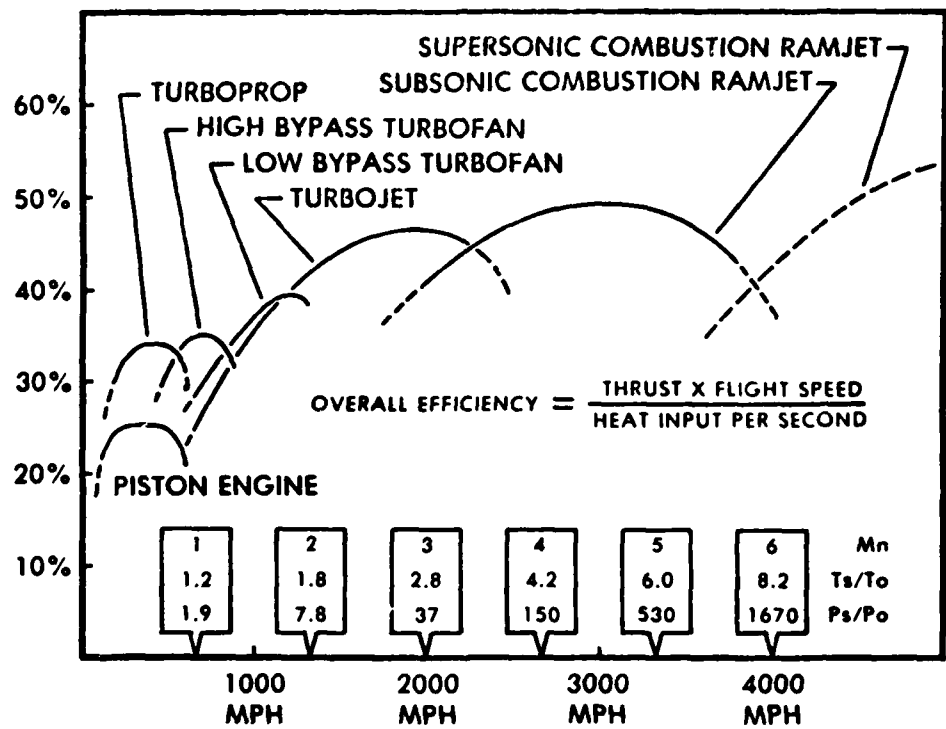


Figure 19. Trends in Aeropropulsion Efficiency

- i. For transonic flight the high bypass ratio ducted fan engine is the most suitable engine. At this flight speed the ram pressure begins to contribute to the engine efficiency.
- j. In low supersonic flight, Mach 1.5, a low bypass ratio ducted fan engine can be slightly better than the turbojet. Engine pressure ratio can be reduced due to high ram pressure.
- k. At higher supersonic flight speeds, Mach 2 to 3, the ram pressure becomes most significant and a low pressure ratio straight turbojet represents the best propulsion system.
- l. Beyond Mach 3 the ram pressure becomes so high that a turbojet would not contribute to overall efficiency, and the subsonic combustion ramjet is the best propulsion system.
- m. Beyond Mach 6 ram pressure and ram stagnation temperature are too high for a subsonic

combustion ramjet. Therefore, the air at the beginning of the combustion is decelerated only to a lower supersonic speed which led to the term supersonic combustion ramjet.

It is interesting to note that the overall efficiency of aeropropulsion systems increases as their operational flight Mach number increases. The speed and altitude regimes for the various types of propulsion systems are shown in Figure 20.

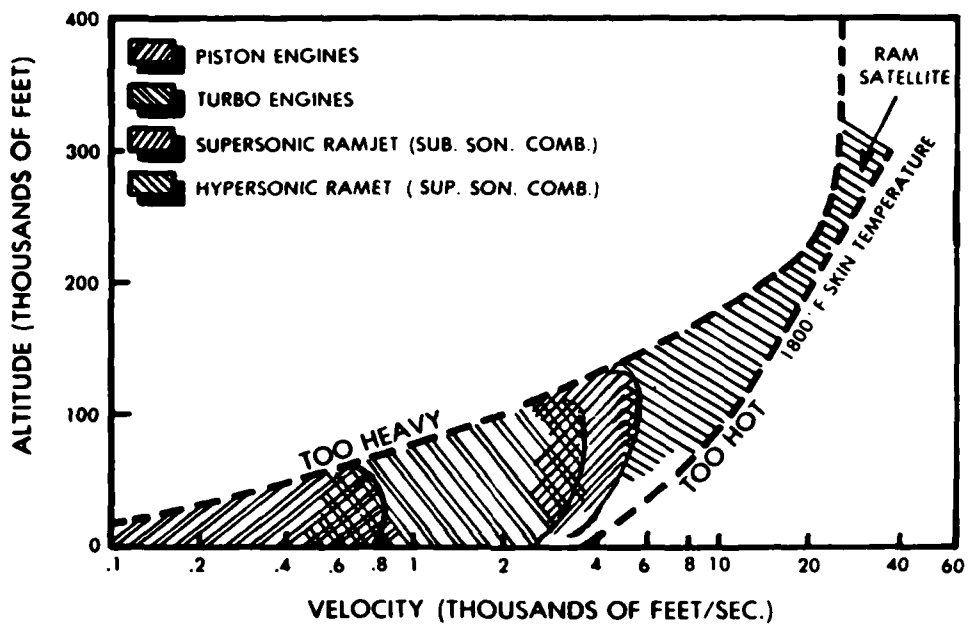


Figure 20. Speed and Altitude Regimes

With the advent of supersonic flight, emphasis was placed on efficient flight operation, not only at one specific supersonic flight speed but over a large regime of flight speeds. For example, a supersonic passenger transport requires not only very efficient engine operation at supersonic design speed but also at transonic speeds for climbing, flying over the American continent, or crossing half the Atlantic in case one engine fails. Another quite different type of multimission would be a Vertical or Short Take Off and Landing (V/STOL) aircraft with efficient transonic or supersonic cruise requirements. Engines which have to operate efficiently in different flight speed regimes are often called "Variable Cycle Engines." In the broadest sense, they have the objective to achieve a reasonable compromise in total efficiency over a range of anticipated flight speeds. Of course, over this anticipated speed range, engine thrust must be matched to aircraft thrust requirements, and engine massflow to the massflow capturing characteristics of the inlet duct for avoiding spillover drag.

The idea of the variable cycle engine is more than two decades old, and some supersonic engines actually have what could be called variable cycle features. The variable cycle engine to its full extent is a future objective; it depends perhaps greatly on the ingenuity of a specific variable cycle engine concept -- whether performance gains and fuel savings will outweigh the increased weight and complexity of engine

and control system.

Broadly sketched, these were the ways the evolution of aircraft gas turbine engines progressed from the simple, low performance, short-life turbojets 35 years ago to the complex, high performance long-life engines of today.

#### D. Future Aeropropulsion Systems

Now, I would like to address two questions which are often raised:

(1) Is the current state of engine evolution at a point where further technological advancements are of diminishing returns?

(2) Is the current gas turbine situation similar to that of the piston engine in the mid 1930s, when a major breakthrough in the form of a radically new engine was just around the corner?

To the first question, the answer is NO: Future technology advancements of strictly evolutionary nature will have an enormous impact on future propulsion systems. Specifically, beneficial effects will be obtained on the following engine characteristics: Reliability; operational characteristics; manufacturing cost; fuel economy; maintenance; range of engine applications; flight envelope; maneuverability. The compounded effects of those technology advancements over the next decades will give the impression of a technological breakthrough in comparison to our current state-of-the-art engines. The underlying estimates of technology advancement are as follows: The overall efficiency, which currently is already as high as that of a diesel engine, may advance by 15 percent to 20 percent, and the thrust to weight ratio may well increase by a factor two. Variable cycle technology very likely will advance, which may furthermore contribute to fuel saving.

To the second question: It is not possible to predict or rule out the coming of radical innovations. One might speculate, however, in what areas radical innovations could have a strong impact on propulsion. Examples for such areas could be:

(1) Application of new energy sources and energy release processes to propulsion including air-rocket hybrid systems for high speed propulsion.

(2) New methods of efficiently transferring energy to environmental air (current methods are limited to turbomachinery, and waves employed, e.g., in the complex).

(3) Radically new methods of functional integration of aero-vehicle and aeropropulsion system.

These examples should illustrate that "radical" innovation must not immediately be equated with "antigravity" or violations of the basic laws of Newton or thermodynamics.

To the other part of question 2, namely: is the current gas turbine engine situation similar to that of the piston engine of the 1930s? The answer is NO:

In the mid 1930s, it was shown that the aero-vehicle could fly at high transonic and supersonic speeds, while the propeller/piston engine could not exceed about 450 mph, or at best 500 mph. Therefore,

the new gas turbine propulsion system in the mid 1930s unlocked a new frontier in flight speed. This situation does not exist today. Today, in any flight speed-altitude regime where an aero-vehicle conceivably can fly, an aeropropulsion system can operate. Therefore, whenever a major breakthrough in aeropropulsion should occur, it will not unlock a new flight speed frontier, but could lead to more efficient, less expensive, lighter propulsion systems, potentially with application for V/STOL.

Let us now discuss some other promising areas for future technology efforts:

Important future technological advancements can be expected from the area of engine airframe integration. Currently, the major concern is to achieve a full understanding and finally a reduction of engine installation drag under all major flight conditions. An additional area which promises potentially great future gains is the area of "functional engine airframe integration." From this area evolutionary as well as radical innovations may emerge. The evolutionary efforts may be concerned with the following topics:

- (1) Improved methods of preventing flow separation by boundary layer control through employing fan air without loss in overall propulsive thrust.
- (2) Drag reduction and efficiency improvement through propulsion by boundary layer acceleration.
- (3) Thrust augmentation; thrust vectoring for V/STOL applications.
- (4) Improved methods of engine induced supercirculation.

Another very important future endeavor is total cost reduction. Efforts will be directed toward improved manufacturing processes, design simplifications, reduction of maintenance time, increase in life and reliability, and also improved performance such as increased overall efficiency and thrust-to-weight ratio.

The last and most fascinating frontier may be the evolutionary approach toward supersonic and possibly hypersonic long-range transportation. Ironically, one major obstacle to high speed transportation is that portion of the journey which takes place on the ground between home and embarking the aircraft and between debarking and place of destination. In essence, remodeling the total airport system is one of the most important and challenging tasks for supersonic transportation to become more widely accepted.

Another obstacle, of course, is the economical problem of supersonic flight. Fuel is a strong factor and engines with variable cycle features will be needed. The solution will not come alone from the engine. Work on a better L/D of the airframe will be equally or even more important.

Finally, the environmental problems, whatever they may be, must be clarified and solutions must be found.

In my opinion, it is most likely that supersonic transportation on a much broader scale than currently with the Concorde will come, but it is difficult to estimate the time. We may have to think in decades rather than in years.

From the Wright brothers' first aircraft engine in 1903, the evolution of aeropropulsion systems

USAFA-TR-81-11

progressed with ever-increasing vigor to the present. Ahead of us still lies probably a greater time span until this evolution reaches a plateau.

**DATE  
ILME**